Department of Chemical Engineering

Solubility and Crystal Growth of Sodium Nitrate from Mixed Alcohol – Water Solvents

Angelina Jane Rossiter

This thesis is presented for the Degree of
Master of Chemical Engineering
of
Curtin University of Technology

August 2009

Declaration

To the best of my knowledge and belief this thesis contains no material previously published by any other person except where due acknowledgment has been made.

This thesis contains no material which has been accepted for the award of any other degree or diploma in any university.

Signature: …….

Date: ……...

Acknowledgements

I would like to express my deep gratitude to my supervisor, Professor Ming Ang, for his support, advice and invaluable guidance. I am also greatly indebted to him for taking me on as his student near the end of my Masters study. Without his supervision and support I would not have been able to complete my Masters study. I would also like to thank my co-supervisor Dr Parvis Safaeefar for his assistance in the solubility work. I would also like to sincerely thank my former supervisor Professor Dongke Zhang for his support and guidance. I also gratefully acknowledge the assistance of my former co-supervisor Dr Sawsan Freij who laid down a foundation of knowledge of this project during the start of my Masters.

I would also like to specially thank Professor Kouji Maeda at University of Hyogo in Japan for his help in NRTL modelling.

I would also like to acknowledge the assistance provided by Centre members at Curtin Centre for Advanced Energy Science and Engineering (CCAESE), especially the Centre's director, Professor Chun-zhu Li for his support. I gratefully acknowledge the help provided by Cyril Kelly and Barry Tindall in setting up the solubility rig, helping me with pump problems and keeping the algae at bay, and for Cyril's motivational speeches. Thanks to Dr John Bromly, Dr Richard Gunawan and Dr Alex Elliot for their advice, assistance, support and friendship. Special thanks to Dr Richard Gunawan for helping me format and collate my thesis. Special thanks to Tasneem Dawood, Meining Song and Yii Leng Chan for their friendship and support and for the friendship of the students that have now graduated, Dr Huiling Wee, Dr Esther Ng, Dr Lingngee Ngu, Dr Setyawati Yani, Dr Nurul Widiastuti and Dr Kongvui Yip. The contribution in the lab work from Kane Black and Winny Phylicia is also greatly appreciated.

I would also like to thank Felicia Lee with her help in AFM work, Elaine Miller from the Applied Physics department for her help in SEM work, Dr Tuna Dincer and Dr Amal Freij for their help and advice on setting up the modified growth cell, Professor Mark Ogden and Dr Thomas Becker from Applied Chemistry for loan of the

modified growth cell set up, and to the Technical staff at Chemical Engineering for the loan of equipment.

I gratefully acknowledge the financial support received for part of this research from Dyno Nobel Asian Pacific Ltd under the ARC Linkage Project scheme. I also acknowledge the financial support received from Chemical Engineering for my scholarship.

Last but not least, special thanks to my family for their love, support and encouragement during my Masters study.

Publications

A. Rossiter, P. Safaeefar, K. Black, K. Maeda, H. M. Ang, "Measurement of the solubility of sodium nitrate in ethanol and water solutions", Chemeca, Burswood Entertainment Complex Perth, Australia, 27 – 30th September 2009 (accepted for presentation)

A. Rossiter, S. Freij and D. Zhang, "An in-situ optical microscopic study of sodium nitrate crystallisation", Chemeca, Sofitel Melbourne, Australia, 23rd – 26th September 2007

Abstract

Due to the ductile nature of the sodium nitrate crystal which deforms plastically under high levels of strain, most of the crystal growth studies in aqueous solution have focussed on the influence of tensile strain, supersaturation and dislocation, using x-ray surface topography to characterise the dislocation structure of the crystal. Most of the crystal growth studies have also focussed on growth from the melt since single crystals of sodium nitrate find application in optical pumping experiments, are a potential substitute for calcite in the preparation of polarising prisms and are interesting for the study of plastic properties because two types of plastic deformation, glide and twinning, take place in these crystals at room temperature. Its crystal habit is also difficult to modify and many researchers have used dyes to investigate its effect. Sodium nitrate is also a highly soluble substance with 96g of sodium nitrate dissolving in 100g of water at 30.0°C, making aqueous solutions of this salt and its supersaturation extremely unstable. Literature on its solubility in organic solvents, such as methanol, ethanol and isoproponal, are quite outdated and limited to specific conditions.

This study involved the determination of the solubility of sodium nitrate in aqueous methanol, ethanol and isopropanol solutions at different temperatures and weight percents of the organic solvents. Splitting into two liquid phases was observed when using isopropanol, however this phase separation does not occur at low and high mass fractions of alcohol, as at lower concentrations of one solvent the two solvents are miscible. Whereas in the presence of methanol and ethanol the solubility of sodium nitrate in water was significantly reduced, with the solubility decreasing with increasing molecular weight of the alcohol. The experimental data for methanol and ethanol was used for the determination of the ion-specific Non random two liquid (NRTL) parameters by correlating with the modified extended NRTL model. It was observed for both methanol and ethanol that the model was found to satisfactorily correlate the data at low to moderate concentrations of alcohol. However, as the concentration of alcohol rises the model prediction was found to be less satisfactory,

probably due to the interaction parameters of NRTL between alcohol and the ions not being able to represent the low solubility of electrolytes.

The growth rates of individual faces of sodium nitrate crystals grown in situ in a batch cell and observed with an optical microscope were measured at different temperatures (20.0, 30.0 and 40.0°C) and relative supersaturations (0.02, 0.04, 0.06, 0.08 and 0.1) to determine the kinetics of growth for homogeneous nucleation. A combined growth order, of 1, and activation energy of 23,580 J/mol was obtained indicating that crystal growth in these sets of experiments was diffusion controlled. Crystal growth rates were also obtained for sodium nitrate crystal seeds grown at 20.0°C at a supersaturation of 0.02 and 0.04, in a modified growth cell where the saturated solution was circulated at a flow rate of 4mL/min. The crystal growth rates obtained were much lower in comparison to the growth rates obtained by homogeneous nucleation. In both sets of experiments size independent growth was observed.

The surface morphology of the crystals was also observed by optical microscopy, scanning electron microscopy (SEM) and atomic force microscopy (AFM) for the crystals grown by homogeneous nucleation to elucidate the mechanism of growth. Liquid inclusions were observed by optical microscopy for crystals that were grown at high temperatures and for a long duration. SEM revealed the presence of pitting on the crystal surface due to the high solubility of sodium nitrate, while AFM images showed the presence of growth hillocks which suggests that crystal growth is surface integration controlled. However, the presence of growth hillocks could have been caused by the formation of some nuclei and surface artefacts when the crystal was taken out from solution. In seeded crystal growth experiments the solute was observed by optical microscopy to deposit onto the crystal surface.

The effect of solvent composition on the growth rate and habit modification of sodium nitrate was also investigated with aqueous solutions of methanol and ethanol. Crystal growth rates of sodium nitrate crystals grown in situ in a batch cell by homogeneous nucleation in aqueous ethanol at 30.0°C at 20, 50 and 90 weight percent of ethanol and crystal seeds grown at 20.4°C at a supersaturation of 0.02 and 0.04 at 30, 50 and 90 weight percent of ethanol, in a modified growth cell was

measured. It was found that growth rates decrease with increasing amounts of ethanol and the habit of the crystal remains unchanged. The growth rate was also observed to be much lower than the growth rates obtained from pure aqueous solution. For crystals grown by homogeneous nucleation it was observed that with increasing supersaturation, decreasing weight percent of ethanol and with increasing crystal size the number of liquid inclusions observed on the crystal surfaces increased, whereas for seeded crystal growth solute was observed to deposit on to the crystal surface mainly at low alcohol weight percents. Sodium nitrate crystals grown in aqueous methanol was also observed to behave similarly to crystals grown in ethanol, with lower growth rates obtained. For all cases size independent growth was observed.

The influence of additives, DOWFAX 3B2 and amaranth was also investigated on the habit modification of sodium nitrate for crystals grown by homogeneous nucleation at 20.0°C at a supersaturation of 0.04. Both additives were observed to be effective in changing the crystal habit of sodium nitrate, with the appearance of triangular truncations or octahedral facets at the corners of the sodium nitrate crystal due to the additive being adsorbed onto the crystal surface. The influence of the additives on the crystal habit modification can be explained due to the presence of the anionic polar group, the sulphonate group. The growth ratio value for DOWFAX 3B2 was also found to decrease with increasing additive concentration.

It is believed that the results of this thesis provides up to date data on the solubility of sodium nitrate in aqueous ethanol and for temperatures and weight percents that have not been reported before in literature for the aqueous methanol system. The work reported on crystal growth studies by homogeneous nucleation and using crystal seeds, the effect of solvent and DOWFAX 3B2 on crystal growth rates and habit modification is also new and has not been reported in literature before.

Table of Contents

List of Figures

List of Tables

Chapter 1
INTRODUCTION

Sodium nitrate has many applications and in the late nineteenth century was used extensively as a fertiliser and as a raw material for the manufacture of gunpowder, however in the first decades of the twentieth century its value declined dramatically after cheaper means were found to make fertilisers and explosives (Wikipedia 2007). It's other applications include being used as an ingredient in glass and pottery enamel, as a food preservative since it has antimicrobial properties, for the production of nitric acid (Wikipedia 2007), manufacture of sulphuric acid, nitrate of potash, arseniate of soda, fireworks, fusing mixtures, steel, minium and for making chlorite in the manufacture of bleaching powders (Myers 1899). It has also been successfully used to control the morphology of platinum nanoparticles (Herricks et al. 2004). Single crystals of sodium nitrate also find application in optical pumping experiments (Gopalakrishnan et al. 1991) and can be used as a substitute for calcite in the manufacturing of polarising prisms (Komnik & Startsev 1969).

Sodium nitrate is highly soluble in water, with 96g of sodium nitrate dissolving in 100g of water at 30°C (Mullin 1993). To reduce its solubility in water sodium nitrate can be dissolved in mixed solvent systems, which are commonly organic solvents such as alcohol added to an aqueous solution, with this process commonly referred to as 'salting-out' or 'drowning-out' crystallisation. This method offers several advantages over other methods of crystallisation by cooling and evaporation because ambient temperature may be employed, which is highly desirable if heat labile substances are being processed, which is therefore an energy saving alternative to evaporative crystallisation if the solvent can be separated at low (energy) costs, and crystals of high purity are normally produced (Nowee et al. 2008). The literature on the solubility of sodium nitrate in aqueous ethanol is quite outdated and for other systems is not available at the conditions and composition of interest. Given this

situation the solubility of the system must either be calculated, a viable alternative when thermodynamic data is available, or measured.

Most of the crystal growth studies of sodium nitrate in aqueous solution have focussed on the influence of tensile strain, supersaturation and dislocation due to the ductile nature of the sodium nitrate crystal which deforms plastically under high levels of strain. Crystal growth rates have also been determined by secondary nucleation at low relative supersaturation (Jones et al. 2000). There has not been any reported work on crystal growth studies of sodium nitrate from homogeneous nucleation or from crystal seeds. X-ray surface topography studies have also been used to characterise the dislocation structure of the crystal (Jones et al. 2000). No other surface topography studies have been carried out to study its mechanism of growth. Very little work has also been carried out on the effect of solvent on the growth and habit modification of sodium nitrate. Only Oosterhof *et al* (Oosterhof et al. 1999) has studied in a microscopic setup the growth of sodium nitrate from mixtures of water and isopropoxyethanol (IPE).

Sodium nitrate is a difficult crystal to modify. Researchers have mainly used dyes to investigate and study the effect of additives on the crystal habit modification of sodium nitrate (Butchart & Whetstone 1949; Weinland & France 1932; Whetstone 1955ab). This is an area of great industrial importance since certain crystal habits are disliked in commercial crystals, such as needles and plates, because they give the crystalline mass a poor appearance; others make the product prone to caking, induce poor flow characteristics, or give rise to difficulties in the handling, packing or filtration of the material. Normally a granular or prismatic habit is usually desired (Mullin 1993). A review of the literature indicates that no recent work has been performed on using dyes or additives to change the crystal habit of sodium nitrate.

Therefore the objectives of the work described in this thesis are to acquire updated solubility data on the solubility of sodium nitrate in aqueous ethanol and to determine its solubility in other aqueous alcohol systems, and determine the ion-specific NRTL parameters by correlating with the extended NRTL model. The solubility data for the aqueous ethanol system will then be used for “salting out” crystal growth studies, comparing this to growth rates of single crystals of sodium nitrate formed by

homogeneous nucleation and crystal seeds of sodium nitrate using the technique of in situ optical microscopy. Growth measurements will be carried out from aqueous solution over a wide range of supersaturations at different temperatures to investigate the mechanisms of growth. The presence of growth rate dispersion (GRD) will also be investigated. The surface topography of the crystals will also be investigated to elucidate its mechanism of growth by optical microscopy, SEM and AFM and to determine the effect of additives, namely amaranth and DOWFAX 3B2 on the crystal habit of sodium nitrate.

The thesis is organised into 6 chapters, in which the experimental and analytical techniques used are presented in Chapters 3 to 5, which are interlinked with each other as shown in Figure 1-1. Each chapter opens with a brief introduction which conveys the motivation of the chapter, with the main points and findings presented in a summary at the end of each chapter.

Chapter 1: Introduction

This chapter presents the background and defines the scope and overall aims of the present study, closing with a detailed outline of the chapters in the thesis.

Chapter 2: Literature review

This chapter starts of with a review on basic crystallisation theory and the effect of additives and solvent on crystallisation. It also reviews the literature on crystal growth, solubility studies and the influence of additives on the growth rate and habit modification of sodium nitrate. This chapter also identifies the existing gaps in the literature, which form the specific objectives of this thesis

Chapter 3: Measurement and correlation of the solubility of sodium nitrate in mixed solvents

The solubility of sodium nitrate in water and in aqueous alcohols (methanol, ethanol and isopropanol) at different temperatures is presented in this chapter. The resulting data for the aqueous methanol and ethanol systems are used for the determination of

the ion-specific NRTL parameters by correlating with the modified extended NRTL model. The experimental techniques used are also described in this chapter.

Chapter 4: Growth rates and surface morphology of sodium nitrate grown from aqueous solution

In this chapter the growth kinetics of the pure aqueous sodium nitrate system grown by homogeneous nucleation in a batch cell at different temperatures (20.0, 30.0 and 40.0°C) and relative supersaturations σ (0.02, 0.04, 0.06, 0.08 and 0.1), the effect of growth rate dispersion and surface morphology is presented. These results are also compared to the aqueous ethanol system grown by the same method at 30°C at 20, 50 and 90 weight percent of ethanol. The results for the pure aqueous and ethanol system are also compared to the seeded crystal growth experiments conducted at 20.0°C for the aqueous pure system and 20.4°C for the ethanol system using a modified growth cell. The effect of aqueous methanol at 20.0°C on the surface morphology is also briefly discussed. The experimental and analytical techniques used are also described in this chapter.

Chapter 5: Effect of additives on the habit modification of sodium nitrate

This chapter discusses the effect of the additives DOWFAX 3B2 and amaranth on the crystal habit modification of sodium nitrate. The experimental techniques used are also described in this chapter.

Chapter 6: Conclusions and Recommendations

This chapter provides a concise account of the conclusions over the whole study and outlines recommendations for future research.

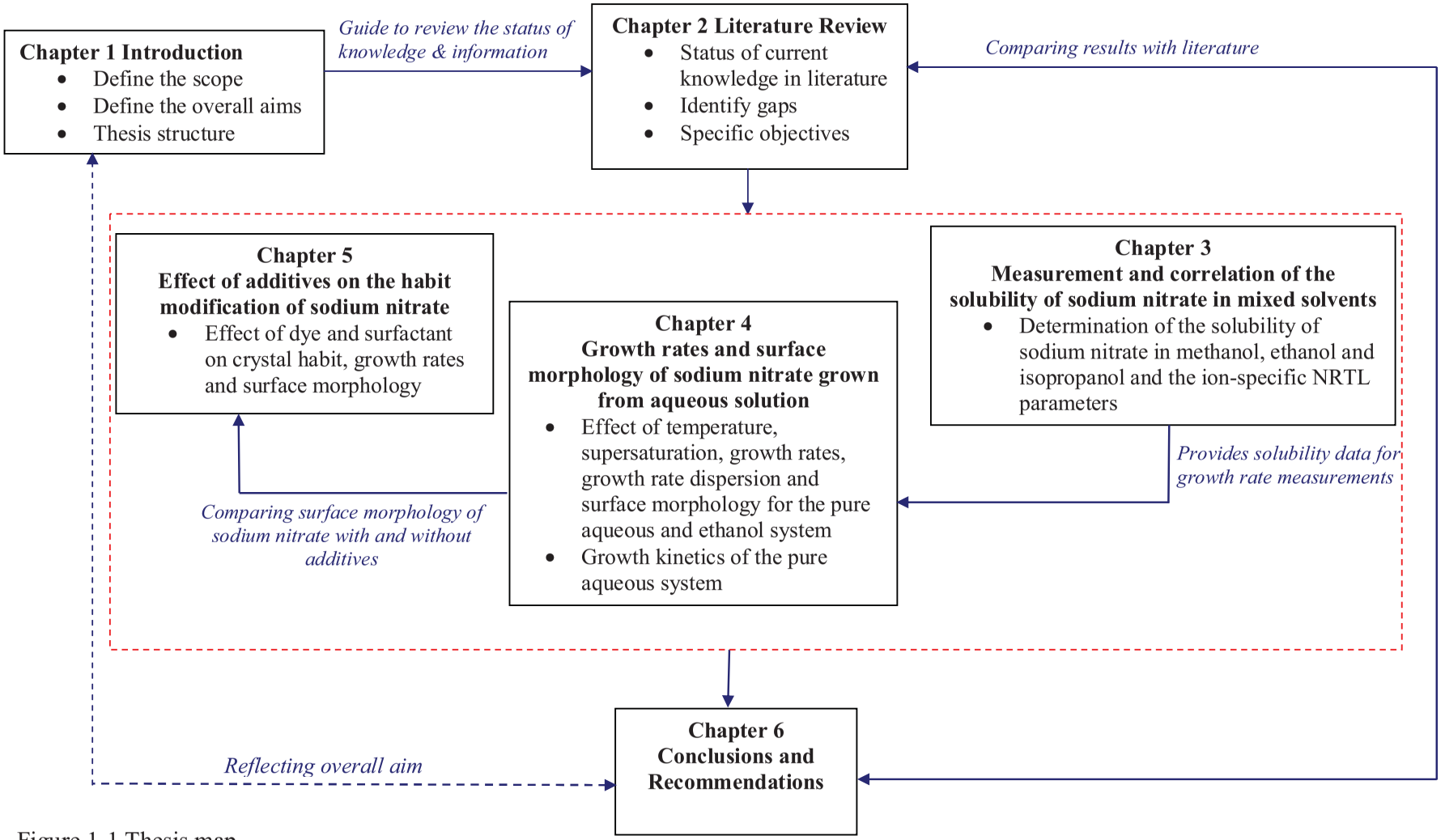

Figure 1-1 Thesis map

Chapter 2
LITERATURE REVIEW

2.1 INTRODUCTION

This chapter provides a brief overview on the basic crystallisation theory, crystal growth mechanisms, additives, solvent, and a review on sodium nitrate crystal growth rate, solubility studies and on the influence of additives and solvent on the growth rate and habit modification of sodium nitrate.

2.2 CRYSTALLISATION

Crystallisation is a technique widely employed in the separation and purification of solids and it is also an important process for the manufacture of many products. The control of crystallisation is also of fundamental importance in many areas such as in the stability of emulsion explosives where crystallisation of the disperse phase can occur caused by homogeneous and heterogeneous nucleation of the supersaturated droplets which weakens the emulsion and makes them relatively unstable (Villamagna & Whitehead 1995).

Crystallisation from solution can be considered as a two step process, namely nucleation and crystal growth. Nucleation is the formation of the crystallisation phase or “birth” of new crystals and crystal growth is the growth of the crystallisation phase into larger sizes. These two processes continue to occur simultaneously only if the solution is supersaturated; hence the rate of nucleation and growth is governed by the level of supersaturation. The following sections will discuss the supersaturation and the crystallisation kinetics in detail.

2.3 SUPERSATURATION AND METASTABILITY

As discussed in the previous section a supersaturated solution is required for crystallisation to occur. This means that the solution has to contain more dissolved solids than it would contain under equilibrium (saturation) concentration at a given temperature (Myerson 1993). The amount of solute that can dissolve in a given amount of solvent at a given temperature is termed the solubility and for the majority of cases the solubility increases with increasing temperature. For some solutes, their solubilities can also decrease with increasing temperature (Myerson 1993). Creating a supersaturated solution can be achieved by various methods such as by temperature change (cooling), chemical reaction, evaporation of solvent, changing the pH and by changing the solvent composition (Myerson 1993). A supersaturated solution is not in equilibrium so it will crystallise in order for it to relieve the supersaturation by a combination of nucleation and crystal growth so it can move towards equilibrium. Figure 2-1 shows the solubility-supersolubility diagram which is typically used to explain the phenomenon of the crystallisation process in terms of supersaturation.

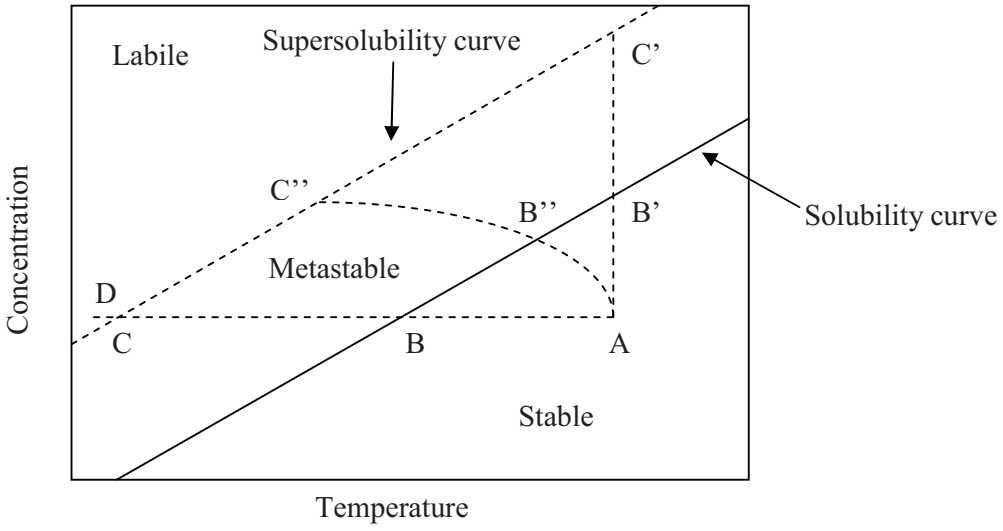

Figure 2-1 The solubility – supersolubility diagram (Mullin 1993)

The solubility curve can be determined and located with precision, whereas the supersolubility curve which represents the temperature and concentration at which

uncontrolled spontaneous crystallisation occurs, is not that well defined since its location on the diagram is affected by, amongst other things, the rate at which supersaturation is generated and the intensity of agitation (Mullin 1993).

From Figure 2-1 three zones can be distinguished, one well defined and the other two variable to some degree, which are (Mullin 1993; Myerson 1993):

1. The stable (unsaturated) zone, where crystallisation is impossible since more crystals can still be dissolved into the solution as the solubility of the solute has not been reached.

2. The metastable (supersaturated) zone, between the solubility and the supersolubility curves, where spontaneous crystallisation is improbable. Knowledge of the width of this zone is also important in crystallisation because it aids in understanding the nucleation behaviour of each system.

3. The unstable or labile (supersaturated) zone, which represents temperatures and concentrations at which spontaneous crystallisation is probable but not inevitable.

Point A on Figure 2-1 represents a solution which is undersaturated. If this solution is cooled without loss of solvent to point B the solution will be saturated and if the solution is cooled further past point C into the labile zone crystallisation may take place rapidly in order to relieve the highly supersaturated conditions so it can return back to equilibrium or it may be induced by seeding, agitation or mechanical shock. Further cooling to point D may be necessary before crystallisation can be induced, especially with very soluble substances since the solution may have become highly viscous and could even set to glass preventing crystallisation. As previously mentioned, supersaturation can also be achieved by solvent evaporation, which is represented by the path AB'C' at constant temperature. In practice, a combination of cooling and evaporation is employed which is represented by the path AB"C". All the conditions above only apply to homogeneous solutions since if a crystal of the solute was placed in the metastable region, growth would occur on it (Mullin 1993).

2.3.1 Expressions of supersaturation

Supersaturation is the fundamental driving force for crystallisation which is commonly expressed as the concentration driving force, Δc, the supersaturation ratio, S, and the absolute or relative supersaturation, σ, which are defined by the following equations:

$$\Delta c = c - c^* \tag{2-1}$$

$$S = \frac{c}{c^*} \tag{2-2}$$

$$\sigma = \frac{\Delta c}{c^*} = S - 1 \tag{2-3}$$

where c is the solution concentration, and c* is the equilibrium saturation at the given temperature.

2.4 NUCLEATION

Nucleation or the formation of the crystalline phase is typically classified into either primary or secondary nucleation mechanisms, with primary nucleation involving either homogenous or heterogeneous mechanisms, and secondary nucleation involving several possible mechanisms which includes initial breeding, dendritic, polycrystalline breeding, macroabrasion, fluid shear and contact which is the most common mechanism (Myerson 1993). Figure 2-2 provides a breakdown of these nucleation mechanisms.

The difference between primary and secondary nucleation is that primary nucleation occurs in systems that do not contain crystalline matter, whereas secondary nucleation is induced by crystalline matter which has a catalysing effect on the nucleation, therefore resulting in nucleation occurring at a lower supersaturation than needed for spontaneous nucleation, and also from its interaction with the environment such as crystalliser walls and impellers (Hartel 2001; Mullin 1993; Myerson 1993).

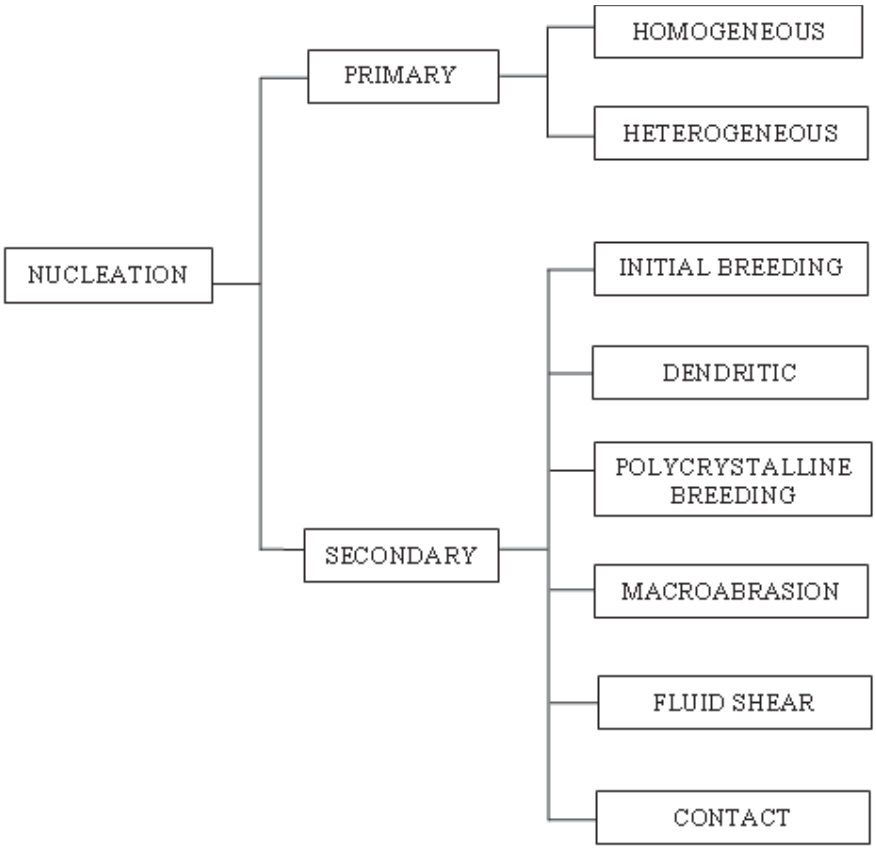

Figure 2-2 Mechanisms of Nucleation

2.4.1 Primary nucleation

Primary nucleation can be subdivided into homogeneous and heterogeneous nucleation. Homogeneous nucleation involves the formation of a crystal lattice structure based on the growth of molecules into a stable size whereas heterogeneous nucleation is usually induced by the presence of dissolved impurities and by foreign surfaces such as vessel walls, dust and colloids that promote the formation of a nucleus (Hartel 2001). Homogeneous nucleation rarely occurs in practice since it is difficult to prepare systems that are free from impurities such as the presence of atmospheric dust which may act as nucleation catalysts, and also physical features such as retaining vessel walls, stirrers and baffles which may frequently catalyse nucleation (Mullin 1993). Homogeneous nucleation also requires a high level of

supersaturation and in most situations heterogeneous nucleation takes place before reaching conditions suitable for homogeneous nucleation.

2.4.1.1 *Homogeneous nucleation*

The classical theory of nucleation (Nielsen 1964; Volmer 1939) assumes that clusters of molecules are formed in solution from a sequence of bimolecular additions that continues until a critical size (i.e stable nucleus) is reached, according to the following scheme (Mullin 1993; Myerson 1993):

$$A + A \rightleftharpoons A_2$$

$$A_2 + A \rightleftharpoons A_3$$

$$A_{n-1} + A \rightleftharpoons A_n \text{ (critical cluster)}$$

where 'A' represents a single solute ion or molecule, which contains n ions or molecules, A_n

The rate of nucleation, J, eg the number of nuclei formed per unit time per unit volume, by this mechanism can be expressed as an Arrhenius type of expression (Mullin 1993; Myerson 1993):

$$J = A\exp\left(\frac{-\Delta G}{kT}\right) \tag{2-4}$$

where A is the pre-exponential factor and has a theoretical value of 10^{30}nuclei/cm^{3}s (Myerson 1993), ΔG is the overall excess free energy between a small solid particle of solute and the solute in solution, k is the Boltzmann constant and T is the temperature in Kelvin.

The classical theory of nucleation was initially based on the condensation of a vapour to a liquid, which may be extended to crystallisation from melts and solutions. The free energy changes associated with the process of homogeneous nucleation may be considered as follows (Hartel 2001; Mullin 1993; Myerson 1993; Randolph & Larson 1988). For a spherical nucleus to form, the work of formation can be broken

down into a surface term and a bulk term. The free energy change of a crystal nucleating homogeneously from solution is given by:

$$\Delta G = \Delta G_s + \Delta G_v \tag{2-5}$$

$$= 4\pi r^2 \gamma + 4/3\pi r^3 \Delta G_v \tag{2-6}$$

where ΔG_s is the surface excess free energy (i.e the excess free energy between the surface of the particle and the bulk of the particle), ΔG_v is the volume excess free energy (i.e the excess free energy between a very large particle ($r = \infty$) and the solute in solution), ΔG_v is the free energy change of the transformation per unit volume, γ is the interfacial tension and r is the nucleus radius. ΔG_s is a positive quantity and is proportional to the surface area and thus the square of the nucleus radius, while ΔG_v is a negative quantity due to the latent heat of fusion released upon the phase change and is proportional to the nucleus volume and thus the cube of the radius. The net free energy change during nucleation is the sum of these terms as shown in Figure 2-3.

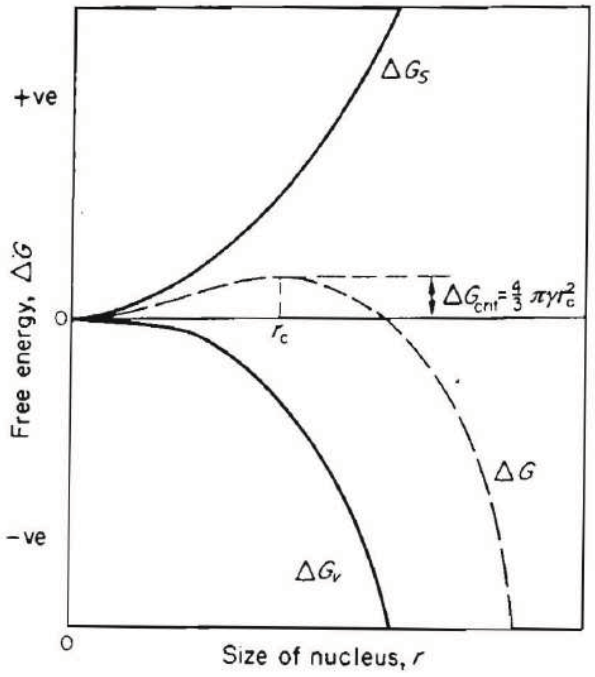

Figure 2-3 Free energy diagram for nucleation showing free energy versus cluster size (Mullin 1993).

From Figure 2-3 it can be seen that the free energy of formation goes through a maximum at some critical size, r_c, corresponding to the critical nucleus size which represents the minimum size of a stable nucleus. Clusters greater than this critical size, result in a decrease in free energy and results in viable nucleus thus contributing to the nucleation process while the growth clusters with a size smaller than the radius, r_c, to grow requires an increase in free energy. The maximum value, ΔG_{crit}, corresponds to the critical nucleus, r_c, and for a spherical cluster it can be obtained by maximising Equation 2-6, setting $d\Delta G/dr = 0$.

$$\frac{d\Delta G}{dr} = 8\pi r\gamma + 4\pi r^2 \Delta G_v = 0 \tag{2-7}$$

therefore

$$r_c = \frac{-2\gamma}{\Delta G_v} \tag{2-8}$$

where ΔG_v is a negative quantity. From Equation 2-6 and 2-8 we get

$$\Delta G_{crit} = \frac{16\pi\gamma^3}{3(\Delta G_v)^2} = \frac{4\pi\gamma r_c^2}{3} \tag{2-9}$$

The growth of the clusters is governed by the Gibbs-Thomson equation

$$\ln\frac{c}{c^*} = \ln S = \frac{2\gamma v}{kTr} \tag{2-10}$$

where v is the molecular volume

Substituting for r_c in equation 2-9 from equation 2-10 we get

$$\Delta G_{crit} = \frac{16\pi\gamma^3 v^2}{3(kT\ln S)^2} \tag{2-11}$$

The nucleation rate can now be obtained from equation 2-4

$$J = A\exp\left[\frac{-16\pi\gamma^3 v^2}{3k^3T^3(\ln S)^2}\right] \tag{2-12}$$

This equation indicates that three main variables govern the rate of nucleation: temperature, T, degree of supersaturation, S, and interfacial tension, γ. The difficulty with this equation is that it predicts nucleation only at extremely high supersaturations, far in excess of supersaturation levels observed in most inorganic crystallisation schemes.

2.4.1.2 *Heterogeneous nucleation*

As mentioned previously homogeneous nucleation is thought to occur quite rarely in real life situations since the presence of foreign particles may catalyse the nucleation process by reducing the energy barrier to nucleation, so that nucleation takes place at much lower supersaturation than those required for homogeneous nucleation (Brecevic & Kralj 2000; Hartel 2001). Thus the overall free energy change associated with the formation of a critical nucleus under heterogeneous conditions must be less than the corresponding free energy change associated with homogeneous nucleation (Brecevic & Kralj 2000). The decrease in free energy depends on the contact (or wetting) angle of the solid phase between the crystalline deposit and the foreign solid surface.

$$\Delta G_{\text{hom}} = \phi\Delta G_{het} \tag{2-13}$$

$$\phi = \frac{(2+\cos\theta)(1-\cos\theta)^2}{4} \tag{2-14}$$

where ΔG_{hom} is the Gibbs free energy for homogeneous nucleation, ΔG_{het} is the Gibbs free energy for heterogeneous nucleation, the factor ϕ is less than unity, the angle θ corresponds to the angle of wetting in liquid-solid systems (angle of contact between the crystalline deposit and the foreign solid surface).

In the case of $\theta = 180^o$ i.e when there is no wetting, the Gibbs energies for heterogeneous and for homogeneous nucleation are equal. When θ is between 0 and 180^o, i.e partial wetting of a solid with a liquid, the overall excess free energy

required is less than that for homogeneous nucleation so nucleation is easier to achieve. When $\theta = 0^o$ i.e complete wetting, the energy required for homogeneous nucleation is zero which means that spontaneous nucleation could take place. However, no such systems exist in practice (Mullin 1993; Myerson 1993).

2.4.2 Secondary nucleation

Secondary nucleation results when crystals of the solute are already present or deliberately added to a supersaturated solution. These crystals have a catalysing effect on the nucleation phenomena, and thus, nucleation occurs at lower supersaturation than needed for spontaneous nucleation (Myerson 1993). There are several possible mechanisms for the formation of secondary nuclei as shown in Figure 2-2 and described in the following paragraphs below, with contact nucleation the most common mechanism.

In initial or dust breeding, secondary nuclei originate from the seed crystals. The surface of the seed crystals are covered with tiny crystallites which are formed during drying of the adhering mother liquor after their preparation, or due to fragmentation during storage. When the crystals are introduced into the supersaturated solution, the adhering tiny crystallites are freed and can act as nucleation sites. This would only occur if the seeds were dry and were directly introduced into the crystalliser. Since these crystallites are usually much larger than the critical nucleus size, and as a result, the rate of nucleation is independent of the supersaturation of the solution or the stirring rate. In practice, this nucleation mechanism is important only in batch crystallisation. However, it is important to minimise the effect by pre-treating the seed crystals by submerging them in a solvent or in an unsaturated solution (Myerson 1993; J. Nyvlt et al. 1985).

Dendritic or needle breeding occurs at high levels of supersaturations resulting in needle like or dendritic growth on crystals. These crystals fragment in the solution and serve as nucleation sites (Myerson 1993; Randolph & Larson 1988). This phenomenon can be reduced by reducing the agitation and suspension density, reducing the supersaturation or using an appropriate additive to change the crystal habit or tendency to form dendrites (Randolph & Larson 1988).

Polycrystalline breeding occurs at higher levels of supersaturations than dendritic or needle breeding so the crystals do not grow regularly, but form irregular polycrystalline aggregates. Fragmentation of these aggregates which occurs especially at lower supersaturation or on mechanical abrasion, can serve as nucleation centres. Nucleation by this mechanism is not considered very likely in industrial crystallisation (Myerson 1993; J. Nyvlt et al. 1985).

Macroabrasion, collision or attrition breeding occurs in systems where the suspensions are subjected to intense stirring, violent agitation or high velocity pumping and from crystal-crystal interaction at high suspension densities. Macroabrasion of the crystals results in fragments that serve as nucleation sites. This phenomenon results in the rounding of edges and corners of crystals. The rate of nucleation by this mechanism is a function of the crystal hardness, the concentration of the suspension, and the retention time. This mechanism can also be obscured by other mechanisms of secondary nucleation. This phenomenon can be reduced by reducing the agitation or pumping, by reducing the suspension density, or by using soft linings and coverings on the crystalliser walls and impellers (Myerson 1993; J. Nyvlt et al. 1985; Randolph & Larson 1988).

Nucleation by fluid shear results when the fluid velocity relative to the crystal velocity is large and some of the “adsorbed layer” is removed (Randolph & Larson 1988). The adsorbed layer being entirely solute, will nucleate if the clusters are sufficiently large.

In contact nucleation nuclei are generated when crystals contact other crystals, crystalliser walls, pump, flow lines, or the stirrer in an agitated tank. Secondary nuclei are generated either by microabrasion with the major production of nuclei from the displacement of the adsorbed layer of the solute that has not yet crystallised (Myerson 1993; Randolph & Larson 1988).

2.5 CRYSTAL GROWTH

Crystal growth involves diffusion controlled (steps 1 and 2) and integration controlled (step 3) processes, which may be considered to occur in the following stages:

1. Volume diffusion of molecules from the bulk of the mother phase to the surface

2. Surface diffusion of the molecules from the surface of the crystal towards a step

3. Incorporation of the molecules absorbed onto the step to the kink site

These diffusional processes are illustrated in Figure 2-4 where it can also be observed that there are three types of sites; kink, step and terrace sites, on the crystal surface that the molecules or growth units can attach to. When crystal growth occurs very slowly the kink site is more energetically favourable compared to the other sites. As growth rate increases, the growth units fit into less energetically favourable sites and the crystal typically grows imperfectly. Thus, slow growth generally leads to perfect crystals, while fast growth leads to crystals with many more imperfections (Hartel 2001; Mullin 1993; Myerson 1993; J. Nyvlt et al. 1985).

One or more of the above stages may control the growth rate, with the slowest stage always being the rate determining step. If the rate of crystal growth is limited by the rate of diffusion through a laminar layer of solution, growth will be diffusion controlled, as is the case in many non agitated systems (Myerson 1993; Randolph & Larson 1988). As the relative crystal-solution velocity is increased the crystal growth rate increases because the stationary diffusion field around the particles are disturbed, thus supplying the solution of higher concentrations closer to its surface (Brecevic & Kralj 2000). When a further increase in velocity no longer increases growth rate, growth is surface integration controlled (Randolph & Larson 1988).

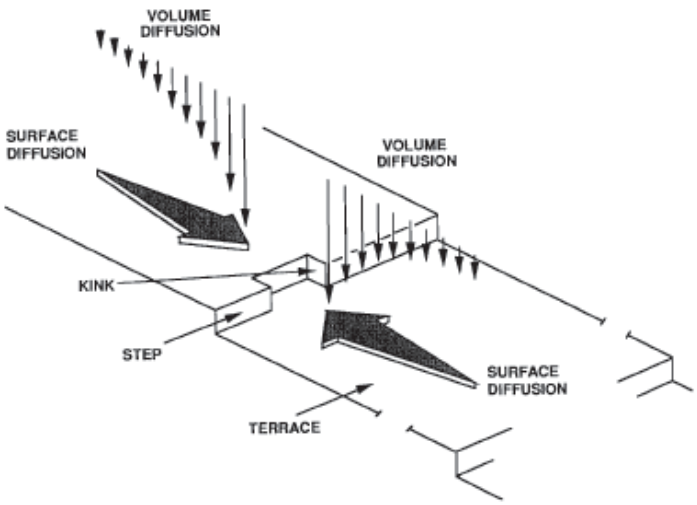

Figure 2-4 Diffusional processes affecting crystal growth (Myerson 1993)

2.5.1 Crystal growth mechanisms

The following section will discuss the three main types of crystal growth mechanisms which are: two dimensional nucleation, Burton-Cabrera-Frank (BCF) surface diffusion model and the diffusion layer model.

2.5.1.1 *Two dimensional growth theories*

For ideal surfaces that are not disarranged eg. by dislocations, a two-dimensional nucleus is needed for the formation of a new lattice plane. Nuclei are formed by the collisions of molecules in the adsorption layer which form clusters. After the critical size of nuclei is attained, growth occurs through further collisions. In general a high degree of local supersaturation is necessary for two-dimensional nucleation to occur.

Basically there are three types of models that exist, mononuclear growth, polynuclear growth and the "Birth and Spread" model, which differ in the concepts of growth of nuclei.

In mononuclear growth, once a surface nuclei is formed it spreads across the surface at infinite velocity ($V = \infty$) with no other nuclei forming until the surface layer is completed. In this model the rate determining step is the formation of surface nuclei, with the growth rate of the crystal expressed as:

$$G = hAI \tag{2-15}$$

or substituting for I

$$G = C_1 hA[\ln(S)]^{1/2} \exp[-C_2 / T^2 \ln(S)] \tag{2-16}$$

where G is the linear growth rate, h is the step height, A is the surface area of the crystal, I is the two-dimensional nucleation rate, C_1 and C_2 are empirical parameters obtained from experimental data, and T is the temperature in Kelvin.

From Equation 2-15 it can be seen that the crystal growth rate of a face is directly proportional to the area of that face, indicating that large faces grow faster than small faces, which is not the case since the fastest growing faces on a crystal have the smallest areas and vice versa. Therefore the mononuclear model is not a useful model (Myerson 1993).

In polynuclear growth, growth does not occur after formation of the critical nucleus, the growth rate of the nuclei is zero (V = 0). However, an infinite number of nuclei can form on the surface until the whole surface is covered. The growth rate can be expressed as follows:

$$G = I\pi r_c^2 h \tag{2-17}$$

or

$$G = \left(C_3 / T^2 [\ln(S)]^{3/2}\right) \exp[-C_2 / T^2 \ln(S)] \tag{2-18}$$

where r_c is the radius of a critical cluster and C_2 and C_3 are empirical parameters obtained from experimental data.

This model predicts that the growth rate will increase with increasing nucleation rate, however, the growth rate will decline with decreasing critical nucleus size. The model also predicts that growth rate should display a maximum in G at some supersaturation, that will decline if the supersaturation is increasing or decreasing which seems unlikely and has not been observed (Myerson 1993).

The Birth and Spread model allows spreading of the nuclei at a finite constant rate anywhere on the surface of the crystal, including incomplete layers or on top of an earlier nucleus that is now growing and it also assumes that there is no intergrowth between the nuclei. Figure 2-5 shows the schematic of the development of polycrystalline growth by this model. The growth rate expression for this model as derived by Ohara and Reid (Ohara & Reid 1973) can be expressed as:

$$R = C_4 (S-1)^{2/3} [\ln(S)]^{1/6} \exp\left[-C_5 / T^2 \ln(S)\right] \tag{2-19}$$

where C_4 and C_5 are empirical parameters obtained from experimental data.

This model predicts that the growth rate G increases with increasing superaturation and increasing temperature. It is the only model that allows a growth order of g>2.

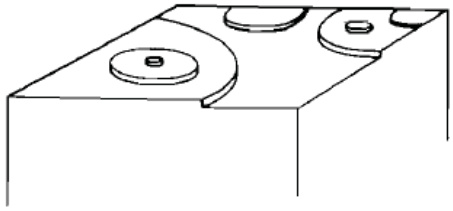

Figure 2-5 Development of polycrystalline growth by the birth and spread mechanism (Mullin 1993).

2.5.1.2 *Burton-Cabrera-Frank (BCF) surface diffusion model*

Since growth is observed at low supersaturation where two-dimensional nuclei are not yet generated, another permanent step source has to exist. The emergence of screw dislocations on a crystal face, results in regenerating spiral dislocations which provide continual kink sites for incorporation of growth units in the lattice. A completely smooth surface never appears under conditions of spiral growth, so surface nucleation is not necessary, and the crystal grows as if the surface was covered with kinks. After a layer is completed, the dislocation is still present. The rate of growth is then limited by surface diffusion of the growth units to the regenerating spiral dislocation (Hartel 2001; Mullin 1993; Myerson 1993). A simple example of growth by screw dislocation is shown in Figure 2-6.

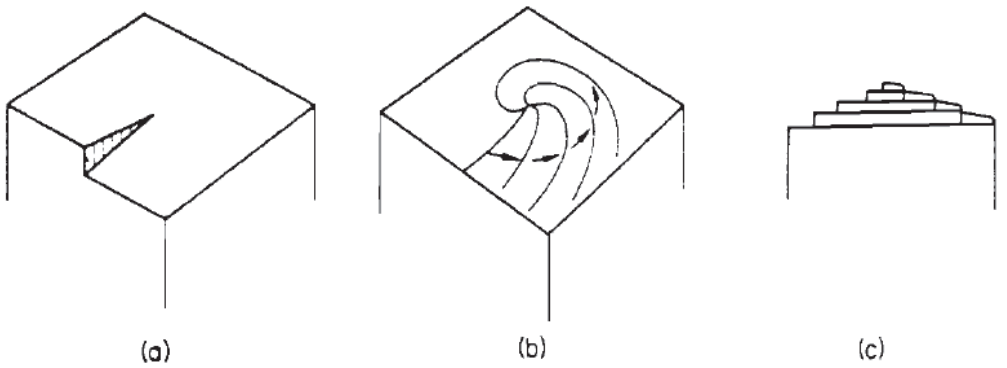

Figure 2-6 Development of a growth spiral from a screw dislocation (Myerson 1993)

A kinetic theory of growth was developed by Burton, Cabrera and Frank (Burton et al. 1951) in which the curvature of the spiral near its origin was related to the spacing of successive turns and the level of supersaturation. By the application of Boltzmann statistics they predicted kink populations, and assumed that surface diffusion was an essential step, and were able to calculate the growth rate at any supersaturation (Mullin 1993).

The BCF relationship may be expressed as:

$$R = A\sigma^2 \tanh\left(B/\sigma\right) \tag{2-20}$$

where R is the crystal growth rate, σ is the absolute or relative supersaturation and A and B are complex temperature-dependent constants which include parameters depending on step spacings.

At low supersaturations the BCF equation approximates that growth is proportional to the square of supersaturation, whereas at higher supersaturation, growth increases linearly with supersaturation. Therefore it changes from a parabolic to a linear growth law as the supersaturation increases.

2.5.1.3 *The diffusion layer model*

Generally this model is used in correlating data for industrial crystallisation processes. This model focuses on the diffusion of solute through the boundary layer

for incorporation into the crystal. Noyes and Whitney (Noyes & Whitney 1897) proposed an equation for crystallisation based on the assumption that crystallisation was the reverse of dissolution, and the rates of both processes were governed by the difference between concentration at the crystal surface and in the bulk of the solution:

$$\frac{dm}{dt} = k_m A(c - c^*) \tag{2-21}$$

where m is the mass of deposited solute in time t, A is the surface area of the crystal, c is the solute concentration in the solution, c* is the equilibrium saturation and k_m is the coefficient of mass transfer.

Equation 2-21 was modified by Nernst (Nernst 1904) on the assumption that there would be a thin stagnant film of liquid adjacent to the growing crystal surface, through which molecules of the solute would have to diffuse:

$$\frac{dm}{dt} = \frac{D}{\delta} A(c - c^*) \tag{2-22}$$

where D is the coefficient of diffusion of the solute and δ is the length of the diffusion path.

The thickness δ of the stagnant film depends on the degree of agitation of the system, which implies an almost infinite rate of growth in agitated systems, which does not occur experimentally. Therefore the concept of film diffusion alone is not sufficient to explain the mechanism of crystal growth. Furthermore, crystallisation is not the reverse of dissolution.

Further modification was made to the diffusion theory by Berthoud (Berthoud 1912) and Valeton (Valeton 1924), who proposed that there were two steps in the mass deposition via a diffusion process, whereby solute molecules are transported from the bulk of the solution to the crystal surface, followed by a first-order reaction where the solute molecules arrange themselves into the crystal lattice, which can be represented by the following equations:

$$\frac{dm}{dt} = k_d A(c - c_i) \quad \text{(diffusion)} \tag{2-23}$$

$$\frac{dm}{dt} = k_r A(c_i - c^*) \quad \text{(reaction)} \tag{2-24}$$

where k_d is the coefficient of mass transfer by diffusion, k_r is the rate constant for the surface reaction (integration) process, and c_i is the solute concentration in the solution at the crystal-solution interface.

Figure 2-7 shows a schematic representation of the concentration profile near a growing crystal surface. The region in which the concentration is changing from the bulk solution C to that at the surface of the crystal C* is termed the concentration boundary layer.

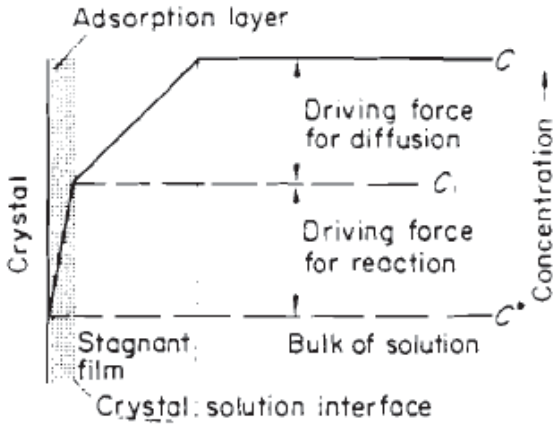

Figure 2-7 Concentration driving forces in crystallisation from solution (Mullin 1993)

The interfacial concentration c_i is difficult to measure, so the term is eliminated from equations 2-23 and 2-24 by considering an 'overall' concentration driving force , c – c* which is quite easily measured. A general equation for crystallisation based on the overall driving force can then be expressed as:

$$\frac{dm}{dt} = K_G A(c - c^*)^g \tag{2-25}$$

where K_G is the overall crystal growth coefficient and the exponent g is the 'order' of the overall crystal growth process and in general is in the range $1 \leq g \leq 2$, and only for less soluble compounds $g > 2$.

If g = 1 and the surface reaction (equation 2-24) is also first-order, the interfacial concentration, ci, may be eliminated from equation 2-23 and 2-24 to give:

$$\frac{1}{K_G} = \frac{1}{k_d} + \frac{1}{k_r} \tag{2-26}$$

If $k_d \leq k_r$ for cases of extremely rapid reaction, $K_G \sim k_d$, and the crystal growth rate will be diffusion controlled. Similarly, if $k_r \leq k_d$ the diffusional resistance is low, $K_G \sim k_r$, and the crystal growth rate will be controlled by the rate of solute incorporation into the crystal.

2.5.2 Crystal growth kinetics

Two basic expressions are used to express the relationship between supersaturation and crystal growth, which are:

$$G = k_g \sigma^g \tag{2-27}$$

$$R_G = K_g \sigma^g \tag{2-28}$$

where G is the linear growth rate of a face, k_g and K_g are temperature dependent constants and R_G is the increase of mass per unit time per unit surface area.

Equation 2-27 employs a linear crystal growth velocity (length/time) while equation 2-28 employs a mass rate of crystal growth (mass/area time).

The constants k_g and K_g are temperature dependent and are usually fit to the Arrhenius equation, to give a general expression for growth rate as a function of temperature, giving the following expression:

$$k_g = k_0 \exp - \left(\frac{E}{RT} \right) \tag{2-29}$$

where k_0 is a constant and E is the activation energy in J/mol. The activation energy can be used to obtain information on whether the rate constant step is diffusion or surface integration controlled. Activation energies for surface integration are typically of the order 40 to 60 kJ/mol, while activation energies for diffusion are usually in the order of 10 to 20 kJ/mol (Mullin 1993).

A crystal growth expression that includes both the effect of temperature and supersaturation on the growth rate can therefore be expressed as:

$$G = k_0 \exp\left(-\frac{E}{RT}\right)\sigma^g \tag{2-30}$$

The value of the exponent g is used for the evaluation of the crystal growth mechanism or limiting step of the process. When diffusion from bulk solution to crystal surface is the limiting step, g is expected to be equal to unity. Higher g values point towards surface integration as the rate controlling step, for spiral growth, a value ≤2 is to be expected while a value >2 indicates growth via two-dimensional nuclei (Rolfs et al. 1997). Crystal growth rates are normally diffusion controlled at high temperatures and surface integration controlled at low temperatures (Mullin 1993).

2.5.3 Size-dependent growth and growth rate dispersion

McCabe (McCabe 1929) first proposed a model to explain the relationship between crystal size and growth rate which states that crystals that are geometrically similar and subjected to identical growth environments (temperature, supersaturation, hydrodynamics etc) grow at the same rate. This model was based on the assumption that the growth rate is independent of crystal size if all the crystals are subjected to the same environmental conditions (Mullin 1993). However, this model fails to explain the different growth rates observed for smaller and larger crystals.

A second model is called size dependent growth which states that larger crystals have higher growth rates than smaller crystals. For crystals in the size range between 200μm to 2mm this effect is closely linked to solution velocity; larger particles have higher terminal velocities than those of small particles and, in cases where diffusion

plays a dominant role in the growth process, the larger the crystals the higher their growth rate. For crystals smaller than about 10μm because of their very small terminal velocity, and size smaller than that of turbulent eddies, they may be growing in a virtually stagnant medium even in a well agitated medium. For crystal sizes smaller than a few micrometers the effect of crystal size is due to the Gibbs-Thomson effect, where crystals of near-nucleic size may grow at extremely slow rates because of the lower supersaturation they experience owing to their higher solubility in comparison to the larger particles (Mullin 1993). The behaviour of these very small crystals considerably influences the performance of continuously operated industrial crystallisers because new crystals are constantly being generated by secondary nucleation in the 1 to 10μm size range which subsequently grow to populate the full crystal size distribution (Pamplin 1980). For larger crystals as they increase in size their total surface area increases, as does the possibility of the occurrence of dislocations on the surface due to mechanical stresses, incorporation of impurity species into the lattice, etc. In addition, the more energetically they will collide in agitated suspensions and the greater is the potential for surface damage, with both of these effects favouring faster surface integration kinetics thus leading to higher growth rates with increasing crystal size (Mullin 1993). If the crystals grow by a BCF type mechanism the larger crystals will likely grow faster than the smaller crystals (Myerson 1993).

While size-dependent growth does occur, studies have shown that in many instances what had been attributed to size dependent growth was due to another phenomenon, known as growth rate dispersion (GRD) where crystals of the same size exposed to identical conditions do not necessarily grow at the same rate. This is not the same as size-dependent growth in which crystals of different sizes display differences in growth rate. White and Wright (White & Wright 1971) first used this term to explain the widening of an initially narrow sized distribution of sucrose crystals in a batch crystalliser. They observed that the standard deviation of an initially narrow sized distribution of crystals increased as time progressed which meant that crystals in their crystalliser were not growing at the same rate.

Studies of GRD have resulted in two distinctly different mechanisms being proposed. In one mechanism termed the constant crystal growth (CCG) model, it is assumed that crystals have a distribution of growth rates but each individual crystal grows at a constant rate. This implies that nuclei are born with a distribution of growth rates and the observation of two nuclei in a crystalliser at steady-state conditions will reveal each nuclei growing at a constant but different rate. The second mechanism termed the random fluctuation (RF) model says that while all crystals have the time-averaged growth rate, the growth rates of individual crystals can fluctuate significantly with time. This mechanism implies that the observation of two different crystals growing under identical conditions might be different at any time that the time-averaged growth rate over a long period of time would be identical (Myerson 1993).

GRD stems mainly from different interferences with the surface integration kinetics on different crystals (Mullin 1993). The primary cause of the observed phenomena is thought to be the surface integration step of the BCF theory of crystal growth. The BCF theory indicates that the growth rate of a crystal is dependent on screw dislocations present on the surface of a growing crystal. Changes in the location or density of screw dislocations can cause large changes in the crystal growth rate (Myerson 1993). For instance crystals with many dislocations grow more rapidly than crystals with fewer dislocations (Bhat et al. 1987). Collisions of the crystals with the impeller, walls, and each other can result in damage to the dislocations and therefore changes in the crystal growth rate, which is especially true with secondary nuclei that could display very different dislocation densities. In addition, the imperfect nature of the crystal growth process could lead to changes in the dislocations of the crystal faces (Myerson 1993). Three other possible mechanisms may lead to GRD (1) differences in surface microstructure due to physical effects (eg roughening), (2) difference in surface coverage of some foreign impurity, and (3) incorporation of a foreign impurity into the lattice to different extent (Hartel 2001).

GRD and size-dependent growth both affect the crystal size distribution obtained from laboratory and industrial crystallisers and therefore must be taken into account when analysing the modelling crystallisation processes (Myerson 1993).

2.5.3.1 *Growth rate dispersion in sodium nitrate*

Jones and Larson (Jones & Larson 1999) characterised the GRD of sodium nitrate secondary nuclei produced as a function of the nucleation and growing supersaturation in a growth cell similar to that developed and used by Garside and Larson (Garside & Larson 1978). They characterised the GRD by analysing the mean, spread and shape of the growth rate distribution. They observed that the average growth rates of secondary nuclei are dislocation controlled at low growing supersaturations and strain controlled at high growing supersaturations, where increasing the nucleation supersaturation causes an increase in both dislocation density and strain. Increasing strain by itself will decrease growth rates, while increasing dislocation density by itself will increase growth rates.

2.5.4 Crystal growth of sodium nitrate

2.5.4.1 *Crystals grown from the melt*

Crystals of sodium nitrate have been grown from the melt by the modified Kyropulos technique using small plates of single crystal mica as seeds (Komnik & Startsev 1969), using a fused quartz or Pyrex ampoule (Sawada & Shichiri 1984), the method of lowering a crucible using epitaxial growth of sodium nitrate on mica (Eckstein et al. 1967), the travelling solvent zone method (Gopalakrishnan, Arivuoli & Ramasamy 1991), zone refining system (Phor et al. 1990), Czochralski method of crystal pulling and the Bridgman technique (Anuradha et al. 1982) and epitaxially on thin mica sheets (Anuradha, Murthy & Raju 1982; West 1945). However, growth of good quality sodium nitrate single crystals is difficult to achieve due to its pronounced anisotropy of thermal conductivity, being a maximum in the direction of the <111> optical axis. The maximum rate of growth proceeds in this direction when crystals are grown from the melt. If the direction of growth does not coincide with the <111> direction, the crystals grow in blocks (Komnik & Startsev 1969). The crystals also exhibit anomalous change of thermal expansion near 275^{o}C, where the phase transition of the second type takes place (Kracek 1931) which further leads to thermal stresses in the blocked single crystals on cooling.

Crystals grown from solution are preferred over growth from the melt since the crystals are merely perfect containing few dislocations, no mosaic structure or small-angle boundaries and the crystals have a better optical quality. However, their preparation is lengthy and their size is not sufficient. Crystals grown from the melt are grown much quicker and larger, however their quality is insufficient, thermal decomposition of $NaNO_3$ to $NaNO_2$ can occur and it is difficult to cool the crystals from melting point down to room temperature without cracking (Eckstein et al. 1967). Therefore in this work crystals of sodium nitrate were grown from solution.

2.5.4.2 *Crystal growth rate studies from aqueous solution*

Crystal growth studies of sodium nitrate grown from aqueous solution have been carried out using a stirred batch crystalliser (Graber et al. 1999), fluidised bed (J. Nyvlt et al. 1985), by solvent evaporation (Ristic et al. 1997) and in a batch cell (Jones & Larson 19992000; Jones et al. 2000; Ristic, Shekunov & Sherwood 1997). Studies have mainly focused on the influence of tensile strain, supersaturation and dislocation on the growth rate of sodium nitrate because sodium nitrate is a very ductile substance deforming plastically under high levels of strain, with these plastic deformations acting as new growth sources in a crystal, resulting in increased growth rates (Jones & Larson 2000). In the literature no data exists for growth rates of sodium nitrate crystals formed by homogeneous nucleation.

Crystal growth rates of sodium nitrate have been determined at low relative supersaturations by Jones *et al* (Jones et al. 2000) and they observed that the effect of integral strain on sodium nitrate secondary nuclei is more pronounced at high levels of growing supersaturations (3.4%) than it is at low levels (0.32%). At low levels of relative supersaturations, $0.04<\sigma<0.45\%$ the growth rates of sodium nitrate crystals are controlled by a dislocation mechanism while at $\sigma < 0.02\%$ the growth rate was extremely low and it was suspected that a 2D nucleation growth mechanism was taking place. This correlates well with the results of Jones and Larson (Jones & Larson 1999) where they observed that the average growth rates of secondary nuclei are strain controlled at high growing supersaturation and dislocation controlled at low growing supersaturation.

Jones and Larson (Jones & Larson 2000) derived a model, an extension of the BCF model, based on the premise that crystals were growing via a screw dislocation mechanism. They observed that the growth rates of sodium nitrate nuclei are time dependant, immediately following nucleation or following an increase in supersaturation. Sodium nitrate exhibits a decreasing growth rate immediately following nucleation, and following a step change increase in supersaturation, the growth rate increases initially and then gradually decreases to a constant level after 3 to 5 minutes, whereas more brittle materials such as potash alum and potassium sulphate secondary nuclei exhibits nearly constant growth rates with respect to time. From these results it can be inferred that sodium nitrate nuclei growth rates do not decrease because of decreasing supersaturation. The same results were observed by Jones and Larson (Jones & Larson 1999) and they concluded that the growth rate decelerated as time progressed as a result of the high ductility of the sodium nitrate crystals.

Graber *et al* (Graber et al. 1999) reported kinetic growth order and activation energy values of 1 and 23,424 J/mol, respectively, using a perfectly stirred batch crystalliser in a temperature range from 10^{o}C to 40^{o}C, with a cooling rate from 1 to 35^{o}C/h and a constant agitation of 500rpm and concluded that growth was diffusion controlled. Nyvlt *et al* (J. Nyvlt et al. 1985) reported crystal growth rates using a fluidised bed at 30^{o}C with relative supersaturations of 0.01 and 0.05 and crystal seed size between 1 and 1.25mm, in the range of 1.61 and 8.05 x 10^{-7} m/s, respectively and a kinetic growth order of 1.

2.6 ADDITIVES

During the crystallisation process the presence of small amounts of impurities can strongly affect crystallisation parameters such as nucleation, growth, crystal habit, agglomeration, polymorphic transitions, size distribution, induction period and many other properties of the system and the solid phase. The most discernable influence is on the growth rate of soluble salts and on the crystal habit (Sarig 1994). Some impurities can suppress, decelerate or enhance growth, while others may exert a

highly selective effect on certain crystallographic faces, thus modifying the crystal habit and changing the relative growth rates of the different crystal faces (Mullin 1993).

Impurities can be defined as any foreign substances other than the material being crystallised, so even the solvent from which the crystals are grown from is considered an impurity (Mullin 1993), unintentionally present in the solution at low concentration (normally below one percent concentration (Sarig 1994)), originating from various sources such as raw materials, from dissociation and other reactions, from corrosion of the equipment etc. If the impurity is intentionally added to the system in order to modify its crystallisation properties, it is called an additive. When the impurity is added in relatively large amounts (up to several percent) the impurities and additives are collectively known as admixtures (Brecevic & Kralj 2000; Mullin 1993; J Nyvlt & Ulrich 1995). Mostly the aim of crystallisation under the influence of additives is to change the habit of the crystal without the additive molecules being incorporated whilst using a minimum amount of the additive (Kipp et al. 1997).

There is no consistent theory available to explain the influence of admixtures on the crystallisation process. In general there are two main mechanisms (Brecevic & Kralj 2000; Hartel 2001; Mullin 1993) by which impurities can affect or influence crystal growth which is:

1. The incorporation of the impurity into the crystal lattice, especially if there is some degree of lattice similarity, which may then disrupt further addition of the lattice structure of the crystallising species as well as causing a reduction of the overall crystal growth rate. This group of impurities primarily refers to inorganic ions and metal complexes, which exert an influence due to the electrostatic interactions between the crystal ions and the impurity species, some of which may easily enter the crystal lattice and substitute for the constituent ions (Brecevic & Kralj 2000).

2. Adsorption of the impurity onto the growing crystal surface which influences the integration of growth units, with the impurity hindering further

incorporation of molecules of the crystallising species since the impurity molecule has to be displaced before surface incorporation can occur. This affects the rate of growth of a particular face or all of the faces present in the growing crystal thus the adsorption of impurities may cause a change in the crystal morphology. This group of impurities refers to substances such as polyelectrolytes, multifunctional long-chained molecules, and small organic compounds which exert an influence based on the formation of bonds between the functional groups or negatively charged ligands and the cations at the crystal surface (Brecevic & Kralj 2000).

Impurities can also change the properties of the solution or the equilibrium saturation concentration as the impurity can influence either solubility or melting point, which can affect the driving force for crystallisation, which will hence effect the supersaturation and growth rate (Hartel 2001; Mullin 1993; Randolph & Larson 1988).

The adsorption of impurities and their specific effect on growth processes can be explained by the Kossel model. Utilising the Kossel model there are three sites where the impurity species may become adsorbed and disrupt the flow of growth layers across the face viz at a kink, at a step or on a terrace (see Figure 2-4). For kink site adsorption growth retardation is affected at very low impurity levels in the solution, more impurity is needed for step site adsorption to occur while much higher levels of impurity are required if adsorption occurs on the terrace surface (Mullin 1993). Kink sites are the most probable position for solute integration because the highest bonding energy associated with integration occurs here, while flat surfaces are the least energetically probable sites for incorporation (Lacmann et al. 1999; J Nyvlt & Ulrich 1995).

Impurities can be classified as (1) completely “immobile” and refers to impurities which adsorb and remain fixed at the site where they first reached the crystal surface and they also form strong bonds on the surface (Myerson) since they are chemically bonded (J. Nyvlt et al. 1985); and (2) completely “mobile” impurities which refers to impurities that can choose to adsorb at steps, kinks, or terraces at the crystal-solution interface and then diffuse “two-dimensionally” on the surface as they form relatively

weak bonds since they are physically adsorbed and are swept away in the advance of steps and have a much smaller effect on the reduction in growth rate. Overall strong adsorbing impurities are more likely to cause noticeable changes in the crystallisation behaviour than weakly interacting ones (Myerson 1993).

Additives employed for aqueous solutions can be subdivided into several groups:

a) Free acids and/or bases

b) Inorganic additives; and

c) Organic additives

In free acids and/ or bases the pH value of the solution is adjusted with the acids or bases most commonly used usually having a common ion with the crystallising substance. The pH modifies the nature and the concentration of ions in solution, particularly when the latter contains salts of weak acids or bases (J Nyvlt & Ulrich 1995). pH can also influence the rate of crystal growth (Ruiz-Agudo et al. 2008) and influence the morphology and structure of the crystal (Colfen & Qi 2001; Prymak et al. 2006).

Inorganic additives that are used include the highly active polyvalent cations such as Fe^{3+}, Cr^{3+}, Al^{3+}, Cd^{2+} and Pb^{2+}, with the higher the charge on the cation the more powerful the inhibiting effect (Mullin 1993), as well as anions like WO_4^{2-}, MoO_4^{2-}, PO_4^{3-}. Very low concentrations (0.001 to 0.1 wt %) of these additives are sufficient to exhibit a dramatic effect on crystallisation, with much higher concentrations (1-10 wt %) required in order to obtain a similar effect when less active additives are used (J Nyvlt & Ulrich 1995). The presence of trace amounts of inorganic cations can also exert an influence on the crystal habit of inorganic salts. For instance some cations act by simple substitution in the lattice as a result of similar ionic radii and charge eg. Cd^{2+} for Ca^{2+} in calcium salts or Ca^{2+} for Mg^{2+} in magnesium salts. Trivalent cations, particularly Cr^{3+} and Fe^{3+} , have a powerful effect on the morphology of salts such as ammonium and potassium dihydrogenphosphates, while complex cations like $Fe(CN)_6^{4-}$ at concentrations of less than 1ppm, modifies the crystal habit of NaCl from cubic crystals to hard dendrites (Mullin 1993). The chromium (III) impurity has

also been reported to suppress the growth rates of several inorganic salts in aqueous solution (Mullin & Davey 1974), cause unsteady growth behaviour (Guzman et al. 1997) and growth hysteresis (Kubota et al. 1988).

Surface active substances (surfactants) and organic dyestuffs are the most frequently used organic additives. They exhibit a strong effect on the growth rate of inorganic crystals since their large molecules are attached to the crystal surface through their polar or hydrocarbon portions which prevents the access of the macrocomponent molecules to the crystal surface (J. Nyvlt et al. 1985; J Nyvlt & Ulrich 1995). The effect of large organic molecules is usually not specific to that molecule, because a substance can modify the growth of several macrocomponents and a similar modification can be obtained using very different organic additives. This property can be attributed to the fact that large organic molecules can be adsorbed at any site on the crystal surface so that their size is a deciding feature (J Nyvlt & Ulrich 1995). Organic dyes have been used for crystallisation kinetics (Rauls et al. 2000), growth kinetics (Kuznetsov et al. 1998), growth rate studies (Girolami & Rousseau 1985; Kipp, Lacmann & Rolfs 1997; Kuznetsov, Okhrimenko & Rak 1998; Maeda et al. 2004; Mauri & Moret 2000; Rousseau et al. 1976), surface characterisation studies (Maeda et al. 2004; Mauri & Moret 2000) and have been used to colour potassium dihydrogen phosphate (KDP) crystals (Hirota et al. 2002; Kahr et al. 1994; Maeda et al. 2004; Rifani et al. 1995).

Many dyestuffs also act as powerful habit modifiers for inorganic salts (Hirota et al. 2002; Kipp, Lacmann & Rolfs 1997; Kumaresan et al. 2008b). However, these additives do not nowadays find any significant industrial application (Mullin 1993). Surface-active agents are also frequently used to change crystal habits (Mahmoud et al. 2004; Michaels & Tausch Jr 1961; Usui 2009) since their molecular structure allows a lot of energetically favourable conformations, so that the kinetics of the precipitation process can be greatly influenced (Brecevic & Kralj 2000). Common anionic surfactants include the alkyl sulphates, alkane sulphonates and aryl alkyl sulphonates, while quaternary ammonium salts are frequently used as cationic agents and non-anionic surfactants are used as habit modifiers (Mullin 1993).

Polymeric substances such as polyvinyl alcohol, polyacrylates, polyglutamates, polystyrene sulphonates, and long chain proteinaceous materials like sodium carboxymethylcellulose, gelatin and phosphoproteins etc act as useful habit modifiers. As well as sodium triphosphate, sodium pyrophosphate, organic derivatives of phosphonic acid, low molecular weight organic acids and their derivatives (Mullin 1993).

2.6.1 Effects of additives on the growth rate and crystal habit modification of sodium nitrate

Sodium nitrate is a difficult crystal to modify (Buckley 1951). Researchers have mainly used dyes to investigate and study the effect of additives on the habit modification of sodium nitrate. Weinland and France (Weinland & France 1932) found that certain dyes such as quinoline yellow, diamine sky blue F.F., bismark brown and dye numbers 4 and 5 modified the sodium nitrate crystal habit by causing the appearance of triangular truncations or octahdedral facets replacing one or more corners of the crystal (i.e of the forms {111} and {11-1}). Butchart and Whetstone (Butchart & Whetstone 1949) found that in the change from the orthorhombic to trigonal system, the effectiveness of dyes such as amaranth in modifying crystal habit is apparently lost, and dyes such as induline, gallophenine and acid green GG extra were found effective in bringing about habit modification. Whetstone (Whetstone 1955a) studied the effect of selected orientations of sulphonate groups in azo-dye molecules containing naphthalene 3:6-disulphonate components on the crystal habit modifying power of sodium nitrate. Whetstone (Whetstone 1955b) also studied the effect of polar group orientation of the dye molecule with ionic sites of particular crystal planes on the crystal habit modification of sodium nitrate. Sodium nitrate has also been grown in the presence of nitric acid (Franke et al. 1981) and curved face growth of sodium nitrate crystals have been studied under the action of the $(NH_4)_2Mo_2O_7$ impurity (Punin & Franke 2004). Table 2-1 provides a summary of the admixtures that have been used in literature and their effect on sodium nitrate.

Table 2-1 Summary of the admixtures in literature that have been used in sodium nitrate crystal growth studies

Admixture	**Effect**	**Reference**
$CdCl_2$, surfactants	Ostwald ripening	(Winzer 1979)
Cr^{3+}	Nucleation	(Furves & Larson 1980)
Fe^{3+}	Distribution	(Iskhakova et al. 1979)
HNO_3, Na_2CO_3, NaCl, $NaNO_2$, Fe_2O_3	Crystal size, crystal habit	(Perelman & Strakhova 1938)
Pb^{2+}, Ca^{2+}	Nucleation, crystal growth	(*Czech Patent* 1964)
Solid impurities	Unfavourable	(J Nyvlt 1960)
Aniline sulphonate, Wool Scarlet, Chlorazol Sky Blue F.F, Acid Green GG extra, Soluble Blue, Induline, Gallophenine D	Crystal habit / 001/ faces on a rhombohedron	(Butchart & Whetstone 1949)
Quinoline yellow, Diamine Sky Blue F.F, Bismark Brown, France dye #4 and #5	Crystal habit	(Weinland & France 1932)
Laurylamino hydrochloride	Caking	(*Pol. Patent.* 1966)
$(NH_4)_2Mo_2O_7$	Curved face growth	(Punin & Franke 2004)
Surfactants	Hydrophobization	(Wolf & Holzweissig 1968)
Trisulphonated p-rosaniline, trisulphonated rosaniline and acid magenta N.D. m:m'-disulphonated Dobner's Violet, Ink Blue p:p':p"-trisulphonated triphenyl-rosaniline, m:m':p"-trisulphonated N:N'-dibenzyl methyl p-rosaniline, 1:4:5:8-tetramino-anthraquinone 2-sodium sulphonate m:m':p"-trisulphonated Dobner's Violet, 1-naphthylamine 3:6-disulph → 2-naphthol 4-sulph, 1-naphthylamine 3:6-disulph→ 1-naphthol 14-sulph, o-amino-p-sulphonic acid → m-phenylene-diamine, 2-napthylamine 6:8-disulph → salicylic acid, 2-napthylamine 5:7-disulph → 1-napthylamine 7 sulph → 2 naphthol 3:6 disulph, 2-napthylamine 5:7-disulph → 1-napthylamine → naphthol 3:6 disulph, 1 naphthylamine 3:6:8 –trisulph →1-napthylamine 7 sulph → 2-naphthol 3:6 disulph,1 naphthylamine 3:6:8 –trisulph →1-napthylamine →2 naphthol 3:6-disulph	Crystal habit - Strong modification / 001 face Crystal habit - Moderately strong modification / 001 face	(Whetstone 1955b)
5:7-disulpho β-naphthylamine → α- naphthylamine → 3:6-disulpho β -naphthol, 5:7-disulpho β -naphthylamine → 7-sulpho α -naphthylamine → 3:6-disulpho β -naphthylamine 5:7-disulpho β -naphthylamine → 7-sulpho α -naphthylamine → 3:6-disulpho β -naphthol	[0001] tablets [0001] tablets [0001] plates	(Whetstone 1955a)
Bismark Brown G, France Dye #4 and #5, France Dye: M- α- OH-3, France Dye: P- β- NH_2-5, France Dye: P- β- NH_2-(6 or 7), Quinoline Yellow, Sunset Yellow		(Kahr & Gurney 2001)
France Dye #4 and #5, Quinoline Yellow		(Kahr & Gurney 2001)

2.7 SOLVENTS

The selection of the solvent is of key importance in the design of crystallisation processes, as it determines the productivity and yield of the process. A poor initial choice of solvent can thermodynamically and kinetically limit the effectiveness of the separation, irrespective of all other factors, including crystalliser design and cost (Myerson 1993). The composition of the solvent also determines the solubility and thus influences the supersaturation, may influence the nucleation rate as well as the relative growth rate of each crystal face, may effect the size distribution of the entire crystallised mass, and may also influence aggregation/agglomeration properties (Granberg & Rasmuson 2005). The solvent can also influence crystal structure and can have a significant effect on crystal size, morphology, and purity by modifying solution properties (such as density, viscosity, and component diffusivities), as well as the structure of the crystal-liquid interface (Myerson 1993). The control of crystal habit is of particular importance for crystals produced in the pharmaceutical industry since crystal size and morphology affect the ease of separating, washing, drying, packaging, handling and storage (Karunanithi et al. 2009), as well as the efficacy and performance of the final solid dosage forms (Nie et al. 2007).

When selecting a solvent for crystallisation processes, an ideal solvent should (Mullin 1993; Myerson 1993; Pamplin 1980):

- Be miscible in all proportions with the solvent and the solute should be relatively insoluble in it and not chemically react with it
- Yield a prismatic habit in the crystal
- Have a high, positive, temperature coefficient of solute solubility
- Have low volatility to reduce the possibility of uncontrolled loss of solvent during lengthy periods of growth and from filters and other processing equipment which may be both costly and hazardous.

- Have a density less than that of the bulk solute and low viscosity since it is desirable that the growing crystal should not float and that is should be well agitated.
- Be as clean and pure as possible
- Be stable under operating conditions i.e it should not decompose nor oxidise

Other factors in selecting a solvent include product characteristics (eg. impurity level, crystal size, morphology, and product yield), health and safety (eg. solvent toxicity, inflammability, chemical reactivity, and environmental impact), and economics (eg. solvent cost, recycling and disposal) (Myerson 1993). However, some compromise must inevitably be made since several undesirable characteristics may have to be accepted to secure the aid of one important solvent property, or the cost of solvent recovery may override other considerations (Mullin 1993).

Based on the above points the solvents chosen in the solubility determinations for Chapter 3 were methanol, ethanol and isopropanol since these lower alcohols are miscible in water, volatile, has a lower density than sodium nitrate and water, and have boiling points around 20 to 35^{o}C less than water making them easily separable by distillation.

2.7.1 Effect of mixed solvents on the crystal morphology

The influence of solvent on the modification of crystal habit is well known and has been researched for many different types of systems. For example, succinic acid crystals grown from aqueous solutions are plate-like while those grown from isopropanol solution are needle-like (Davey et al. 1982). The habit of paracetamol changes from a rounded to a rectangular and flat shape with increasing water concentration in acetone-water mixtures (Granberg & Bloch 1999). In pure acetone and DMF, 11α-hydroxy-16α, 17α-epoxyprogesterone (HEP) crystallises as long prismatic crystals, while in pure chloroform it crystallises as blocks (Nie et al. 2007). The crystal shape of carbamazepine is micronised flaky or thin plate-like, whereas the crystals obtained from alcohol are polyhedral prismatic (Nokhodchi et al. 2005).

Unique crystal morphologies are obtained of hydrophobic calcium carbonate crystals grown in a mixture of water and tetrahydrofuran (THF) (Keum et al. 2003). The morphology of potassium dihydrogen phosphate (KDP) transforms from tetragonal prism to sharp needles when grown in ethanol (Xu et al. 2005). The drug tolbutamide when processed from acetone or ethyl acetate crystallises as polyedres and in a crystal lattice typical of Form I. When ethanol is added to acetone elongated particles are formed together with a needle population (Subra-Paternault et al. 2007).

The polarity of the solvent also plays an important role in determining the crystal morphology. Normally highly polar solvents tend to produce crystals that are isometric with low aspect ratios, and non polar solvents tend to produce crystals that are elongated with high aspect ratios. For example, crystals of alizarin (1,2-dihydroxy-9,10-anthraquinone) crystallises as very long needles from acetone, acetonitrile, hexane, toluene and acetic acid with an aspect ratio of at least 10. If dry ethanol, methanol or propanol are used as the solvent, flat crystals having an isosceles triangular shape are obtained (Algra et al. 2005). Crystals of 1,4-di-tert-butylbenzene (DTBB) grown from polar methanol and ethanol have a tabular habit with lengths and widths of the faces nearly equal while if a less polar alcohol such as isopropyl-alcohol is used it causes the DTBB to crystallise in tabular habits with an aspect ratio of 2. In acetone the DTBB crystals are acicular with an aspect ratio of 6 while clear crystals with a high aspect ratio of about 10 are deposited from hexane, and crystals grown from benzene produce needles with many occlusions (Garti et al. 1981). Crystals of meta-nitroaniline grown in non-polar toluene produces needles while more polar solvents like ethanol and acetone produce plates (Cang et al. 1998). Isometric shaped crystals are observed when ibuprofen is grown from polar ethanol whereas growth from non-polar ethyl acetate result in elongated platelets (Cano et al. 2001). However, this trend of highly polar solvents producing crystals that are isometric and non polar solvents producing crystals that are elongated is not always observed (Martino et al. 2007) and while there is ample literature on the above, there is not a systematic study and comprehensive explanation of the phenomenon for a particular class of solutes (Karunanithi et al. 2009).

2.7.2 Effect of mixed solvents on the crystal growth rate

Changing the solvent composition also plays an important role in changing the crystal growth rate and can affect the driving force (thermodynamic effect) or the mechanism of crystal growth (kinetic growth). The solvent may influence the growth mechanism by an influence on the surface roughness, with the net effect on the crystal growth of increasing solubility of the solvent is that the growing surface becomes rougher, thus leading to more rapid growth. This is supported by experimental results (Bourne & Davey 1976; Human et al. 1981; Olech & Hodorowicz 1990; Skoda & van den Tempel 1967). However, specific adsorption of solvent molecules at the growing crystal surface can result in a lower growth rate despite a higher solubility, as has been experimentally observed for organic molecules with polar faces such as α-resorcinol (Davey et al. 1988) and succinic acid (Davey, Mullin & Whiting 1982).

In the literature it has been observed that the growth rates of crystals are much higher than in the pure aqueous solvent. Omar (Omar 2006) observed that the addition of alcoholic solvents (20 wt% methanol, ethanol and propanol) to the ascorbic acid/water system results in a significant increase in the growth rate of ascorbic acid, higher than in the pure aqueous solvent, and significantly reduces the mass transfer rate and enhances the surface integration process. In acetone and water mixtures, the growth rate is higher than in the pure solvents and the growth rate of paracetamol increases to a maximum at approximately 40 mass percent water before it decreases in a similar manner as does the solubility of paracetamol in these mixtures (Granberg & Bloch 1999). The opposite trend is also observed where the growth rates of crystals are much lower than in the pure aqueous solvent. This is observed for sodium nitrate grown in mixture of isopropoxyethanol (IPE) (Oosterhof et al. 1999), for cyanzine crystals grown in aqueous ethanol solutions (Hurley et al. 1997) and for potassium chloride II grown in the water-ethanol system (Lopes & Farelo 2006).

2.7.3 Effect of solvent on growth rate and crystal habit modification of sodium nitrate

While there has been a lot of literature reporting the effect of additives on the crystal habit modification of sodium nitrate, very little work has been carried out on the effect of solvent on the growth and habit modification of sodium nitrate. Oosterhof *et al* (Oosterhof et al. 1999) studied in a microscopic setup the growth of sodium nitrate grown from mixtures of water and isopropoxyethanol (IPE) and investigated the influence of the weight fraction IPE on the growth rate, shape and purity of the crystal. The growth rate was found to be dependent linearly on the concentration difference, the mass transfer constant k_D was found to decrease with increasing weight fraction of IPE in the mixture and no changes in the crystal habit was observed.

2.8 SOLUBILITY

The solubility of a substance is defined as the amount of solute that can dissolve in a given amount of solvent at a given temperature. In the majority of cases the solubility increases with increasing temperature but can also decrease with increasing temperature with sparingly soluble materials (Myerson 1993). The solubility of many inorganics in aqueous solution as a function of temperature is available in the literature (Linke 1965; Mullin 1993; Stephen & Stephen 1964). The solubility characteristics of a solute in a given solvent has a considerable influence on the method of crystallisation and crystalliser system, influences the design and optimisation of production processes, and the maximum possible yield of crystalline phase.

2.8.1 Effect of mixed solvents on solubility

An organic liquid, which is miscible with water, is often used to precipitate a solute, and with increasing proportions of organic liquid the solubility of the original solute decreases. This method is often used to generate supersaturation, which is often referred to as “drowning out” or “salting out”. This method is advantageous where

the substance to be crystallised (solute) is highly soluble, has solubility that is a weak function of temperature, is heat sensitive or unstable at high temperatures because it is generally operated at ambient temperature without additional cooling or heating, produces crystals of high purity, and is an energy-saving alternative to evaporative crystallisation if the solvent can be separated at low (energy) costs (Nowee, Abbas & Romagnoli 2008). This salting out method has been used by many researchers (Cho et al. 2009; Gonzalez & Rasmuson 1997; Hash & Okorafor 2008; Nowee, Abbas & Romagnoli 2008; J Nyvlt 1992; Toth et al. 2005).

2.8.2 Solubility of sodium nitrate

Sodium nitrate is highly soluble in water with its solubility from Mullin (Mullin 1993) tabulated in Appendix A1 and shown graphically in Figure 2-8 where it can be observed that with increasing temperature the solubility of sodium nitrate in water increases exponentially.

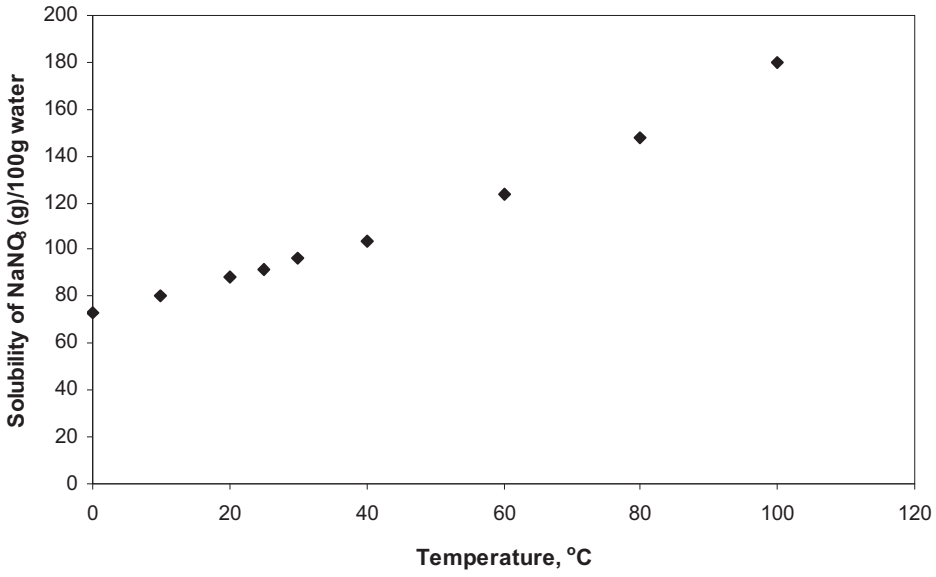

Figure 2-8 Solubility curve of sodium nitrate in water (Mullin 1993)

The solubility of sodium nitrate in water has also been determined at higher temperatures up to its melting point (Kracek 1931). More recently Archer (Archer 2000) reported a calculated solubility of 10.839m sodium nitrate [92.1g of $NaNO_3$ (100g of water)$^{-1}$] at 25°C and 13.453m sodium nitrate [114.34g (100g of water)$^{-1}$] at

50°C. Kiryanova (Kiryanova 2003) also found that there are temperature solubility oscillations for the solubility curve of the nitratine ($NaNO_3$) – water system, bearing maxima, minima or salient points, which is caused by subtle crystallogenetic phenomena and, thus, can only be detected by thorough precise investigations.

The solubility of sodium nitrate in various systems has also been determined. A compilation of solubility data of sodium nitrate in aqueous solution over a wide range of temperatures is available from Linke (Linke 1965) and Stephen and Stephen (Stephen & Stephen 1964). More recently solubility data has been reported for binary and ternary systems for the following sodium nitrate systems: sodium nitrate-sodium fluoride and sodium nitrate-sodium phosphate in water and sodium hydroxide at 25°C and 50°C (Selvaraj et al. 2008), sodium nitrate-lithium nitrate-potassium nitrate in water at different salt ratios (Vargas et al. 2008), sodium nitrate-ammonium nitrate in water at the temperature range 20 – 50°C (Trypuc & Druzynski 2008), sodium nitrate-sodium sulphate in water and sodium hydroxide at 25, 35 and 50°C (Toghiani et al. 2008), sodium nitrate-sodium vanadate in water at the temperature range 20 – 50°C (Trypuc & Druzynski 2007), sodium nitrate in 2-hydroxyacetamide over a limited concentration range (Vitali & Berchiesi 1989) and sodium nitrate-urea in water at 0°C (Kim et al. 1988).

No recent studies have been carried out on the solubility of sodium nitrate in solvents such as methanol, ethanol or isopropanol. The compiled data from (Linke 1965) on the solubility of sodium nitrate in these solvents dates back to some 100 years ago. Therefore in this work solubility determinations were focussed on sodium nitrate in solvents.

2.8.3 Thermodynamic model for solubility data

Accurate solubility data is a crucial part of the design, development and operation of a crystallisation process (Myerson 1993). In crystallisation processes, often the desired properties cannot be obtained with pure solvents so a solvent mixture is used. The mixing of solvents can result in a large change in the solubility of the solute in the solution and any impurities present in the solvent can also have a considerable effect on the solubility. The availability of solubility data in mixed solvents or on the

effect of other species on solubility is difficult to find and usually not available and must either be measured or calculated. However, accurate solubility measurements demand laboratory facilities and experimental skills and can be very time-consuming since equilibrium needs to be achieved and measurements may need to cover a wide range of variables. Calculation is a viable alternative when thermodynamic data is available for the pure components (in solution) making up the multicomponent mixture. Using a thermodynamic model allows minimisation of the required experimental work and facilitates interpolation and extrapolation in the whole range of industrial operating conditions.

The industrial production and treatment processes dealing with inorganic compounds usually involve electrolyte solutions. However, as mentioned earlier for many multicomponent systems the solubility data available is scarce and difficult to find and usually not available. Also, since the construction of a multicomponent phase diagram can take a considerable length of time depending on the number of solubility measurements necessary and number of components, representation of solid-liquid equilibrium of aqueous multicomponent electrolyte systems is a fundamental problem in the design and operation of many industrial processes involving electrolytes. This problem can be overcome by using the activity coefficient, which represents the phase equilibrium properties of the aqueous phase, over the temperature and concentration ranges of interest. However, the activity coefficient data of binary aqueous electrolyte solutions are not sufficient in the calculation of the phase equilibrium in an aqueous multielectrolyte solution, since the addition of other electrolytes affects the phase equilibrium of the electrolyte of interest. Also, the concentration of the added electrolytes affects the phase equilibrium, with an increase in concentration resulting in a greater effect on the phase equilibrium. Crystallisation is based on solid-liquid equilibrium, or the solubility product defined by the activity coefficient and molality of aqueous ions. Therefore, the desired activity coefficient model would be capable of representing the activity coefficient behaviour of a given ion in a wide concentration range and also in multielectrolyte solutions (Kuramochi et al. 2005).

In terms of inorganic chemical industries such as waste water treatment, hydrometallurgy, desalination, and crystallisation processes, activity coefficient models are still being developed, as well as for the understanding of electrolyte solutions (Kuramochi et al. 2005). Most methods are based to some extent on the modified Debye-Huckel equations, which describes the excess Gibbs energy due to long-range (electrostatic) interaction and generally, the activity coefficient of an electrolyte in a dilute solution (less than 0.1 mol kg^{-1}) can be expressed by this equation. In early studies, Pitzer (Pitzer 19731980; Pitzer & Kim 1974; Pitzer & Mayorga 1973) derived the thermodynamic equations for the activity coefficient of an electrolyte solution using the Debye-Huckel model, suggesting the equation be followed by a virial expansion of terms. In 1978, Cruz and Renon (Cruz & Renon 1978) first considered the Non random two liquid (NRTL) model combined with the Debye-Huckel model. The former and latter models represent short-range and long-range interactions, respectively. In the 1980's Chen *et al* (Chen et al. 1982; Chen & Evans 1986) applied the electrolyte NRTL model to electrolyte solutions, taking into account both short-range and long-range interactions and obtained good correlation of the activity coefficients of electrolytes between measured and calculated values over a wide range of salt concentration in aqueous solution. More recently Jaretun and Aly (Jaretun & Aly 19992000) applied additional empirical parameters to the electrolyte NRTL model for better representation of aqueous activity coefficient of electrolytes. Similarly, Lu and Maurer (Lu & Maurer 1993) and Thomsen *et al* (Thomsen et al. 1996) developed the electrolyte-Universal Quasichemical (UNIQUAC) model and the extended UNIQUAC model, respectively, using the UNIQUAC model as the local composition term. Among all the above mentioned models, Chen's electrolyte NRTL model is the simplest and requires fewer parameters in the calculation. Unfortunately this model is not suitable in extending to multi-electrolyte solutions since it requires some additional parameters besides binary NRTL parameters between an electrolyte and water. However, this disadvantage can be solved by replacing the electrolyte-specific NRTL binary interaction parameters used in this model with ion-specific ones.

2.9 SODIUM NITRATE

2.9.1 Properties

Sodium nitrate, also variously known as caliche, Chile saltpetre, salt peter, and soda niter, closely resembles potassium nitrate in appearance and chemical properties. It is also soluble in water, alcohol and liquid ammonia (NationMaster), with its properties shown in Table 2-2 and a photograph of typical sodium nitrate crystals shown in Figure 2-9.

Table 2-2 Properties of sodium nitrate

Property	
Chemical formula	$NaNO_3$
Appearance	White powder or colourless crystals
Melting point	307°C
Decomposition temperature	380°C
Density	$2.26 g/cm^3$
Crystal structure	Trigonal

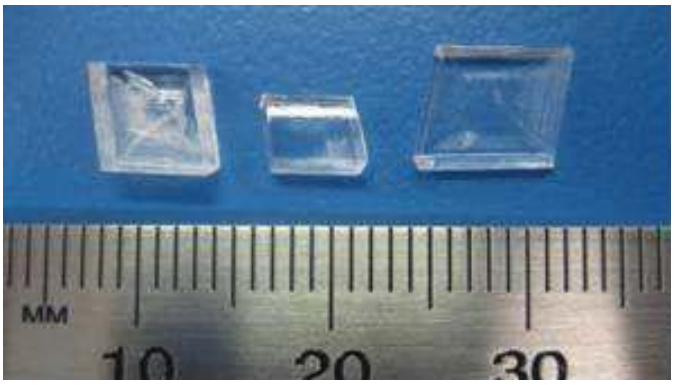

Figure 2-9 Photograph of sodium nitrate crystals

2.9.2 Occurrence and uses

Sodium nitrate can either be obtained by the processing of caliche ore, a crude, impure nitrate rock or gravel, with large reserves found naturally in arid regions of Chile, Peru, Argentina and Bolivia (The Columbia Encyclopedia 2008), or by

synthesising industrially by neutralising nitric acid with soda ash as shown by the following equation:

$$2HNO_3 + Na_2CO_3 \longrightarrow 2NaNO_3 + H_2CO_3 \qquad (2\text{-}31)$$

Sodium nitrate has many applications and in the late nineteenth century was used extensively as a fertiliser and as a raw material for the manufacture of gunpowder. In this same period a review was written on its origin, production and destruction of nitrates in the soil (Myers 1899), highlighting its importance as a source of nitrogen and its role as fertiliser in agriculture. However, in the first decades of the twentieth century its value declined dramatically after cheaper means were found to make fertilisers and explosives (Wikipedia 2007). It's other applications include being used as an ingredient in glass and pottery enamel, as a food preservative since it has antimicrobial properties, for the production of nitric acid (Wikipedia 2007), manufacture of sulphuric acid, nitrate of potash, arseniate of soda, fireworks, fusing mixtures, steel, minium and for making chlorite in the manufacture of bleaching powders (Myers 1899). It has also been successfully used to control the morphology of platinum nanoparticles (Herricks, Chen & Xia 2004). Single crystals of sodium nitrate also find application in optical pumping experiments (Gopalakrishnan, Arivuoli & Ramasamy 1991) and can be used as a substitute for calcite in the manufacturing of polarising prisms (Komnik & Startsev 1969).

2.9.3 Crystal Structure

Sodium nitrate has a rhombohdedral crystal structure and belongs to the space group D63d with the unit cell having dimensions a = 6.3247Å and α= 47°16' at 25^{o}C (Wyckoff 1964) and dimensions of a = 6.56Å and α= 45°35' at 280^{o}C (Kracek et al. 1931). But it is more conveniently described as a hexagonal system with a'o=5.0708Å and C'o=16.818Å, and D63d (R3c) space group (Wyckoff 1964). Sodium nitrate is also a structural analogue of calcite, the same crystal type found in anhydrous lithium nitrate, and at the high temperature modification of potassium nitrate and rubidium nitrate (Kracek, Posnjak & Hendricks 1931), and belongs to the trigonal system and has the symmetry 3m (Punin & Franke 2004).

The Miller indices for the sodium nitrate faces are shown in Figure 2-10 where it can also be observed that the faces of sodium nitrate are crystallographically equivalent.

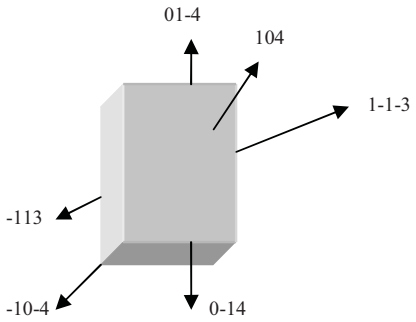

Figure 2-10 Miller indices for sodium nitrate (Jones & Larson 1999)

2.10 CONCLUSIONS

2.10.1 Conclusions from the literature

From the literature the following conclusions can be made:

- Crystals grown from solution are preferred over growth from the melt since the crystals grown from solutions contain few dislocations, no mosaic structure or small-angle boundaries and the crystals have a better optical quality. Thus, this point must be considered when choosing which method to grow crystals.

- Most of the crystal growth studies on sodium nitrate have focussed on the influence of tensile strain, supersaturation and dislocation due to the ductile nature of sodium nitrate which deforms plastically under high levels of strain. In these studies the growth rates of secondary nuclei have been measured and in the literature no data exists for the growth rates of sodium nitrate crystals formed by homogeneous nucleation. Thus further work is required in this area.

- In the literature, surface topographical studies have used x-ray surface topography for characterising the dislocation structure of the crystal. No surface studies have been carried out on the crystal to determine its mechanism of growth.

- The literature on the solubility of sodium nitrate in solvents such as methanol, ethanol and isopropanol is quite old, dating back some 100 years ago, and is only available for certain temperatures and weight percents. Thus this work is outdated and further work is required in this area.

- Sodium nitrate is a difficult crystal to modify and researchers have mainly used dyes to investigate and study the effect of additives on the habit modification of sodium nitrate. No recent studies have been carried out.

- From the literature not much research has been carried out on the effect of solvent on the growth and habit modification of sodium nitrate. Thus further work on the effect of solvent on sodium nitrate is required.

2.10.2 Specific objectives of the present research

Based on the literature review and the gaps identified, the main objectives of the present study are as follows:

- To determine the solubility of sodium nitrate in various solvents such as methanol, ethanol and isopropanol.

- To determine the kinetics of growth of sodium nitrate formed by homogeneous nucleation and compare the growth rates to seeded experiments.

- To identify the growth mechanism of the sodium nitrate crystal by using optical microscopy, SEM and AFM.

- To study the effect of additives and solvent on the growth rates and habit modification of sodium nitrate.

Chapter 3
MEASUREMENT AND CORRELATION OF THE SOLUBILITY OF SODIUM NITRATE IN MIXED SOLVENTS

3.1 INTRODUCTION

A solution is a homogeneous mixture of two or more substances formed by the addition of a solid solute to a solvent. The amount of solute that can dissolve in a given amount of solvent is temperature dependent, for the majority of cases the solubility increases with increasing temperature. For some solutes, their solubilities can also decrease with increasing temperature (Myerson 1993). The maximum amount of solute that can dissolve in a given amount of solvent at a given temperature is termed the solubility of a substance. The solubility of a typical substance is represented by the solubility curve shown in Figure 2-1.

Traditional methods to generate supersaturation and induce crystallisation is by cooling and evaporation, with the choice of method used, to a large extent, dependent on the shape of the solubility curve and on the magnitude of the solubility (Pamplin 1980). For instance cooling cannot be used to generate supersaturation if the solubility of the material changes very little over the temperature range of interest. Similarly if the solvent is not volatile enough and the product is heat sensitive then the evaporation method is unsuitable (Myerson 1993) and is at its best where the overall solubility is low (Pamplin 1980).

A third option of creating supersaturation, which is often referred to as “drowning out” or “salting out”, is by adding another solvent to the system which greatly reduces the solubility of the solute in the original solvent. Use of this method requires an appropriate solvent miscible in all proportions with the solvent and the

solute should be relatively insoluble in it and the final solvent-precipitant mixture must be readily separable, eg. by distillation. This method offers several advantages because ambient temperature may be employed, which is highly desirable if heat labile substances are being processed, and is therefore an energy saving alternative to evaporative crystallisation if the solvent can be separated at low (energy) costs (Nowee, Abbas & Romagnoli 2008), and frequently the mixed solvent mother liquor has a high retention for impurities resulting in very pure crystals (Pamplin 1980). The disadvantage of using this method is the need for a solvent recovery unit to separate the mixed solvents, the stringent operating conditions required since most organic solvents are inflammable (Mullin 1993) and its high-dependence on mixing, for instance, where poor mixing regimes exist, high local supersaturation at antisolvent induction zones exists leading to excessive primary nucleation (Nowee, Abbas & Romagnoli 2008).

The availability of solubility data in mixed solvents or on the effect of other species on solubility is difficult to find and is usually not available at the conditions and composition of interest. Given this situation the solubility of the system must either be calculated, a viable alternative when thermodynamic data is available, or measured, since it is unlikely that data will be available in the literature for the solubility of the solute in the actual working solution with all impurities present (Myerson 1993).

To satisfy this need for experimental data, this chapter presents the solubility data for solutions of sodium nitrate in aqueous alcohols (methanol, ethanol and isopropanol) at various weight percents (0 – 90%) at different temperatures of 20.0°C (for methanol and isopropanol), 20.4°C (for ethanol), and 30.0°C and 40.0°C (for methanol and ethanol), and in water in the temperature range from 10.0°C to 40.0°C. The experimental data was used for the determination of the ion-specific NRTL parameters by correlating with the extended NRTL model. This model allows the minimisation of the required experimental work and significantly facilitates interpolation and extrapolation in the range of operating conditions.

3.2 EXPERIMENTAL SET-UP

Numerous techniques are available for the measurement of the solubility of solids in liquids. However, no single method can be identified as being generally applicable to all possible types of systems, since the choice of the most appropriate method must be made in the light of the system properties, the availability of apparatus and analytical techniques, the skill and experience of the operator and the precision required and so on (Mullin 1993). The measurement of solubility appears to be quite simple; however, it is a measurement that can easily be done incorrectly resulting in very large errors (Myerson 1993). Solubility should always be measured at a constant isothermal temperature with agitation employed, which is necessary to bring the liquid and solid phases into intimate contact and facilitate equilibrium. Equilibrium is usually achieved after several hours, and in some cases days or even weeks. The long period of time is necessary because dissolution rates become very slow near saturation, and if shorter periods of time is used (one hour or less), the solubility will generally be underestimated (Myerson 1993). Generally solutions that are viscous, at relatively low temperature and substances of low solubility require long contact times (Mullin 1993).

3.2.1 Materials

The chemicals used in the solubility experiments were sodium nitrate (BDH AR, ≥99.5%), absolute ethanol (Pronalys, 99.5%), methanol (BDH Normapur, 99.8%), isopropanol (Pronalys, 99.5%) and deionised water. They were all used without further purification. Appendix B details the specifications for sodium nitrate.

3.2.2 Apparatus

Solubility measurements were conducted in a solubility cell, using the same experimental set up that was designed and used by (Safaeefar 2007) as shown in Figure 3-1. The system comprised of the following main components: a 47 litre plastic solubility tank, stainless steel holders to hold the flasks in place in the solubility tank, a thermostatic heater/water bath to control the temperature of the system, two centrifugal pumps located at the input and output of the tank to circulate

water from the thermostatic heater, glass flasks (solubility cells) and magnetic stirrers and bars to agitate the solutions.

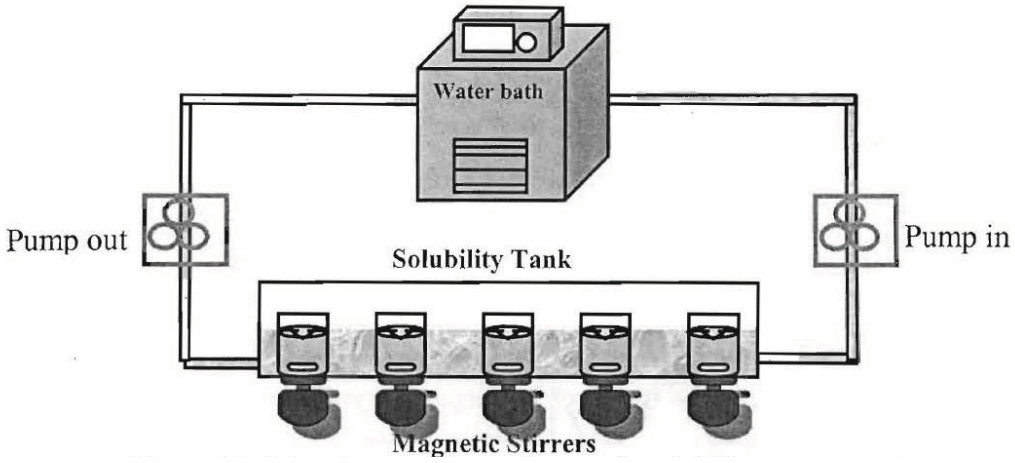

Figure 3-1 Experimental set-up for solubility measurements (Safaeefar 2007)

3.3 SOLUBILITY MODEL

3.3.1 Introduction

Electrolyte solutions are usually encountered in industrial production and treatment processes that deal with inorganic solutions, such as waste water treatment, extractive distillation, solution crystallisation, sea water desalination, mineral scale formation in steam systems and gas scrubbing. It is important to understand the thermodynamic properties of these aqueous strong electrolyte systems which is essential for the design and simulation of the above mentioned chemical processes (Loehe & Donohue 1997). Separation processes that include crystallisation or precipitation, solvent extraction, sorption, and ion-exchange, are used in the recovery or removal of these inorganic salts, with these processes predicated on the phase equilibrium between an aqueous phase and one other additional phase (Kuramochi et al. 2005).

Crystallisation is based on solid-liquid equilibrium, or the solubility product defined by the activity coefficient and molality of aqueous ions. The activity coefficient

represents the phase equilibrium properties of the aqueous phase and can be used to calculate the real behaviour of fluid mixtures. However, the activity coefficient data of binary aqueous electrolyte solutions are not sufficient in the calculation of the phase equilibrium in an aqueous multielectrolyte solution, since the addition of other electrolytes affects the phase equilibrium of the electrolyte of interest. Also, the concentration of the added electrolytes affects the phase equilibrium, with an increase in concentration resulting in a greater effect on the phase equilibrium. For crystallisation purposes it is necessary to have highly concentrated electrolyte solutions. If the concentration of the electrolyte of interest is low or dilute, highly concentrated solutions of other electrolytes must be used. Thus, a model that represents the activity coefficient behaviour of a given ion in a wide concentration range and in multielectrolyte solutions is necessary (Kuramochi et al. 2005).

To study the effect of methanol and ethanol on the solubility of sodium nitrate in aqueous solution, suitable thermodynamic equations should be used to correlate the data. The NRTL model was chosen to be used since it is the most convenient and useful because of its simplicity and its extensive use and it requires less parameters in the calculation. This model has also been widely used to correlate and extrapolate phase behaviours of highly non ideal systems with chemicals, electrolytes, oligomers, polymers and surfactants (Chen & Song 2004). However, this model is not suitable in extending to multi-electrolyte solutions, so this problem was overcome by replacing the electrolyte-specific NRTL binary interaction parameters used in this model with ion-specific ones.

3.3.2 Non random two liquid (NRTL) model

The electrolyte-NRTL model proposed by Chen and co-workers (Chen et al. 1982; Chen & Evans 1986; Mock et al. 1986) was used for predicting the activity coefficients of electrolytes in aqueous systems. However, this model requires additional parameters such as the electrolyte-specific parameters, for multicomponent prediction. Therefore, the electrolyte-specific NTRL binary interaction parameters used in this model were replaced with ion-specific parameters. In addition, the local neutralisation for cations and anions were not considered. These

corrections enable the prediction of the activity coefficient of any ion species in a multicomponent system without any additional parameters. The calculation procedure and explanation of the used equations are described in the following paragraphs below (Kuramochi et al. 2005; Maeda et al. 2002).

Crystallisation is based on solid-liquid equilibrium, or on the solubility product, K_s, of a salt in solution which is defined by the activity coefficient and molality of aqueous ions as follows:

$$K_s = a_+^{\nu+} a_-^{\nu-} = \left(\gamma_+^* x_+\right)^{\nu+} \left(\gamma_-^* x_-\right)^{\nu-} \tag{3-1}$$

where, a and x denote activity and solubility in units of mole fraction, γ^* is the unsymmetrical activity coefficient, the subscripts + and – refer to cation and anion, respectively and $\nu_\pm$ is the stoichiometric number when the salt is perfectly dissociated. The temperature dependence can be expressed as an Arrhenius function of temperature:

$$R \ln K_s = A + \frac{B}{T} \tag{3-2}$$

where, R is the universal gas constant, and the constants A and B are the thermal parameters for the pure salt, and are independent on concentration of salt in the aqueous solution. The solubility data can be converted from molality (m) to mole fraction unit (x) as follows:

$$x_+ = \frac{\nu^+ m}{\frac{1000}{M_S} + m\left(\nu^+ + \nu^-\right)}, \; x_- = \frac{\nu^- m}{\frac{1000}{M_S} + m\left(\nu^+ + \nu^-\right)} \tag{3-3}$$

where, M_s is the molecular weight of the solvent.

It was assumed that an aqueous electrolyte solution consists of water, anions, and cations; with this complete dissociation assumption extended to aqueous mixed electrolyte systems. Since the activity coefficient of an individual ion $i\left(\gamma_i^*\right)$ cannot be

measured, the activity coefficients of aqueous ions are usually expressed as the mean ionic activity coefficient, $\left(\gamma^*_{\pm,ac}\right)$, of neutral electrolytes a-c, and is given by:

$$\ln \gamma^*_{\pm,ac} = \frac{v_a \ln \gamma^*_a + v_c \ln \gamma^*_c}{v_{ac}} \tag{3-4}$$

where, v_a is the stoichiometric coefficient of the anion, which is the number of moles of the anion produced by the dissociation of one mole of a-c; v_c denotes that of the cation, and v_{ac} is:

$$v_{ac} = v_a + v_c \tag{3-5}$$

In the electrolyte-NRTL model proposed by Chen (Chen et al. 1982), the activity coefficient of aqueous ion i is represented by the unsymmetric Pitzer-Debye-Huckel expression:

$$\ln \gamma^*_i = \ln \gamma^*_{i,pdh} + \ln \gamma^*_{i,NRTL} \tag{3-6}$$

The first term on the right hand side of equation 3-6 is the contribution of the long range interaction of ions and is given by the Pitzer-Deye-Huckel equation, which is a function of ionic strength (I) only, and is given by:

$$\ln \gamma^*_{i,pdh} = -\left(\frac{1000}{M_s}\right)^{1/2} A_\phi \left\{ \left(\frac{2z_i^2}{\rho}\right) \ln\left(1+\rho I_z^{1/2}\right) + \left(\frac{z_i^2 I_z^{1/2} - 2I_z^{3/2}}{1+\rho I_z^{1/2}}\right) \right\} \tag{3-7}$$

where, A_ϕ is the Pitzer-Debye-Huckel parameter which has been calculated according to Chen's paper (Chen et al. 1982), z is ion charge, and ρ is the closest approach parameter (=14.9 which is the same value used by Pitzer (Pitzer 1980) and Chen (Chen et al. 1982)). Ion strength, which is based on the mole fraction x is defined by:

$$I_x = \frac{1}{2}\sum_i^N z^2 x_i \tag{3-8}$$

The second term on the right hand side of equation 3-6 is the contribution due to the short-range interaction of any species in solution and is given by the NRTL equation, which is generally expressed as:

$$\ln \gamma_{i,NRTL} = \frac{\sum_{j}^{N} z_j G_{ji} \tau_{ji}}{\sum_{k}^{N} z_k G_{ki}} + \sum_{j}^{N} \frac{z_j G_{ij}}{\sum_{k}^{N} z_k G_{kj}} \left(\tau_{ij} - \frac{\sum_{k}^{N} z_k G_{kj} \tau_{kj}}{\sum_{k}^{N} z_k G_{kj}} \right) \tag{3-9}$$

where, $G_{ij} = \exp(-\alpha \tau_{ij})$; $\tau_{ij} = \frac{\Delta g_{ij}}{RT} = \frac{g_{ij} - g_{jj}}{RT}$ and α = non-random factor (=0.2)

τ_{ij} is the NRTL binary interaction parameter of the i-j combination for any species and Δg_{ij} is defined as the difference in the interaction energy between the i-j and j-j combinations. The NRTL-derived activity coefficient $(\gamma_{i,NRTL})$ is based on symmetric convention, which is different from that of the activity coefficient of aqueous salts. Therefore, the activity coefficient must be transformed to the unsymmetric activity coefficient $(\gamma^{*}_{i,NRTL})$ using the NRTL-derived infinite dilution activity coefficient $(\gamma^{\infty}_{i,NRTL})$ as follows:

$$\ln \gamma^{*}_{i,NRTL} = \ln \gamma_{i,NRTL} - \ln \gamma^{\infty}_{i,NRTL} \tag{3-10}$$

3.4 EXPERIMENTAL SOLUBILITY MEASUREMENTS

The solubility of sodium nitrate in binary and ternary systems was determined by equilibrating crystals and solution in a solubility cell as shown in Figure 3-1. The experimental set up comprised of five glass solubility cells. Each cell consisted of a 250mL flat bottom flask closed by a ground glass stopper, with the contents stirred continuously for 24 hours by a submersible magnetic stirrer. The cells were immersed in a 47L plastic solubility tank, with the thermostatic heater (Thermoline unistat) capable of maintaining the temperature to within ±0.05°C. The temperature

of the tank was measured using a TPS digital temperature probe which had been calibrated against a mercury thermometer with 0.05°C uncertainty.

3.4.1 Binary solubility data

The solubility of the sodium nitrate-water system was determined over the temperature range of 10.0 to 40.0°C by equilibrating crystals and solution in a solubility cell. A fixed amount of water was placed into separate flasks which were each fitted with submersible magnetic stirrers. The flasks were then stoppered and sealed with paraffin film to prevent evaporation of solvent and placed in the solubility tank at the desired temperature until the temperature of the solvent was equilibrated. An accurately weighed out mass (approximately 0.5 to 1g in excess of saturation) of sodium nitrate was then added to each of the flasks, with the solutions continuously stirred at the desired temperature for 24 hours to ensure complete saturation of the solution. After 24 hours the flasks were taken out of the solubility tank, the solutions were filtered by vacuum through a Millipore 47mm sterifil aseptic system using a 0.2μm Supor membrane filter, and the residue was dried in an oven to constant mass at around 110°C. For determinations of solubility at higher temperatures the filtration flask was preheated prior to filtration to eliminate any solution temperature fluctuations. The solubility of the saturated solution was determined by subtracting the amount of undissolved solute from the total amount of solid initially added by using a Shimadzu AW320 analytical balance (accuracy ±0.1mg).

The solubility data for sodium nitrate in water at different temperatures (10.0, 20.0, 30.0 and 40.0°C) and in comparison with literature results taken from Mullin (Mullin 1993) is shown in Figure 3-2 and is tabulated in Appendix A2. Each experimental solubility data reported represents the average value of 3 to 7 independent measurements. From this figure it can be observed that the results are similar to the literature values. In Chapter 2, Figure 2-8 shows the solubility curve from Mullin (Mullin 1993) over the full temperature range of 0 to 100°C. This figure shows that the solubility graph is curved and is highly temperature sensitive for sodium nitrate.

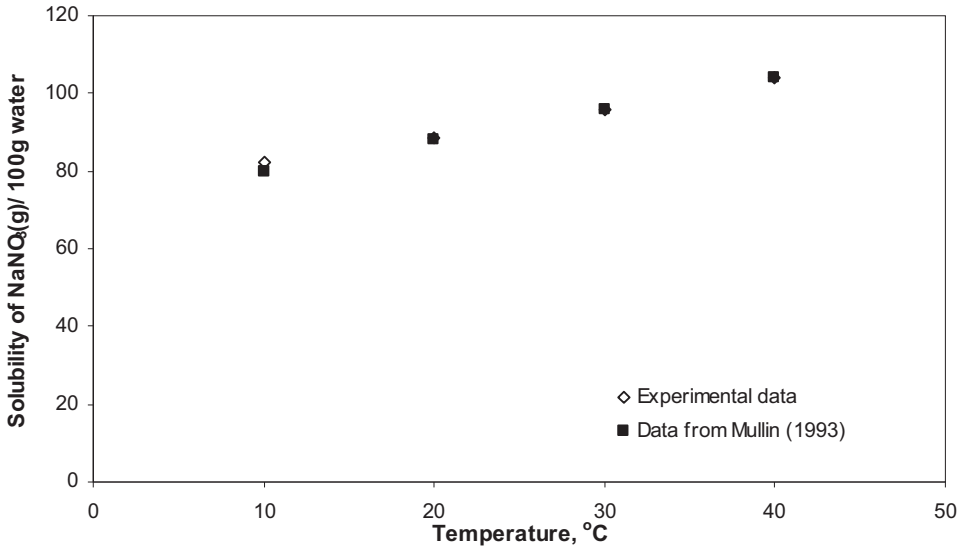

Figure 3-2 Solubility of sodium nitrate in water, comparison of experimental data with literature data from Mullin (Mullin 1993)

3.4.2 Ternary solubility data

The solubilities of the sodium nitrate-water-methanol system and the sodium nitrate-water–ethanol system were determined over the temperature range of 20.0 to 40.0°C by equilibrating crystals and solution in a solubility cell. The solubility of the sodium nitrate-water-isopropanol system was also investigated at 20.0°C. The same apparatus and method was used as for the binary system, except the solute, organic solvent and water was first combined together and then equilibrated to the desired temperature. This method excluded the additional step of opening the flasks while the solvent and solute were at their equilibrated temperature and hence eliminated solvent losses from the system.

The solubility data given on both mass basis (S) and mole basis (m) for the sodium nitrate-water in methanol, sodium nitrate-water in ethanol and sodium nitrate-water in isopropanol solutions is shown in Table 3-1 to Table 3-3 respectively. The solubility data reported represents the average value of 2 to 12 independent measurements (see Appendix A3). For the isopropanol system (Table 3-3) only three data points are presented for low mass fraction (0.0549) and high mass fraction

(0.90) of isopropanol since this system for other mass fractions tested was observed to split into two phases (i.e not miscible). The same data in mole fractions from Table 3-1 and Table 3-2 is also presented in Figure 3-4 and Figure 3-5 for sodium nitrate-water in methanol and sodium nitrate-water in ethanol systems.

Table 3-1 Solubilities of sodium nitrate at different mass fractions (W) of methanol

Mass fraction methanol (W)	Mole fraction methanol (X)	S (g/ 100g solvent[a])	m (mol/kg solvent[a])	m^b_c (mol/kg solvent[a])
t = 20.0°C				
0	0.00	88.46	10.41	10.42
0.0549	0.03	79.22	9.32	9.30
0.1359	0.08	66.23	7.79	7.76
0.1909	0.12	57.93	6.81	6.80
0.3	0.19	42.84	5.04	5.10
0.4	0.27	31.58	3.72	3.77
0.5	0.36	22.96	2.70	2.67
0.6	0.46	15.71	1.85	1.79
0.9	0.84	4.19	0.49	0.51
t = 30.0°C				
0	0.00	95.61	11.25	11.35
0.1	0.06	79.87	9.40	9.28
0.2	0.12	63.68	7.49	7.43
0.3	0.19	49.14	5.78	5.79
0.4	0.27	36.73	4.32	4.37
0.5	0.36	26.48	3.12	3.17
0.6	0.46	18.62	2.19	2.19
0.7	0.57	12.50	1.47	1.43
0.9	0.84	4.71	0.55	0.55
t = 40.0°C				
0	0.00	104.10	12.25	12.40
0.1	0.06	88.45	10.41	10.24
0.2	0.12	70.82	8.33	8.29
0.3	0.19	55.79	6.56	6.55
0.4	0.27	42.61	5.01	5.02
0.5	0.36	31.14	3.66	3.71
0.6	0.46	21.88	2.57	2.61
0.7	0.57	14.25	1.68	1.72
0.9	0.84	5.41	0.64	0.58

a) Solvent refers to the mixed solvent of water and methanol
b) The solubility values calculated from Equation 3-11.

Table 3-2 Solubilities of sodium nitrate at different mass fractions (W) of ethanol

Mass fraction ethanol (W)	Mole fraction ethanol (X)	S (g/ 100g solvent[a])	m (mol/kg solvent[a])	m^b_c (mol/kg solvent[a])
t = 20.4°C				
0	0.00	89.58	10.54	10.38
0.0549	0.02	78.39	9.22	9.19
0.1359	0.06	63.08	7.42	7.56
0.1909	0.08	54.54	6.42	6.55
0.3	0.14	39.77	4.68	4.76
0.4	0.21	28.63	3.37	3.38
0.5	0.28	19.97	2.35	2.25
0.6	0.37	12.92	1.52	1.37
0.9	0.78	1.06	0.13	0.20
t = 30.0°C				
0	0.00	95.61	11.25	11.21
0.05	0.02	85.82	10.10	10.09
0.2	0.09	59.64	7.02	7.09
0.4	0.21	33.49	3.94	3.93
0.6	0.37	14.81	1.74	1.71
0.7	0.48	8.27	0.97	0.96
0.9	0.78	1.24	0.15	0.17
t = 40.0°C				
0	0.00	104.10	12.25	12.27
0.08	0.03	88.48	10.41	10.38
0.26	0.12	57.69	6.79	6.83
0.428	0.23	35.67	4.20	4.15
0.651	0.42	13.43	1.58	1.61
0.872	0.73	2.20	0.26	0.25

a) Solvent refers to the mixed solvent of water and ethanol
b) The solubility values calculated from Equation 3-11.

Table 3-3 Solubilities of sodium nitrate at different mass fractions (W) of isopropanol at 20.0°C

Mass fraction Isopropanol (W)	S (g/ 100g solvent[a])	m (mol/kg solvent[a])
0	88.46	10.41
0.0549	77.34	9.10
0.9	0.81	0.10

a) Solvent refers to the mixed solvent of water and isopropanol

The experimentally determined solubility data can also be predicted by a general equation for any mass fraction of alcohol in the appropriate temperature range as a function of composition by an equation of the form:

$$m = Aw^2 + Bw + C \tag{3-11}$$

where m is the solubility of sodium nitrate in moles of solute per kilogram of mixed solvent, w is the mass fraction of the alcohol, and the constants A, B and C are empirically determined at specific temperatures.

The values of the constants A, B and C along with the calculated root-mean-square deviation (Rmsd) which is defined in Equation 3-12 (Chirico et al. 2003), are listed in Table 3-4 and Table 3-5. The results show that Equation 3-11 can be used to correlate the solubility data quite satisfactorily.

$$Rmsd = \left[\frac{\sum_{i=1}^{N} \left(m_i^{calc} - m_i^{\exp} \right)^2}{N} \right]^{1/2} \tag{3-12}$$

where m_i^{calc} and $m_i^{\exp}$ are the calculated and experimental mole fraction solubilities, respectively, and N is the number of experimental points.

Table 3-4 A, B and C values and the root-mean-square deviations of the measured solubility from the calculated results for methanol

Temperature (°C)	A	B	C	Rmsd
20.0	11.23	-21.12	10.42	0.04
30.0	10.89	-21.80	11.35	0.06
40.0	10.64	-22.70	12.40	0.08

Table 3-5 A, B and C values and the root-mean-square deviations of the measured solubility from the calculated results for ethanol

Temperature (°C)	A	B	C	Rmsd
20.4	12.39	-22.47	10.38	0.11
30.0	11.89	-22.97	11.21	0.04
40.0	11.67	-23.96	12.27	0.03

3.4.2.1 *Comparison of results with literature*

The solubility data for the sodium nitrate-water-ethanol system at 30.0 and 40.0°C was compared to literature from Taylor (Taylor 1897) and Bathrick (Bathrick 1896) which is tabulated in Appendix A4 and is shown in Figure 3-3 below. No recent literature results could be found for this system, or for methanol and isopropanol at the temperatures of interest, so in this section only the sodium nitrate-water-ethanol system was compared to literature. From this figure it can be observed that the experimental and literature results at 30.0°C are very similar, whereas at 40.0°C the experimental data obtained has a much lower solubility than the literature results. The variance in the results could be due to the literature data being outdated (by over one hundred years) when sophisticated systems with precise temperature control and balances with ±0.1mg precision were not available.

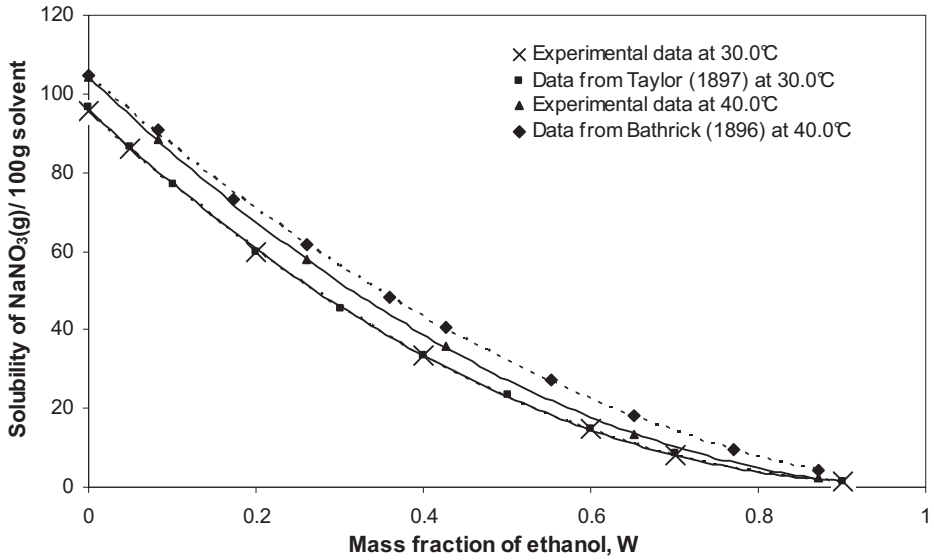

Figure 3-3 Solubility of sodium nitrate in water and ethanol, comparison of experimental data with literature data from Taylor (Taylor 1897) at 30.0°C and Bathrick (Bathrick 1896) at 40.0°C

Figure 3-3 compares the solubility data to mass fraction of ethanol for literature comparisons since this is how Taylor (Taylor 1897) and Bathrick (Bathrick 1896) presented their data. From here on, in the following sections, the solubility data will

be compared to mole fraction, X of the solvent, since this unit is used in the NRTL model, so ease of comparison can be made to the experimental and correlated results.

3.4.2.2 *Effect of temperature on the solubility of sodium nitrate in methanol and ethanol*

Figure 3-4 and Figure 3-5 show the solubility curves for the sodium nitrate-water in methanol and sodium nitrate-water in ethanol systems at different temperatures, respectively. In all cases it can be observed that the solubility of sodium nitrate is significantly reduced by the presence of methanol and ethanol, by up to 90 percent, making the alcohols a suitable salting out agent for the crystallisation of sodium nitrate. It can also be observed that the solubility of sodium nitrate increases with increasing temperature. This effect is more pronounced at the lower mole fractions, since at higher mole fractions the solubilities of sodium nitrate in both alcohols at the three temperatures are quite similar.

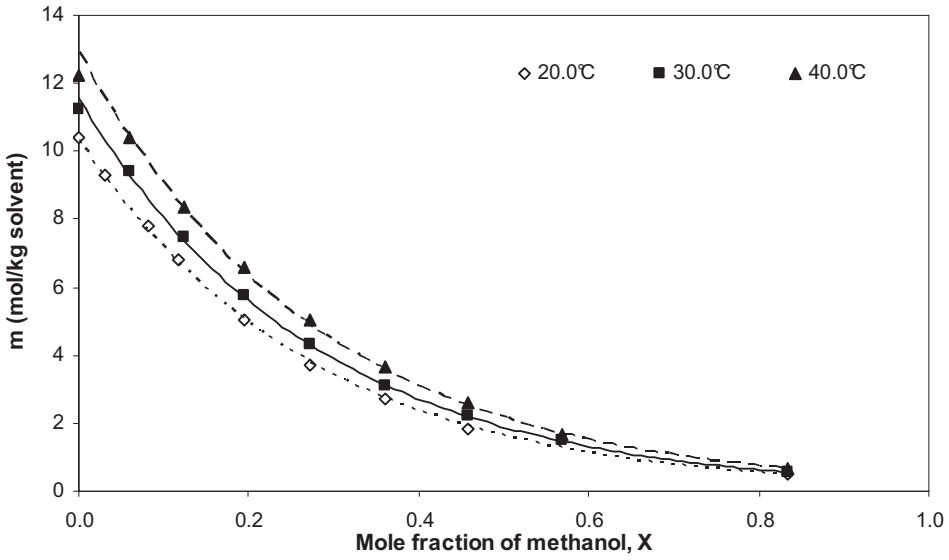

Figure 3-4 Solubility of sodium nitrate (mol/kg solvent) versus mole fraction, X of methanol and water at 20.0, 30.0 and 40.0°C

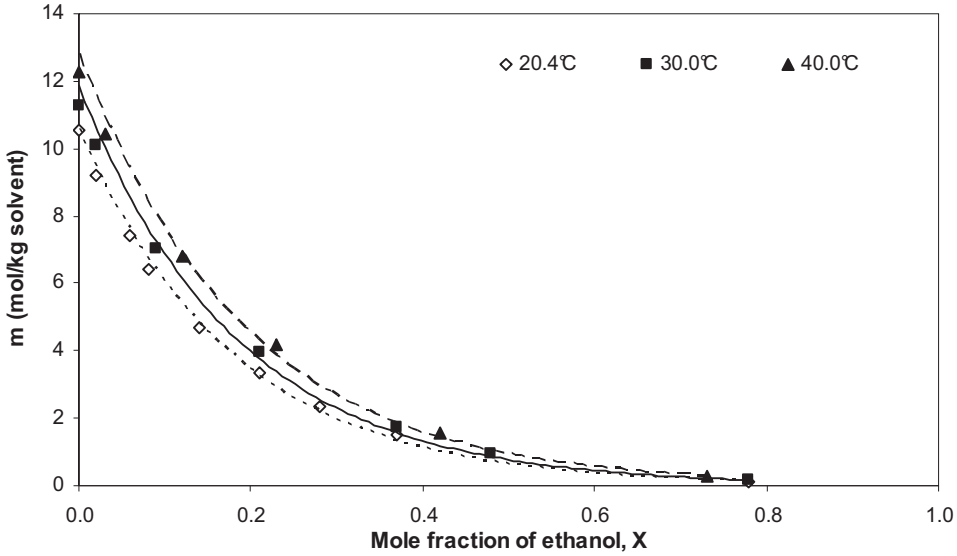

Figure 3-5 Solubility of sodium nitrate (mol/kg solvent) versus mole fraction, X of ethanol and water at 20.4, 30.0 and 40.0°C

3.4.2.3 *Effect of methanol, ethanol and isopropanol on the solubility of sodium nitrate*

Figure 3-6 to Figure 3-8 shows the comparison of the solubility curves for the sodium nitrate-water in methanol and sodium nitrate-water in ethanol systems which have been overlaid on top of each other at each temperature. In all figures it can be observed that sodium nitrate is more soluble in methanol followed by ethanol. For the isopropanol system at 20.0°C for the lowest mass fraction (0.0549) and the highest mass fraction (0.90), the values obtained are lower for those specified mass fractions in comparison to methanol and ethanol. However, as previously mentioned for all other weight percents tested the isopropanol system was observed to split into two phases, resulting in more sodium nitrate dissolving in the water phase, hence resulting in an overestimation in the solubility measurements. Therefore the order of decreasing solubility of sodium nitrate and water is of methanol<ethanol<isopropanol (only for low or high mass fractions). In other words, the solubility of sodium nitrate and water decreases with increasing molecular weight of the alcohol.

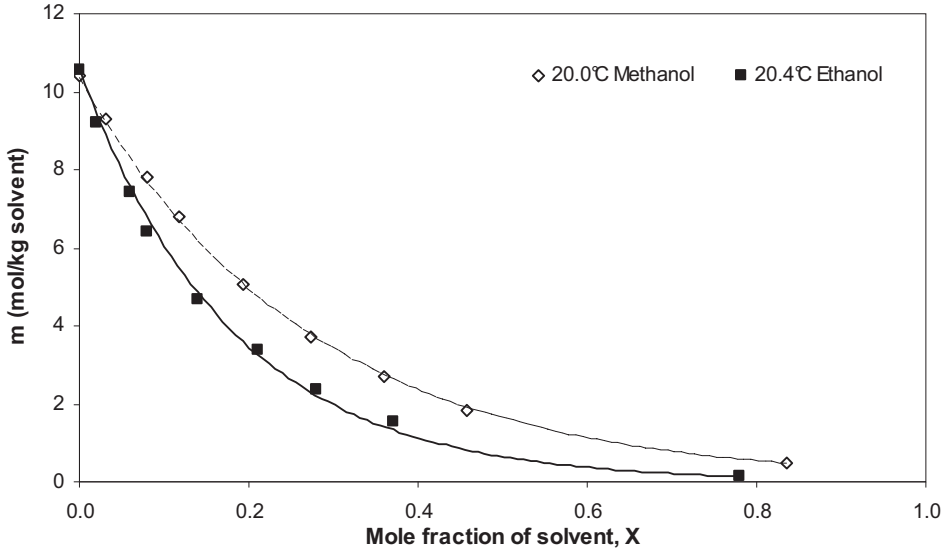

Figure 3-6 Solubility of sodium nitrate (mol/kg solvent) versus mole fraction, X of methanol and water at 20.0°C and ethanol and water at 20.4°C

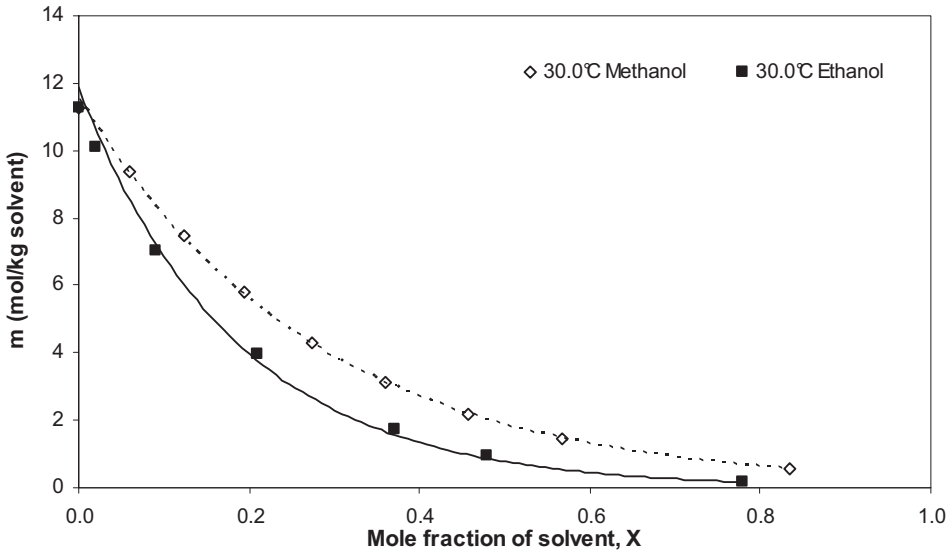

Figure 3-7 Solubility of sodium nitrate (mol/kg solvent) versus mole fraction, X of methanol and water, and ethanol and water at 30.0°C

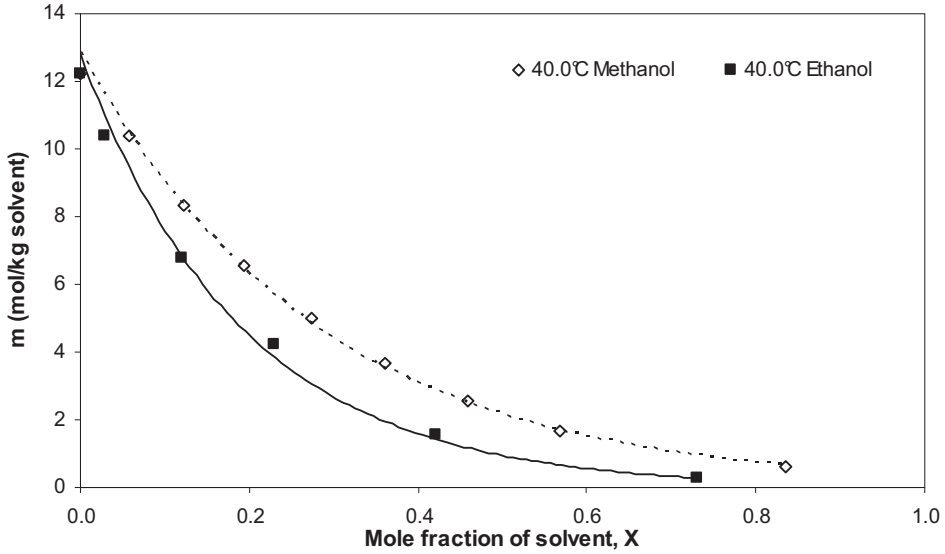

Figure 3-8 Solubility of sodium nitrate (mol/kg solvent) versus mole fraction, X of methanol and water, and ethanol and water at 40.0°C

3.4.3 Correlation of Ternary solubility data

3.4.3.1 *Solubility of sodium nitrate-water-methanol system*

According to the original NRTL equation (see Equation 3-9), in these electrolyte systems, the NRTL parameters (g_{ij}) required were for the water-methanol multielectrolyte system. The ion-specific NRTL parameters consisted of the combination-pairs for water, alcohol, one cation and one anion. Four species exist in this aqueous solution of three substances. Consequently, 12 parameters of g_{ij} are required for the mixed solution system. The NRTL parameters for the water-methanol systems were obtained from the DECHEMA reference book (Sorensen & Arlt 1980) and the universal ion specific parameters were obtained from Kuramochi *et al* (Kuramochi et al. 2005) and they are directly determined by many activity coefficient data (Robinson & Stokes 1965). The required correlative NRTL parameters are listed in Table 3-6 for the methanol-multi-electrolyte system, and they were used for the prediction of the activity coefficients in aqueous multi-electrolyte solutions. The ion specific parameters for the sodium nitrate–methanol system were newly determined in this work.

Table 3-6 Correlative NRTL parameters g_{ij} (J/mol) of the binary pair of i-j species

i-j species	Water	Methanol	Na^+	NO_3^-
Water	0	2717[b]	7150[a]	-1540[a]
Methanol	-1430[b]	0	-3980	-421320
Na^+	-10700[a]	-14740	0	9960[a]
NO_3^-	-13300[a]	-14970	-25200[a]	0

[a] Obtained from Kuramochi *et al* (Kuramochi et al. 2005)
[b] Obtained from Sorensen and Arlt (Sorensen & Arlt 1980)

The solubility data for sodium nitrate in aqueous methanol solution at three different temperatures are listed in Table 3-7 and shown in Figure 3-9 to Figure 3-11. The mole fraction (X) of methanol in the mixed solvent was obtained from Table 3-1 and m^{exp} and m^{cor} are experimental and correlating saturated molality (mol/kg solvent) values respectively. It can be observed that the model satisfactorily correlates the data at low to moderate concentrations of methanol. However, as the concentration of methanol rises the model prediction is less satisfactory, probably due to the interaction parameters of NRTL between alcohol and the ions not being able to represent the low solubility of electrolytes.

Table 3-7 Experimental (m^{exp}) and correlated (m^{cor}) solubility data of sodium nitrate-water-methanol system at 20.0, 30.0 and 40.0°C

20.0°C			**30.0°C**			**40.0°C**		
X	**m^{exp}**	**m^{cor}**	**X**	**m^{exp}**	**m^{cor}**	**X**	**m^{exp}**	**m^{cor}**
0.00	10.41	10.37	0.00	11.25	11.30	0.00	12.25	12.24
0.03	9.32	9.40	0.06	9.40	8.97	0.06	10.41	9.81
0.08	7.79	7.36	0.12	7.49	6.79	0.12	8.33	7.39
0.12	6.82	6.34	0.19	5.78	5.35	0.19	6.56	5.80
0.19	5.04	4.90	0.27	4.32	4.35	0.27	5.01	4.71
0.27	3.72	4.00	0.36	3.12	3.64	0.36	3.66	3.92
0.36	2.70	3.36	0.46	2.19	3.10	0.46	2.57	3.33
0.46	1.85	2.87	0.57	1.47	2.68	0.57	1.68	2.86
0.84	0.49	1.83	0.84	0.55	1.95	0.84	0.64	2.06

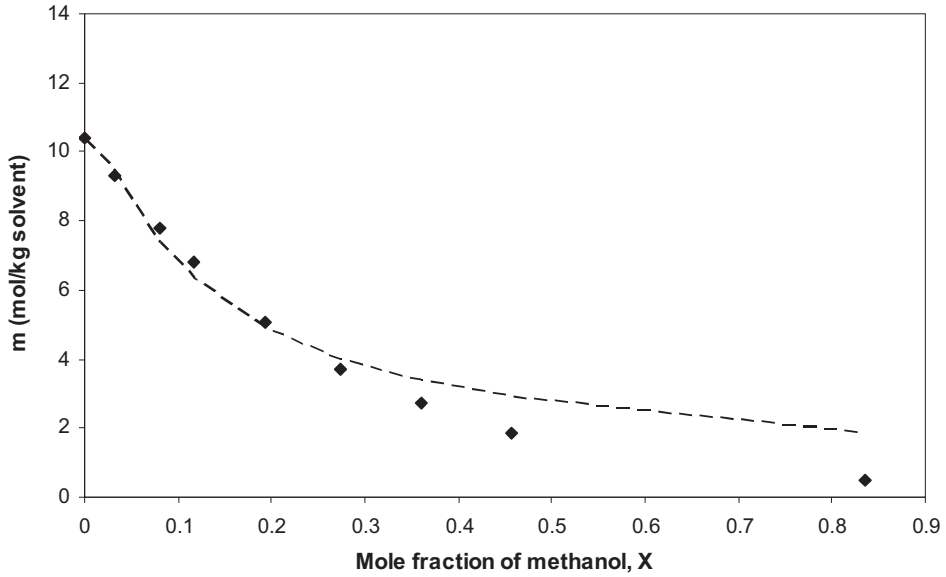

Figure 3-9 Experimental (symbols) and correlated (dotted lines) solubility data of sodium nitrate-water-methanol system at 20.0°C.

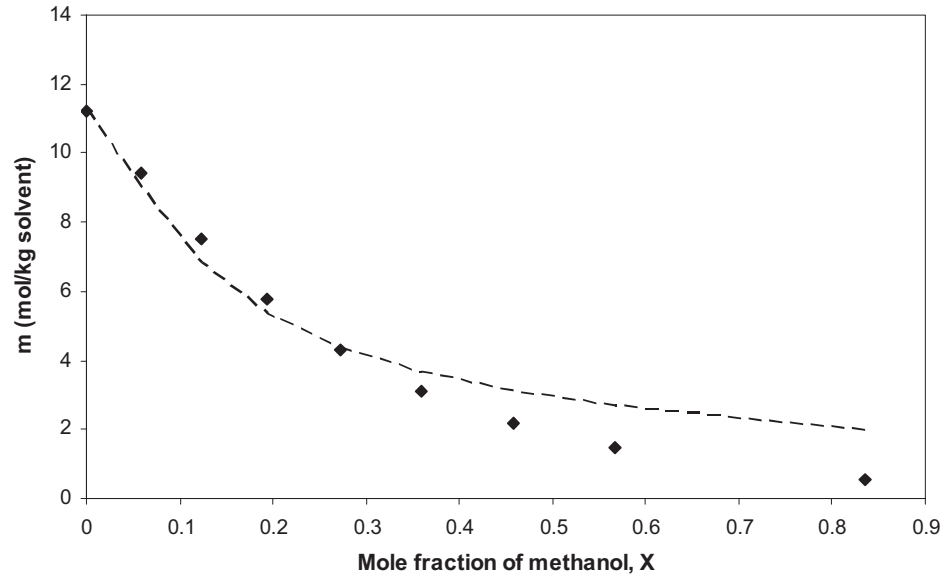

Figure 3-10 Experimental (symbols) and correlated (dotted lines) solubility data of sodium nitrate-water-methanol system at 30.0°C.

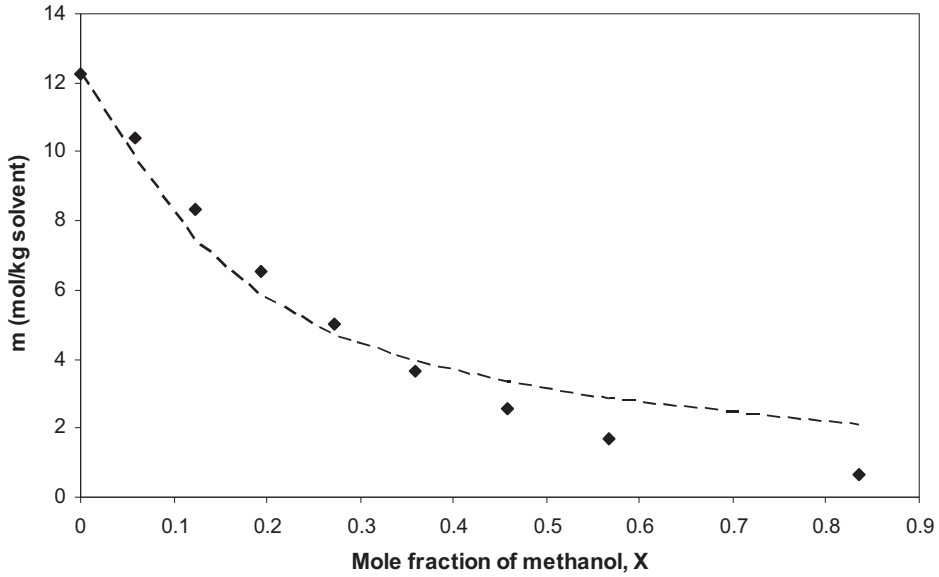

Figure 3-11 Experimental (symbols) and correlated (dotted lines) solubility data of sodium nitrate-water-methanol system at 40.0°C.

3.4.3.2 *Solubility of sodium nitrate-water-ethanol system*

The correlation described in Section 3.4.3.1 for the solubility of sodium nitrate in aqueous methanol is the same except using ethanol instead of methanol. The experimental and correlated solubility data of sodium nitrate-water-ethanol system is listed in Table 3-8 and shown in Figure 3-12 to Figure 3-14.

Table 3-8 Experimental (m^{exp}) and correlated (m^{cor}) solubility data of sodium nitrate-water-ethanol system at 20.4, 30.0 and 40.0°C

20.4°C			**30.0°C**			**40.0°C**		
X	$\mathbf{m^{exp}}$	$\mathbf{m^{cor}}$	**X**	$\mathbf{m^{exp}}$	$\mathbf{m^{cor}}$	**X**	$\mathbf{m^{exp}}$	$\mathbf{m^{cor}}$
0.00	10.54	10.41	0.00	11.25	11.30	0.00	12.25	12.24
0.02	9.22	9.50	0.02	10.10	10.44	0.03	10.41	10.50
0.06	7.42	7.00	0.09	7.02	6.36	0.12	6.79	5.91
0.08	6.42	6.17	0.21	3.94	3.78	0.23	4.20	3.84
0.14	4.68	4.54	0.37	1.74	2.48	0.42	1.58	2.41
0.21	3.37	3.48	0.48	0.97	2.00	0.73	1.26	1.34
0.28	2.35	2.84	0.78	1.15	1.13			
0.37	1.52	2.30						
0.78	1.13	1.05						

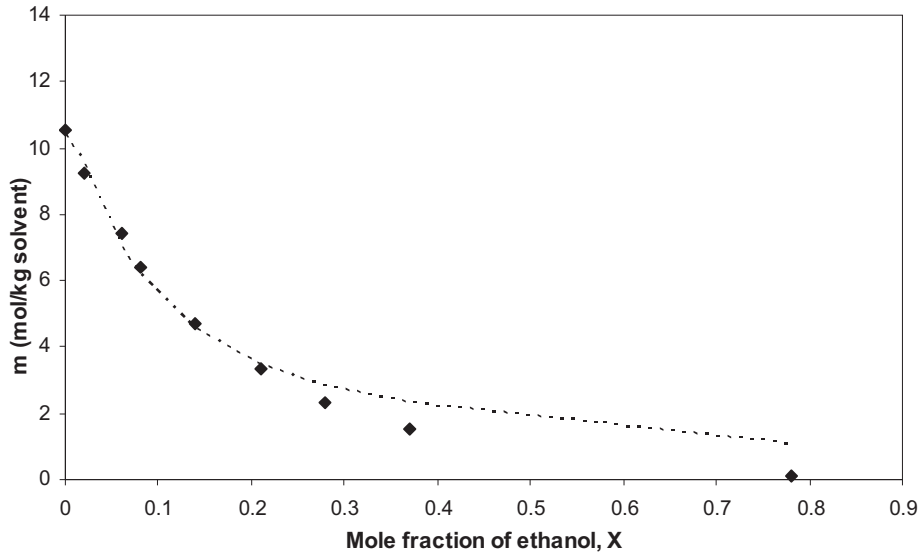

Figure 3-12 Experimental (symbols) and correlated (dotted lines) solubility data of sodium nitrate-water-ethanol system at 20.4°C.

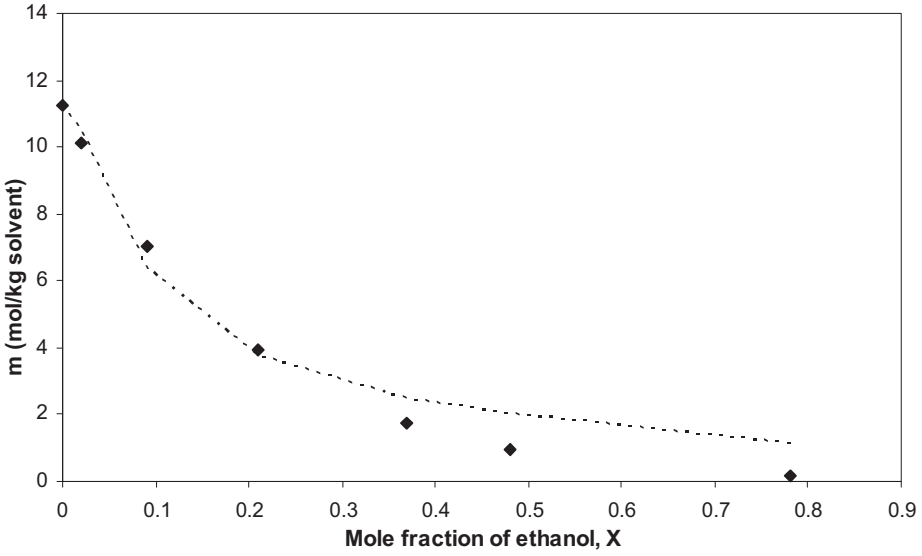

Figure 3-13 Experimental (symbols) and correlated (dotted lines) solubility data of sodium nitrate-water-ethanol system at 30.0°C

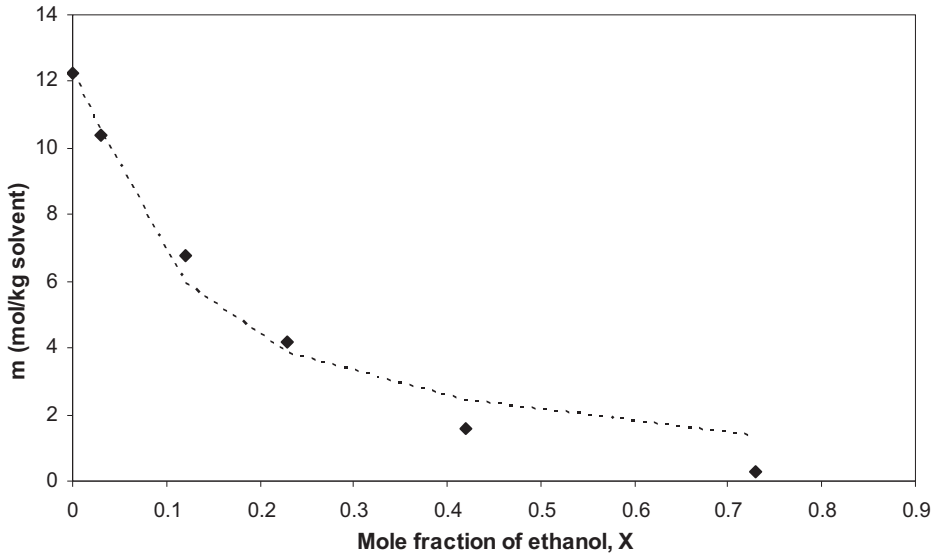

Figure 3-14 Experimental (symbols) and correlated (dotted lines) solubility data of sodium nitrate-water-ethanol system at 40.0°C

The required correlative NRTL parameters are listed in Table 3-9 for the ethanol-multi-electrolyte system, and they were used for the prediction of the activity coefficients in aqueous multi-electrolyte solutions. The ion specific parameters for the sodium nitrate–ethanol system were newly determined in this work.

Table 3-9 Correlative NRTL parameters g_{ij} (J/mol) of the binary pair of i-j species

i-j species	Water	Ethanol	Na^+	NO_3^-
Water	0	5427[b]	7150[a]	-1540[a]
Ethanol	-527[b]	0	-4924	-591100
Na^+	-10700[a]	-13360	0	9960[a]
NO_3^-	-13300[a]	-13720	-25200[a]	0

[a]Obtained from Kuramochi *et al* (Kuramochi et al. 2005)

[b] Obtained from Sorensen and Arlt (Sorensen & Arlt 1980)

The experimental data was modelled with the modified extended NRTL and the model was found to satisfactorily correlate the data at low to moderate concentrations of ethanol. However, as the concentration of ethanol rises the model prediction is less satisfactory, probably due to the interaction parameters of NRTL between alcohol and the ions not being able to represent the low solubility of electrolytes.

Summary

- Due to sodium nitrate's high solubility in water, data on its solubility in aqueous alcohol is essential for salting out crystallisation studies. A survey of the literature indicated that solubility data for sodium nitrate in the presence of ethanol is quite outdated, while solubility data with either methanol or isopropanol does not exist at the temperature range of interest.

- The effect of the addition of methanol, ethanol and isopropanol (the latter only at 20.0°C) on the solubility of sodium nitrate in water was experimentally investigated in the different temperature ranges and various weight percents of alcohol. In all cases the solubility of sodium nitrate in water was significantly reduced by the presence of methanol and ethanol.

- Splitting into two liquid phases was observed when using isopropanol. However, this phase separation did not occur at low mass fractions (0.0549) and high mass fractions (0.90) of alcohol, as at lower concentrations of one solvent the two solvents are miscible.

- The order of decreasing solubility of sodium nitrate and water is of methanol<ethanol<isopropanol (only for low or high mass fractions). In other words, the solubility of sodium nitrate and water decreases with increasing molecular weight of the alcohol.

- The experimental data was used for the determination of the ion-specific NRTL parameters by correlating with the modified extended NRTL model. It was observed for both methanol and ethanol that the model was found to satisfactorily correlate the data at low to moderate concentrations of alcohol. However, as the concentration of alcohol rises the model prediction is less satisfactory, probably due to the interaction parameters of NRTL between alcohol and the ions not being able to represent the low solubility of electrolytes.

Chapter 4
GROWTH RATES AND SURFACE MORPHOLOGY OF SODIUM NITRATE GROWN FROM AQUEOUS SOLUTION

4.1 INTRODUCTION

This chapter presents the results of growth rates of individual faces of sodium nitrate crystals grown in-situ in a batch cell and observed with an optical microscope at different temperatures and supersaturations to determine the kinetics of growth for homogeneous nucleation. Previous studies (Jones & Larson 1999; Jones et al. 2000) have determined crystal growth rates of sodium nitrate formed by secondary nucleation and in the literature no data exists for the growth rates of sodium nitrate formed by homogeneous nucleation. Crystal seeds were also introduced into a modified growth cell and growth rates were compared to the growth rates determined from the unseeded homogeneous nucleation experiments. A similar growth cell set-up has also been used for the measurement of layer velocities on crystal faces (Davey & Mullin 1974), to determine the growth dispersion in a variety of materials, as well as the extent to which contact nucleation is important at various supersaturation levels (Randolph & Larson 1988), for batch contact nucleation experiments (Berglund et al. 1983; Berglund & Larson 1982; Lowe et al. 2002; Shanks & Berglund 1985; Shiau & Berglund 1987) and has also been modified so the saturated solution can be circulated at different flow rates (Carter 2004; Dincer 2000; A.J Freij 2007; Mathis-Lilley & Berglund 1985).

The effect of solvent composition on the growth rate and habit modification of sodium nitrate was also investigated with aqueous solutions of methanol and ethanol. In the literature very little work exists on the effect of solvent composition on the effect of growth rate and habit modification of sodium nitrate. Only Oosterhof *et al*

(Oosterhof et al. 1999) has studied the effect of sodium nitrate grown from mixtures of water and isopropoxyethanol (IPE). The morphology of the sodium nitrate crystals grown was also observed by in-situ optical microscopy, scanning electron microscopy (SEM) and atomic force microscopy (AFM) to elucidate the crystal growth mechanism to verify if crystal growth is diffusion or surface integration controlled.

4.2 METHODOLOGY

4.2.1 Materials

The chemicals used in the crystal growth rate experiments were sodium nitrate (BDH AR, ≥99.5%), absolute ethanol (Pronalys, 99.5%), methanol (BDH Normapur, 99.8%), and deionised water. They were all used without further purification.

4.2.2 Experimental apparatus

In situ optical imaging was conducted using a stainless steel fluid cell similar to that described by Garside and Larson (Garside & Larson 1978). The cell was used to determine the growth characteristics of individual crystals of sodium nitrate growing under different conditions of temperature and supersaturation. A schematic drawing of the batch cell is shown in Figure 4-1.

The cell comprised of two chambers, with the upper section holding 5mL of the supersaturated solution while water from a water bath which was set at a specific temperature was circulated through the lower section (8mL) of the fluid cell so as to maintain the solution in the upper section at a constant temperature. The cell temperature was monitored by placing a thermocouple in the solution compartment. Circular glass cover plates (35mm diameter) were used to separate the solution and water, with neoprene o-rings sealing the cell against fluid loss. The images of the growing crystals were captured at selected time intervals using a digital camera attached to an optical microscope and analysed using the Image Pro software. Figure 4-2 shows the experimental set up used for the growth rate experiments.

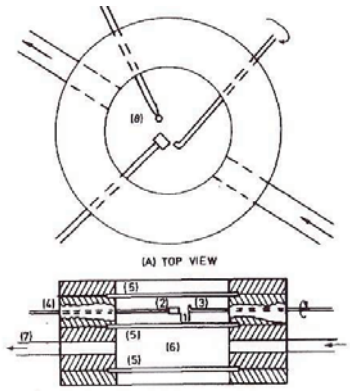

Figure 4-1 Schematic of the batch cell, (a) top view (b) side view (Garside & Larson 1978)

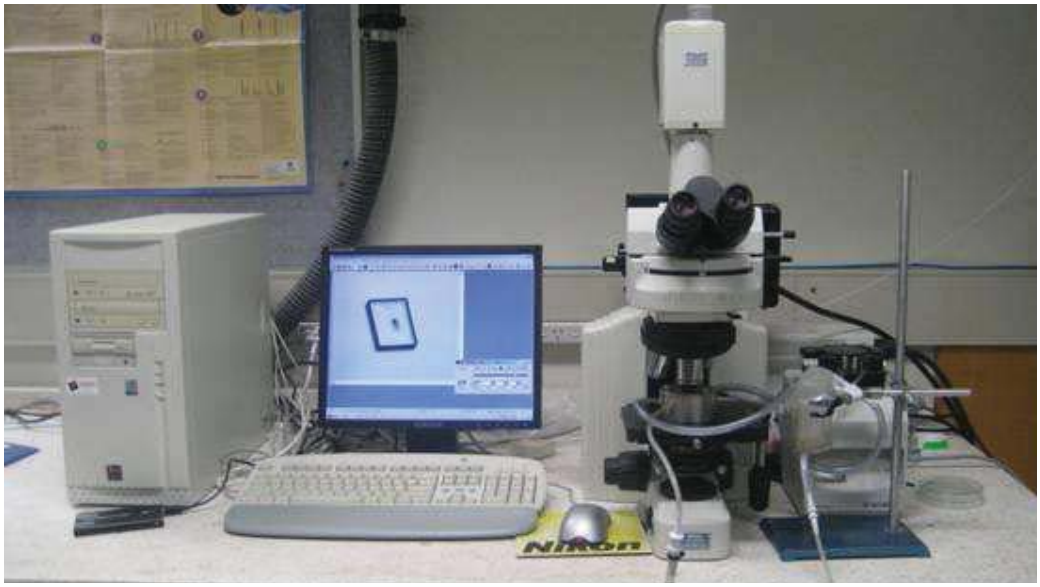

Figure 4-2 Experimental set up used for the in situ growth rate experiments

The batch cell was also modified so that the saturated solution could be circulated at different flow rates by using a peristaltic pump (Watson Marlow 5055/RL, manual control and variable speed) to investigate the growth rate mechanism of sodium nitrate. Water from a water bath was circulated through the lower section of the fluid cell and into a glass jacketed flask (solution reservoir) which contained the supersaturated solution in order to maintain the solution in the upper section of the

growth cell and in the solution reservoir at a constant temperature. Seed crystals were added to the upper compartment (not yet sealed) and the appropriate supersaturated sodium nitrate solution was added to the solution reservoir. A plastic baffle was inserted into the solution reservoir to enable mixing of the solution in the reservoir. The peristaltic pump was used to pump the supersaturated solution from the solution reservoir through the upper section of the fluid cell and back into the reservoir again. The modified growth cell was sealed after all air bubbles were removed from the system. A schematic of the setup if shown in Figure 4-3.

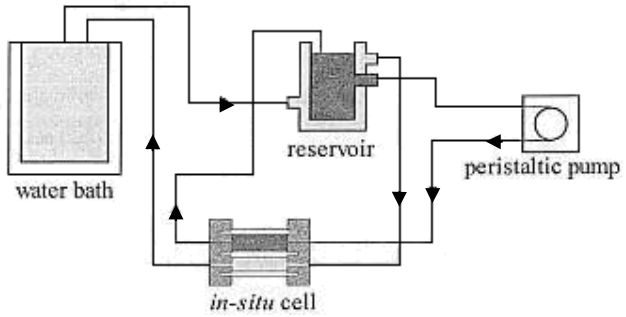

Figure 4-3 Schematic of experimental set up using the modified growth cell (Carter 2004)

4.2.3 Instrumental techniques

4.2.3.1 *Optical microcscopy*

Microscopic observations were made using a Nikon eclipse ME600 metallurgical microscope, with automated video image capture (Nikon DXM1200F digital camera). Crystals were observed using reflected light. The images of the growing crystals were analysed using the Image Pro software. A calibration was first established by taking pictures of a graticule (x and y directions) using the 5, 10 and 20 times magnification lens on the optical microscope and the calibration information was applied to each of the images.

4.2.3.2 *Atomic force microscopy (AFM)*

AFM investigations were carried out in air with a Digital Instrument Dimension 3000 AFM. All the AFM images (height and deflection) were collected in the contact

mode. Wide triangular shaped 100 and 200μm cantilevers made of gold coated Si_3N_4, with a spring constant of 0.58 and 0.12 Nm^{-1} were used. To prepare the sodium nitrate crystals for AFM examination the crystals grown under different conditions (i.e temperature, supersaturation and time) in the growth cell were carefully dried with filter paper in order to avoid drying effect after being taken out of the growth cell.

4.2.3.3 *Scanning Electron Microscopy (SEM)*

SEM images of the surface of sodium nitrate crystals were taken using a Philips XL30 scanning electron microscope fitted with a secondary electron, a backscattered electron and an x-ray energy dispersive detector (SEM-EDS). The SEM was operated at 10kV, spot size 4.0. To prepare the sodium nitrate crystals for SEM examination the crystals that were grown under different conditions (i.e temperature, supersaturation and time) in the growth cell were carefully dried with filter paper in order to avoid drying effect after being taken out of the growth cell, mounted on carbon tape which was stuck onto 10mm diameter stubs, and coated in gold for SEM imaging.

4.3 HOMOGENEOUS NUCLEATION EXPERIMENTS IN A BATCH CELL

Sodium nitrate solutions (approximately 20g) were prepared at relative supersaturations (σ) of 0.02, 0.04, 0.06, 0.08 and 0.1 at several different temperatures (20.0°C, 30.0°C and 40.0°C). The solutions were heated on a hotplate while being stirred continuously with a magnetic stirrer to a temperature slightly higher than the experimental temperature required. Solutions were filtered through a 0.2μm acro disc syringe filter prior to being placed in the growth cell as shown in Figure 4-1. In each experiment performed between one to three crystals were monitored in the growth cell under microscopic examination.

4.3.1 Crystal growth rates

Optical microscopy was used to evaluate rates of crystal growth directly. Crystal growth rates were determined by capturing images of the growing crystal with the optical microscope at selected time intervals and analysing them using the Image Pro software. The characteristic dimension (CD), the square root of the area of the 104 or -10-4 face (refer to Figure 2-10) of selected crystals was plotted as a function of time and the gradient of the straight line obtained from the early stages of crystal growth when the supersaturation was assumed to be constant was taken as the growth rate. Growth rate measurements were made on one to three crystals in each batch cell experiment. Figure 4-4 shows a growth sequence of a typical sodium nitrate crystal (30.0^{o}C σ = 0.1) taken with the optical microscope and grown in the batch cell at different time intervals, with its growth rate profile, the CD plotted against time shown in Figure 4-5.

(a) (b) (c)

Figure 4-4 Optical images of a growth sequence of a sodium nitrate crystal grown in situ in the batch cell, grown at 30.0^{o}C, σ = 0.1 (a) first observation (b) after 12 minutes from first observation, and (c) after 30 minutes from first observation.

From Figure 4-5 it can be observed that the growth rate increases and gradually decreases to a constant level after about 30 minutes. Jones and Larson (Jones & Larson 1999) also used a similar growth cell to determine the growth rates of sodium nitrate nuclei and also noticed that the growth rate decelerated as time progressed, and concluded that this deceleration was a result of the high ductility of sodium nitrate crystals and thus fitted a quadratic equation to get the relationship between size and time. They also noted that when they used more brittle materials such as potash alum and potassium sulphate in the growth cell that they grew in a time

dependant manner. However, in these sets of experiments it was concluded that the deceleration in growth was due to the growth cell design in which the solution is stagnant, therefore not being able to maintain constant liquor composition so the supersaturation decreases over time. Therefore due to this reason it was assumed that the supersaturation only remains constant in the early stages of crystal growth, so data in this region was only analysed. Figure 4-6 displays this region of constant supersaturation for the growth rate profile shown in Figure 4-5 where the growth rate is taken as the gradient which is 29.875 μm/min.

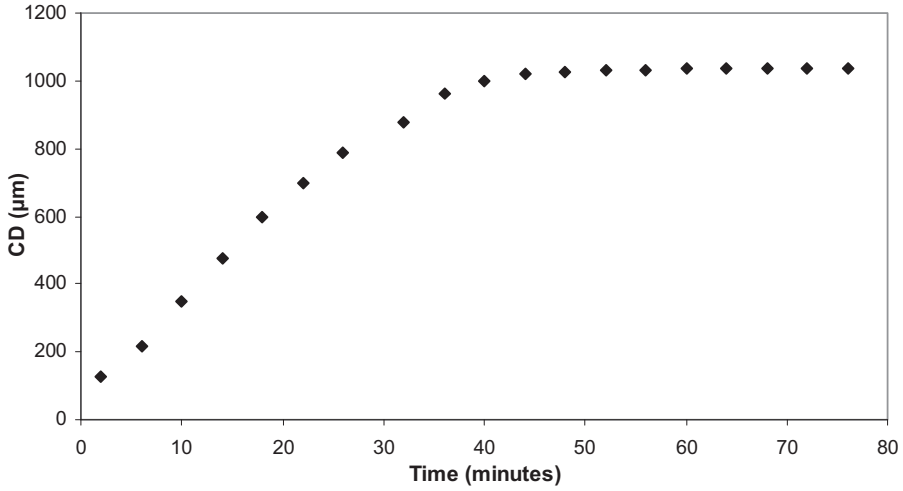

Figure 4-5 Typical plot of the growth rate profile, characteristic dimension vs. time

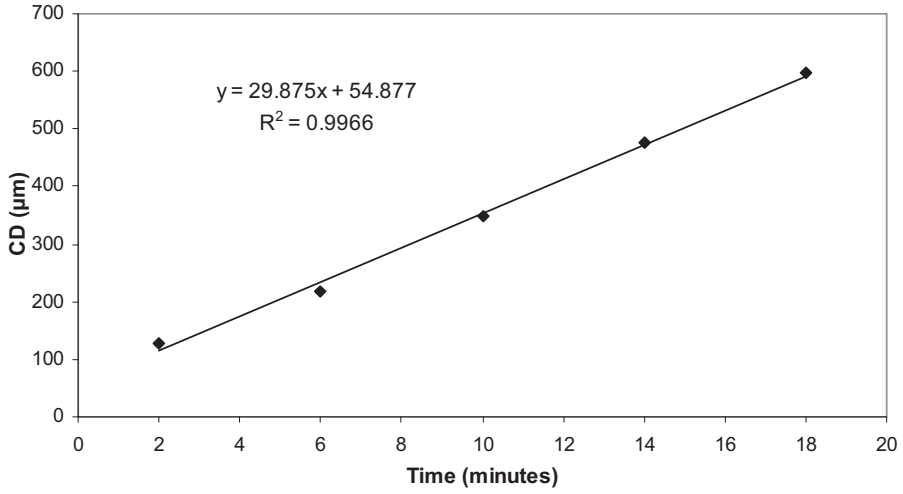

Figure 4-6 Region of constant supersaturation

Table 4-1 to Table 4-3 summarises the crystal growth rates obtained at different temperatures (20.0°C, 30.0°C and 40.0°C) and relative supersaturations, σ (0.02, 0.04, 0.06, 0.08 and 0.1) and the number of crystals that were analysed in the batch cell during an experiment or when replicate experiments were carried out (see Appendix C1 for a tabulated summary of the growth rates).

Table 4-1 Average growth rates of sodium nitrate grown at 20.0°C

σ	Growth rate (μm/min)	Number of crystals analysed
0.02	5.31±1.77	9
0.04	9.74±1.69	16
0.06	13.44±2.61	9
0.08	18.35±3.00	13
0.1	22.97±2.54	8

Table 4-2 Average growth rates of sodium nitrate grown at 30.0°C

σ	Growth rate (μm/min)	Number of crystals analysed
0.02	8.57 ± 1.62	14
0.04	14.04 ± 3.00	26
0.06	18.49 ± 2.24	17
0.08	28.96 ± 1.82	14
0.1	30.22 ± 5.08	18

Table 4-3 Average growth rates of sodium nitrate grown at 40.0°C

σ	Growth rate (μm/min)	Number of crystals analysed
0.02	10.18 ± 3.56	20
0.04	20.74 ± 5.15	19
0.06	28.20 ± 2.93	11
0.08	41.80 ± 3.14	6
0.1	37.95 ± 5.42	13

Figure 4-7 shows the growth rate profiles for replicate experiments that were carried out at 20.0°C, σ = 0.02. A number of replicate experiments were carried out since homogeneous nucleation is spontaneous and unpredictable as observed from the high standard deviations obtained in comparison to the seeded crystal growth experiments presented in Section 4.4. It is also difficult to prepare systems that are free from the presence of atmospheric dust which may act as nucleation catalysts, and physical

features such as vessel walls and stirrers may catalyse nucleation, and in most cases heterogeneous nucleation takes place before reaching conditions suitable for homogeneous nucleation.

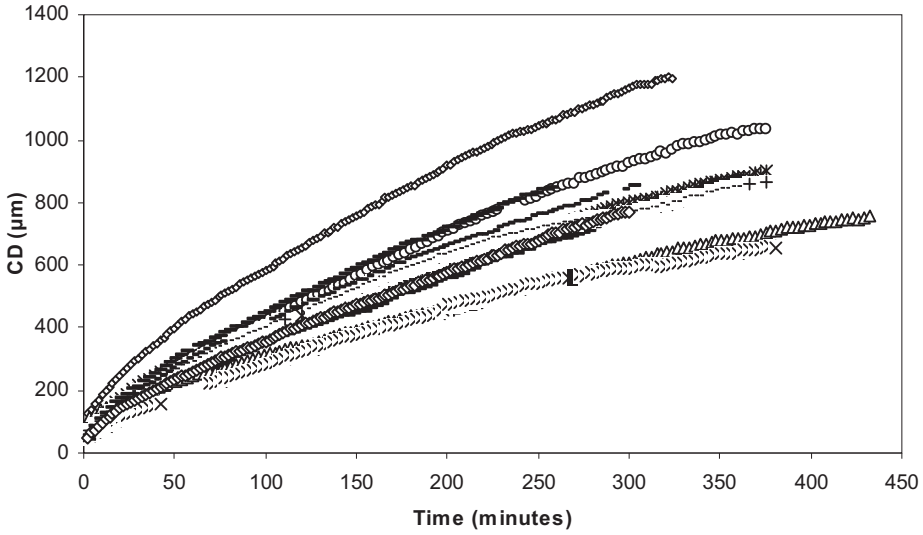

Figure 4-7 Growth rate profiles for replicate experiments of sodium nitrate crystals grown at 20.0°C, σ = 0.02

From Table 4-1 to Table 4-3 it can be observed that the growth rates increase with increasing supersaturation, except at 40.0°C where the relative supersaturation at 0.1 is lower than 0.08, whereas for 30.0°C the relative supersaturation at 0.08 and 0.1 are quite similar. The reason for this observation is because at higher supersaturations excessive nucleation in the batch cell was observed thus resulting in a decrease in the concentration and hence the crystal growth rates. At the higher temperature of 40.0°C this effect is more significant since higher temperatures promote more nucleation. In comparison to literature, Nyvlt *et al* (J. Nyvlt et al. 1985) reported crystal growth rates of 1.61 x 10^{-7} m/s (9.66 µm/min) and 8.05 x 10^{-7} m/s (48.3 µm/min) for relative supersaturations of 0.01 and 0.05 respectively, at 30°C in a fluidised bed. The growth rates obtained are much higher in comparison to the results at 30.0°C in Table 4-2, probably because in the fluidised bed there was agitation employed thus resulting in a thinner boundary layer around the crystals so that the diffusion of molecules onto the crystal surface is higher. Whereas the flow in the batch cell is laminar (see

Section 4.4.2) resulting in a much thicker boundary layer around the crystals and hence resulting in lower growth rates.

4.3.2 Growth kinetics

Average growth rate values were fitted into a combined mass transfer model (Equation 2-30) in order to evaluate the growth mechanism by relating the observed growth to theoretical mechanisms. This equation was then linearised by applying a logarithmic function to give:

$$\ln G = \ln(k_0) - \left(\frac{E}{RT}\right) + g \ln \sigma \qquad (4\text{-}1)$$

The parameters $\ln(k_0)$, E/R and g in Equation 4-1 were obtained by linear regression. The parameter g, the combined growth order, was obtained by plotting lnG versus lnσ as shown in Figure 4-8.

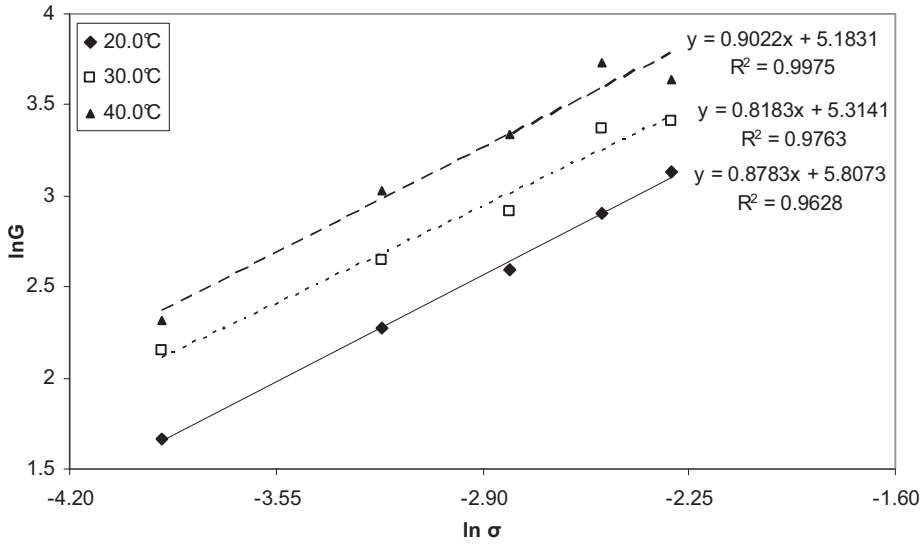

Figure 4-8 Plot of lnG versus lnσ to obtain the growth order, g

The gradient of the lines represent the g value which is 0.88, 0.82 and 0.90 for 20.0, 30.0 and 40.0°C respectively. The intercept values ($\ln(k_0) - E/RT$) obtained from this plot was then plotted versus 1/T as shown in Figure 4-9. The gradient of the line represents –E/R and the intercept value represents $\ln(k_0)$. From this plot it can also

be observed that the R^2 fit is low which is probably due to the limited data points available since only three temperatures were analysed. Using these parameters the following equation was obtained:

$$G = 2.6x10^{6} \exp\left(\frac{-23580}{RT}\right)\sigma \qquad (4\text{-}2)$$

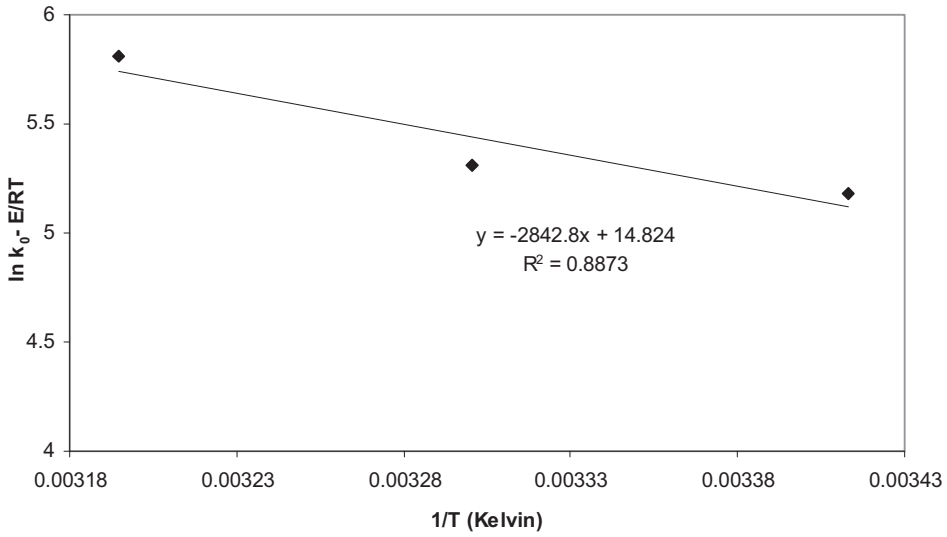

Figure 4-9 Plot of $\ln k_0$ – E/RT versus 1/T to obtain the activation energy and constant k_0

The parameters obtained; a combined growth order g of 1 and activation energy of 23,580 J/mol suggests that in this set of experiments crystal growth might be controlled by diffusion, which is in agreement with the results obtained by Graber *et al* (Graber et al. 1999) and Nyvlt *et al* (J. Nyvlt et al. 1985). Graber *et al* (Graber et al. 1999) obtained a similar activation energy of 23,424 J/mol and a kinetic growth order of 1 and concluded that growth was diffusion controlled, whereas Nyvlt *et al* (J. Nyvlt et al. 1985) calculated a kinetic growth order of 1. However, at low relative supersaturations ($0.04 < \sigma < 0.45$ %), Jones *et al* (Jones et al. 2000) observed that the crystal growth rates of sodium nitrate crystals that were nucleated by contact in a similar batch cell at a growth temperature of 27 °C are controlled by a dislocation mechanism while at σ <0.02% the growth rate was extremely low and it was

suspected that a 2D nucleation growth mechanism was taking place. They also determined that crystal growth rates are strain controlled at high growing supersaturations and dislocation controlled at low growing supersaturation, which correlates well with the results obtained by Jones and Larson (Jones & Larson 1999). However, in these sets of experiments higher supersaturation levels were used, and the results are in agreement with Graber *et al* (Graber et al. 1999) and Nyvlt *et al* (J. Nyvlt et al. 1985).

Predicted curves using equation 4-2 and experimental results are detailed in Figure 4-10 where it can be observed that the increase in growth rate with increasing supersaturation is accentuated when working at higher temperatures. It can also be observed that the predicted curves fit the data better at 20.0°C, probably because at this temperature hardly any nucleation was observed in the batch cell in comparison to 30.0 and 40.0°C where excessive nucleation was observed at higher supersaturations.

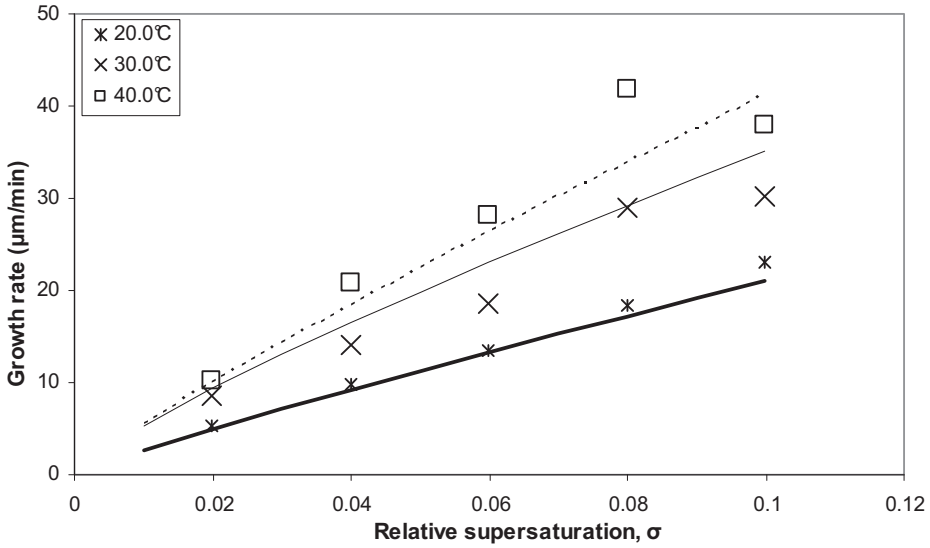

Figure 4-10 Measured (symbols) and predicted (lines) average growth rates of sodium nitrate at different supersaturations and temperatures.

To confirm that crystal growth under these experimental conditions was diffusion controlled, the same method was used to measure growth rates while the saturated

solution was circulated through a modified growth cell using a peristaltic pump. Diffusion controlled growth can be assumed if an increase in the relative velocity of the solution increases the crystal growth rate. The effect of solution flow on the crystal growth rate is illustrated in Figure 4-11 for growth conditions 20.0°C σ = 0.04 and is shown tabulated in Table 4-4. The dotted line in Figure 4-11 represents the average crystal growth rates obtained from Table 4-4.

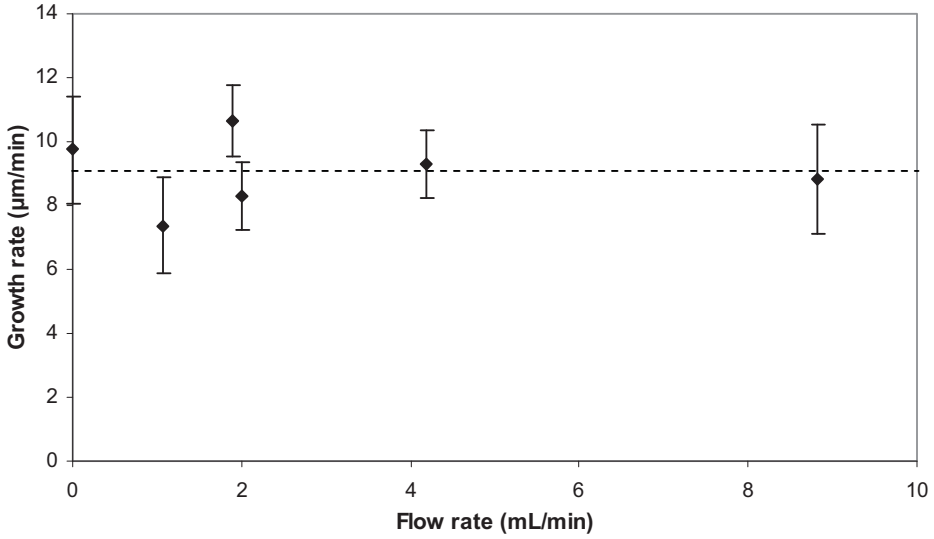

Figure 4-11 Effect of flow rate on the crystal growth rates of sodium nitrate grown in the modified growth cell at 20.0°C σ = 0.04

Table 4-4 Average growth rates of sodium nitrate grown at 20.0°C σ = 0.04 at different flow rates

Flow rate (mL/min)	Growth rate (µm/min)	Number of crystals analysed
0	9.74 ± 1.69	16
1.06	7.37 ± 1.50	4
1.9	10.64 ± 1.11	3
2	8.29 ± 1.07	5
4.18	9.30 ± 1.07	3
8.82	8.83 ± 1.70	5

From Figure 4-11 it can be observed that the mean crystal growth rate does not increase with increasing flow rate, which suggests that crystal growth at 20.0°C σ = 0.04 may be surface integration controlled. However, the Reynolds number calculated in Section 4.4.2 (Table 4-8) in the seeded crystal growth experiments for a

flow rate of 4 mL/min suggests that flow in the growth cell is laminar. Flow was also calculated to be laminar at the higher flow rate of 8.82 mL/min. Therefore since both flow rates are in the laminar region and produce low Reynolds number, from these results it cannot be concluded that growth is surface integration controlled. Experiments at higher flow rates and temperatures could not be performed due to the increased occurrence of nucleation in the cell caused by the pumping action as observed in Figure 4-12.

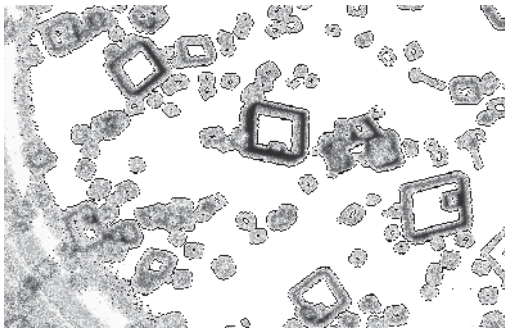

Figure 4-12 Optical images of sodium nitrate crystals growing in situ in the modified flow through cell, grown at 20.0^{o}C σ = 0.04 at a flow rate of 23.68 mL/min, 12 minutes from initial observation.

It was also observed that if the same solution was used in the growth cell at different flow rates, the crystal growth rate decreased, probably due to decreasing supersaturation since precipitate was observed to occur in the lines and solution reservoir. Therefore at each different flow rate fresh solution was used, where between 3 to 6 crystals were monitored for each flow rate. Therefore, in section 4.3.4 the surface morphology of the crystals will be studied to verify if sodium nitrate crystal growth is diffusion or surface integration controlled.

4.3.3 Growth rate dispersion (GRD)

In order to determine the effect of crystal size on the growth rate, initial crystal size (characteristic dimension) of when the crystals were first observed in the growth cell was plotted against growth rate of the crystal. Figure 4-13 to Figure 4-15 show the growth rates of crystals at different supersaturations at each of the different

temperatures. The dotted line represents the average crystal growth rates obtained from Table 4-1 to Table 4-3. It can be clearly seen that there is no increase in growth rate with increasing crystal size, thus the crystals exhibit size independent growth.

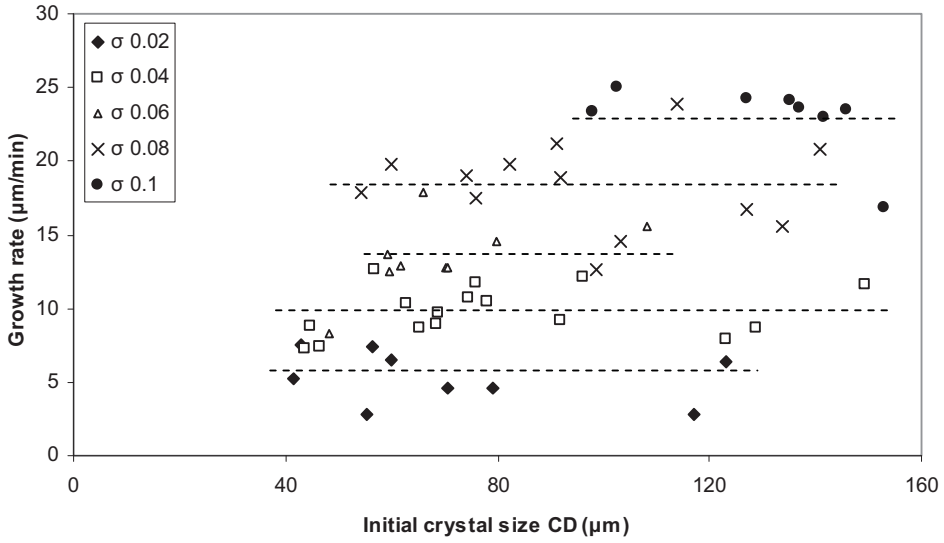

Figure 4-13 Growth rates of sodium nitrate grown at different supersaturations at 20.0°C

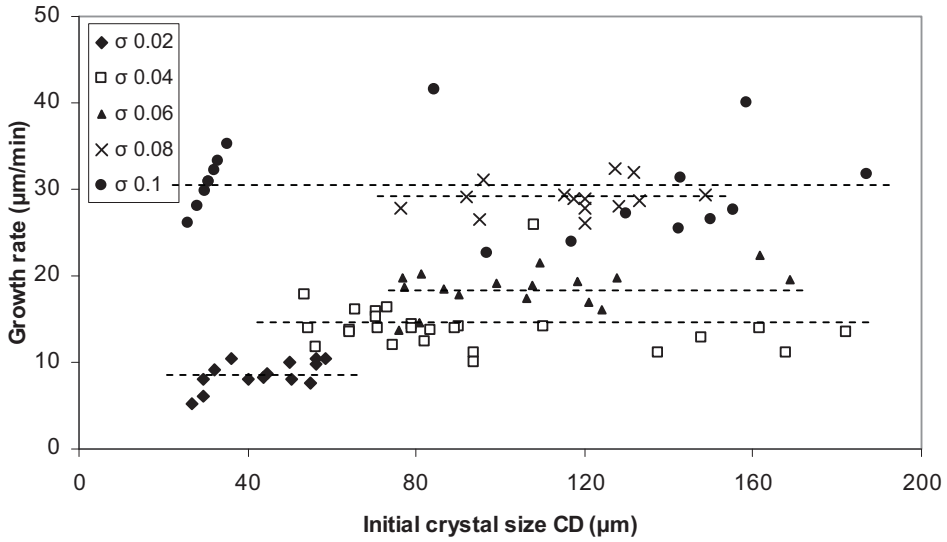

Figure 4-14 Growth rates of sodium nitrate grown at different supersaturations at 30.0°C

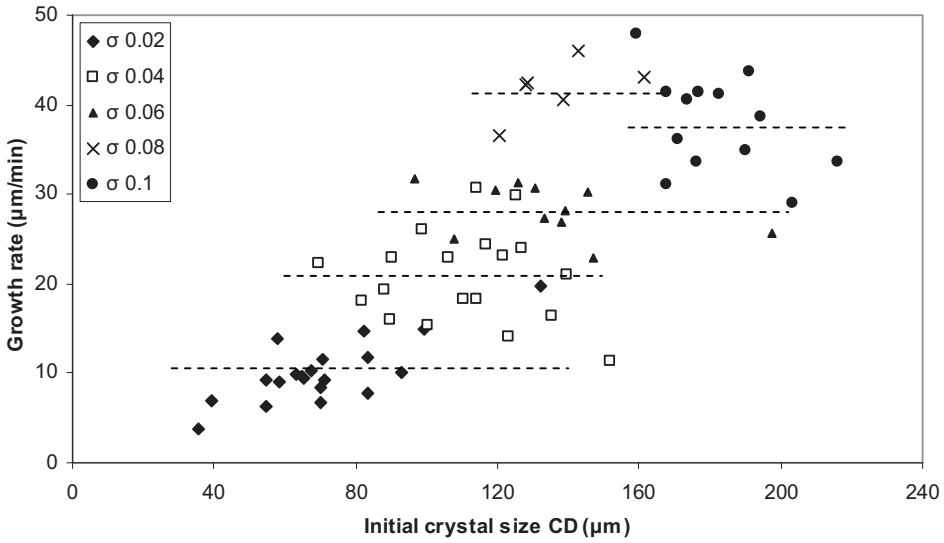

Figure 4-15 Growth rates of sodium nitrate grown at different supersaturations at 40.0°C

Jones and Larson (Jones & Larson 1999) also characterised the GRD of sodium nitrate secondary nuclei produced as a function of the nucleation and growing supersaturation in a similar growth cell, calculating the standard deviation to get the spread of the distribution. When the supersaturation during nucleation and growth in the cell was the same they observed that the spread of the distribution of growth rates increased with increasing supersaturation. This is also observed in Table 4-1 to Table 4-3 where the standard deviation of the growth rates increase with increasing supersaturation, except at 40.0°C where the standard deviation at lower supersaturations is relatively large. Also, as mentioned previously in Section 2.5.3, GRD is thought to occur due to the location or density of screw dislocations for crystals which are growing under surface integration controlled conditions. However, crystals growing under diffusion control conditions may exhibit GRD due to perturbation of the boundary layers during crystal-crystal or crystal-wall collisions, and in this case the dispersion should be rather low compared with crystals growing by a dislocation mechanism (Sohnel & Garside 1992). In these sets of experiments the crystals were grown in a batch cell so there was no chance for the boundary layer to be perturbed during growth for the above reasons, hence minimising the chance of GRD occurring.

4.3.4 Surface morphology

The surface morphology of crystals strongly depends on the supersaturation and temperature used for growth and on the presence and concentration of impurities in the growth medium (Sangwal & Rodriguez-Clemente 1991). Therefore in this section the surface morphology of the sodium nitrate crystals grown at different supersaturations and temperatures were compared by different microscopy techniques; in-situ optical microscopy, SEM and ex-situ AFM to elucidate the crystal growth mechanism, with a comparison between these different microscopy methods presented in Table 4-5. Out of these techniques, AFM has the highest spatial resolution so fundamental growth theories can be assessed directly on a nanoscale. AFM imaging of crystal surfaces also gives detailed information about the surface structure, growth steps, dislocations and molecular packing on crystal surfaces. It has also been used in the identification of growth mechanisms of many crystals (S.J Freij & Parkinson 2005; S.J Freij et al. 2004; Wakihara et al. 2004) and has also been used for surface topography studies (Asakuma et al. 2007; Mauri & Moret 2000; Moret 2000; Shangfeng et al. 1999).

Table 4-5 Comparison of features between the optical microscope, SEM and AFM (Dincer 2000)

	Optical Microscopy	**Scanning Electron Microscopy (SEM)**	**Atomic Force Microscopy (AFM)**
Sample operation environment	Ambient, liquid, vacuum	Vacuum	Ambient, liquid
Depth of field	Small	Large	Medium
Depth of focus	Medium	Small	Small
Resolution	1.5µm, N/A	5nm, N/A	0.01nm, 0.01nm
Magnification range	1-2 x 10^3	10-10^6	10^2-10^8
Sample preparation	Little	Coating	None
Characteristics required of sample	Transparent	Vacuum compatible	No excessive height variations

4.3.4.1 *In situ optical microscopy*

Figure 4-16 shows optical images of different sodium nitrate crystals grown in situ in the batch cell after 14 minutes of growth from their first observation at different

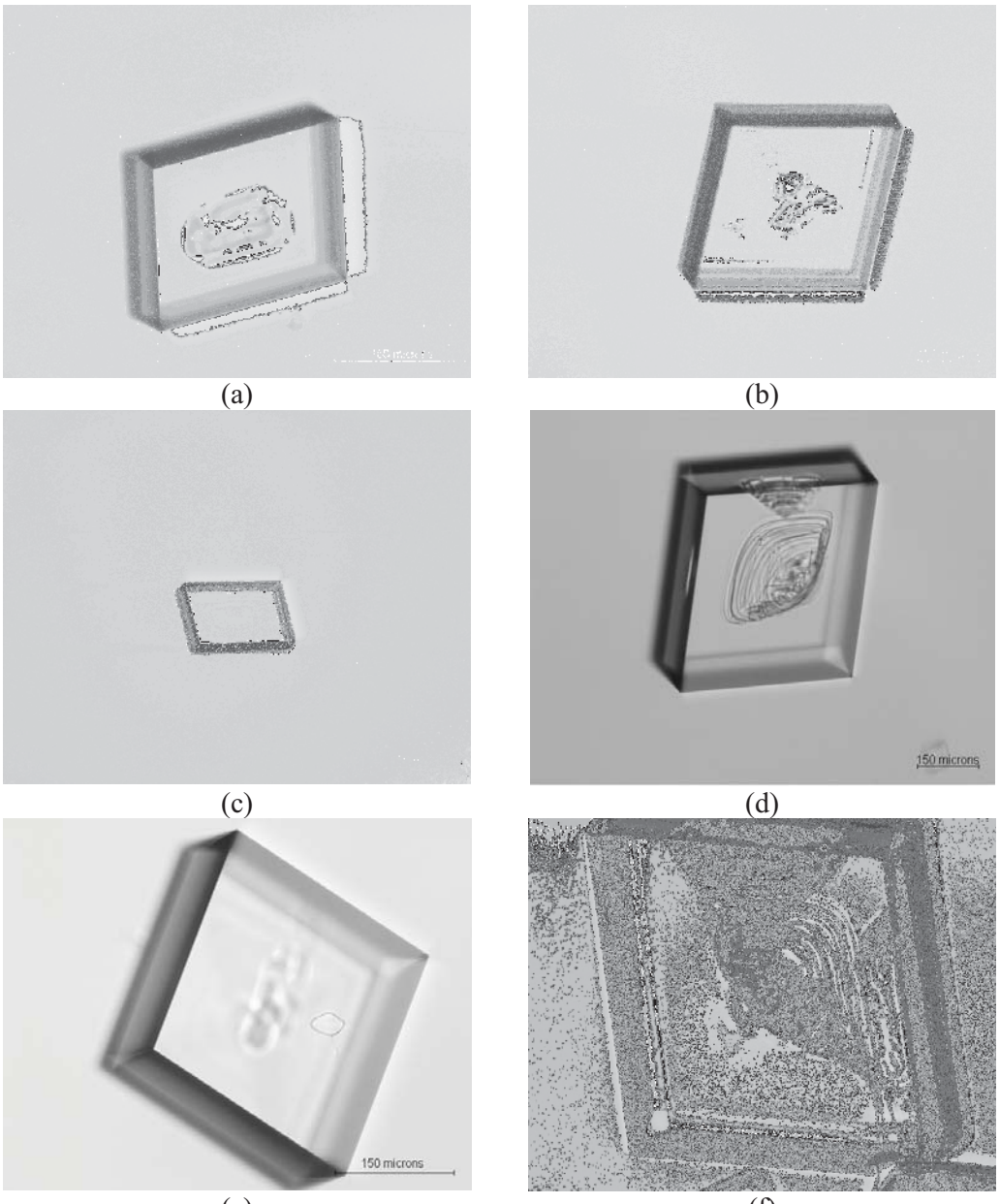

(a) (b) (c) (d) (e) (f)

Figure 4-16 Optical images of sodium nitrate crystals growing in situ in the batch cell after 14 minutes from first observation, grown at (a) 20.0°C σ = 0.02 (b) 20.0°C σ = 0.1 (c) 30.0°C σ = 0.02 (d) 30.0°C σ = 0.1 (e) 40.0°C σ = 0.02, and (f) 40.0°C σ = 0.1.

temperatures (20.0°C (a,b), 30.0°C (c,d) and 40.0°C (e,f)) and supersaturations (σ = 0.02 (a,c,e) and σ = 0.1 (b,d,f)). Liquid inclusions in some of the crystals, Figure 4-16 (d) and (f), that were grown at high supersaturation can be observed which are probably caused by their growth from a stagnant fluid, which causes a higher depletion of growth units near the crystals surface (Oosterhof et al. 1999) or from other factors such as rapid crystal growth (Mullin 1993; Myerson 1993), uneven levels of supersaturation across the crystal interface (Myerson 1993) or from growth at high supersaturations (Sangwal & Rodriguez-Clemente 1991). For the crystals grown at 20.0°C no inclusions were observed after 14 minutes of growth, but when the crystals were grown for a longer period of time liquid inclusions can be observed as shown in Figure 4-17 for the same sodium nitrate crystals shown in Figure 4-16 (a) and (b).

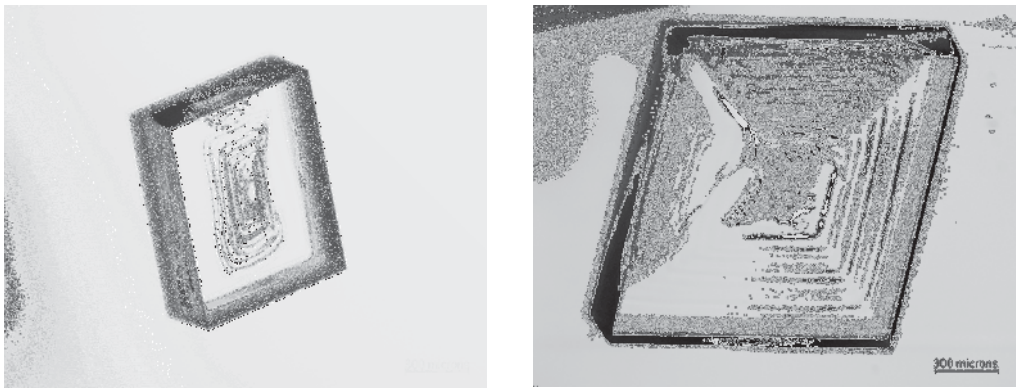

(a) (b)

Figure 4-17 Optical images of sodium nitrate crystals growing in situ in the batch cell at 20.0°C at (a) σ = 0.02 after 176 minutes of growth from first observation, and (b) σ = 0.1 after 60 minutes of growth from first observation.

These liquid inclusions were also observed to develop at the centre of the crystal faces as shown in Figure 4-18, which is the same sodium nitrate crystal shown in Figure 4-16 (a) and Figure 4-17 (a). This is because in growth controlled by volume diffusion the supersaturation on the surface is lower than in the bulk, hence resulting in a supersaturation difference on the surface of the crystal such that the supersaturation is the highest at the edges and corners of the face, and is the lowest at the centre of the face. This results in the bunching of steps whose height increases as

they advance towards to the central regions of the face, and when the step reaches the critical height after a critical distance from the edges and corners, inclusions begin to be trapped on the surface. Consequently as growth proceeds, a crystal filled with inclusions in its interior is formed (Sangwal & Rodriguez-Clemente 1991). Since these inclusions are formed during growth they are classified as primary fluid inclusions, which constitute samples of fluid in which the crystals grew (Mullin 1993).

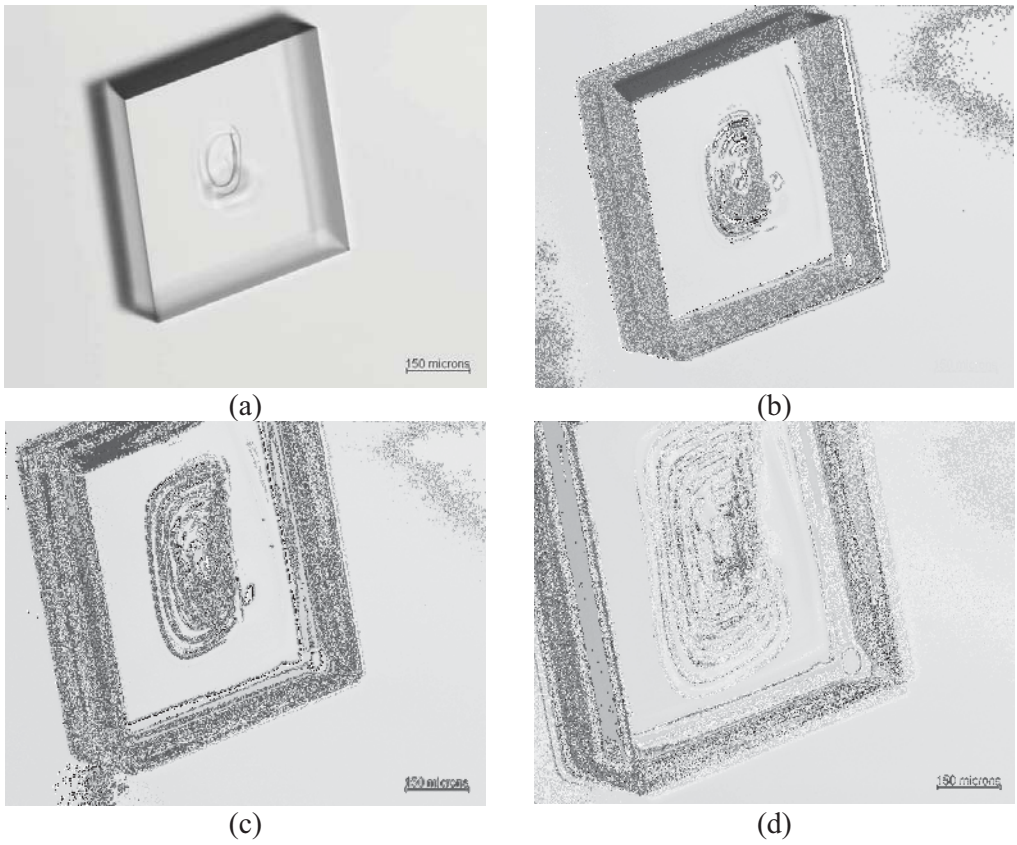

(a) (b)

(c) (d)

Figure 4-18 Optical images of a growth sequence of a sodium nitrate crystal grown in situ in the batch cell, grown at 20.0^{o}C, σ = 0.02 (a) after 80 minutes from first observation (b) after 100 minutes from first observation (c) after 120 minutes from first observation, and (d) after 160 minutes from first observation.

4.3.4.2 *Scanning Electron Microscopy (SEM)*

SEM images of sodium nitrate crystals grown at 30.0°C and 40.0°C at σ = 0.1 are shown in Figure 4-19 (a) and (b) respectively, with Figure 4-19 (c) and (d) showing the magnified secondary electron image and back scattered image of Figure 4-19 (a) respectively. No clear difference in surface roughness was observed between crystals grown at different temperatures. Nuclei observed on the crystal surface are due to the residual solution drying on the crystal surface, when the crystals were taken out from the batch cell. No nuclei on crystal surfaces were observed in optical images as they were in solution (Figure 4-4).

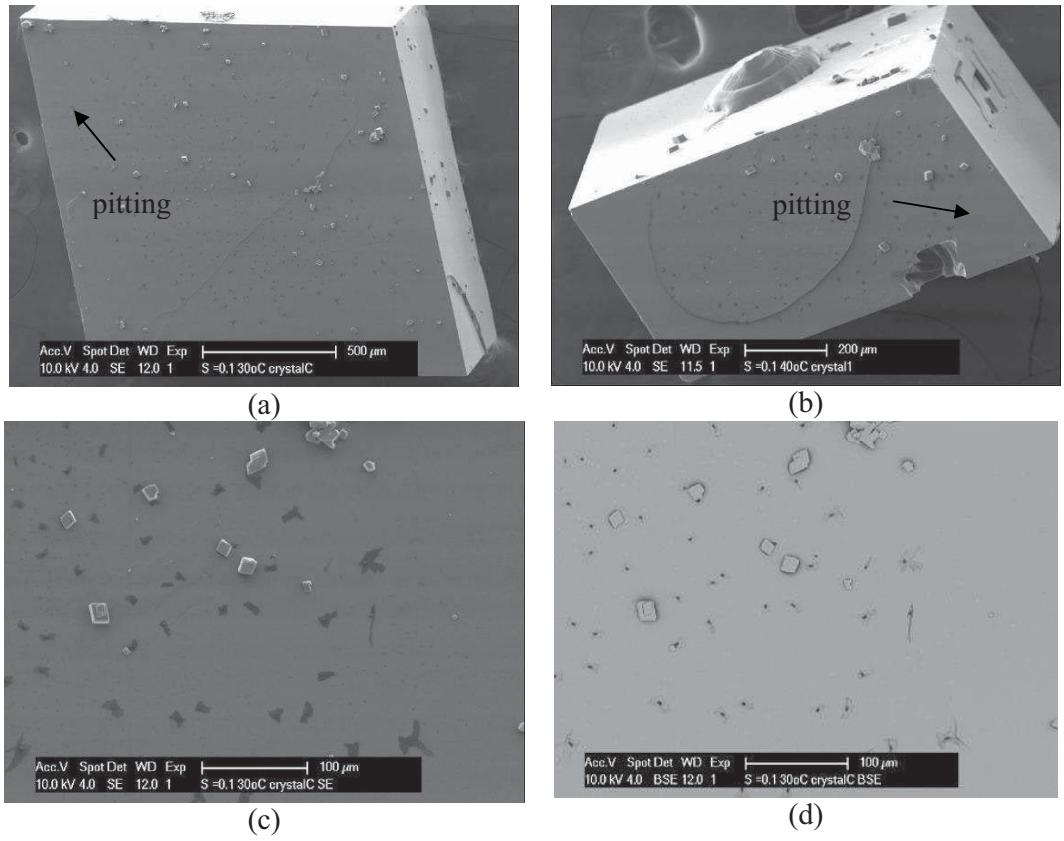

Figure 4-19 SEM images of sodium nitrate crystals grown at σ = 0.1 (a) 30.0°C and taken out of the batch cell after 35 minutes of growth (b) 40.0°C and taken out of the batch cell after 15 minutes of growth (c) the magnified secondary electron image of (a), and (d) the magnified back scattered electron image of (a).

From Figure 4-19 (a) and (b) pitting on the crystal surface can be observed, which is not an artefact due to the coating process, which is confirmed by Figure 4-19 (c) and (d), which are the magnified images of Figure 4-19 (a). The pitting observed could possibly be due to the high solubility of sodium nitrate which causes its dissolution (Hartel 2001; Mullin 1993).

4.3.4.3 *Atomic force microscopy (AFM)*

Figure 4-20 shows AFM deflection (a, c and e) and height (b, d and f) images of a sodium nitrate crystal (20.0^{o}C $\sigma = 0.04$) grown by slow evaporation in a beaker at room temperature for several days. Figure 4-20 (a) shows a growth hillock with no dislocation which suggests that growth occurs by 2D nucleation. These growth hillocks of non dislocation origin are produced by the occurrence of two-dimensional nucleation at some points on the surface, where the supersaturation is higher than the rest of the surface. These points act as centres of repeated two-dimensional nucleation for growth fronts due to this local increased supersaturation, which spread and pile upon one another to produce the hillocks. The number and location of the growth centres of non dislocation hillocks is probably determined by the growth environment, such as size and shape of the growth cell, size of the crystal face, temperature, supersaturation, impurities present in the solution, solution hydrodynamics and so on (Sangwal & Rodriguez-Clemente 1991). The shape of the growth hillock is almost rounded which indicates that growth is isotropic ie. same growth rate in all directions, and is also due to its low surface energy i.e. high solubility, and can also be from other factors such as growth from high temperature and high supersaturation (Sangwal & Rodriguez-Clemente 1991). From the height image, Figure 4-20 (b), it can be seen that the height of the hillock is about 40nm. Irregular etch pits are also observed in Figure 4-20 (c) and (d) due to the high solubility of sodium nitrate. Irregular steps are also observed in Figure 4-20 (e) and (f) and there also appears to be impurities that are present in the pure solution.

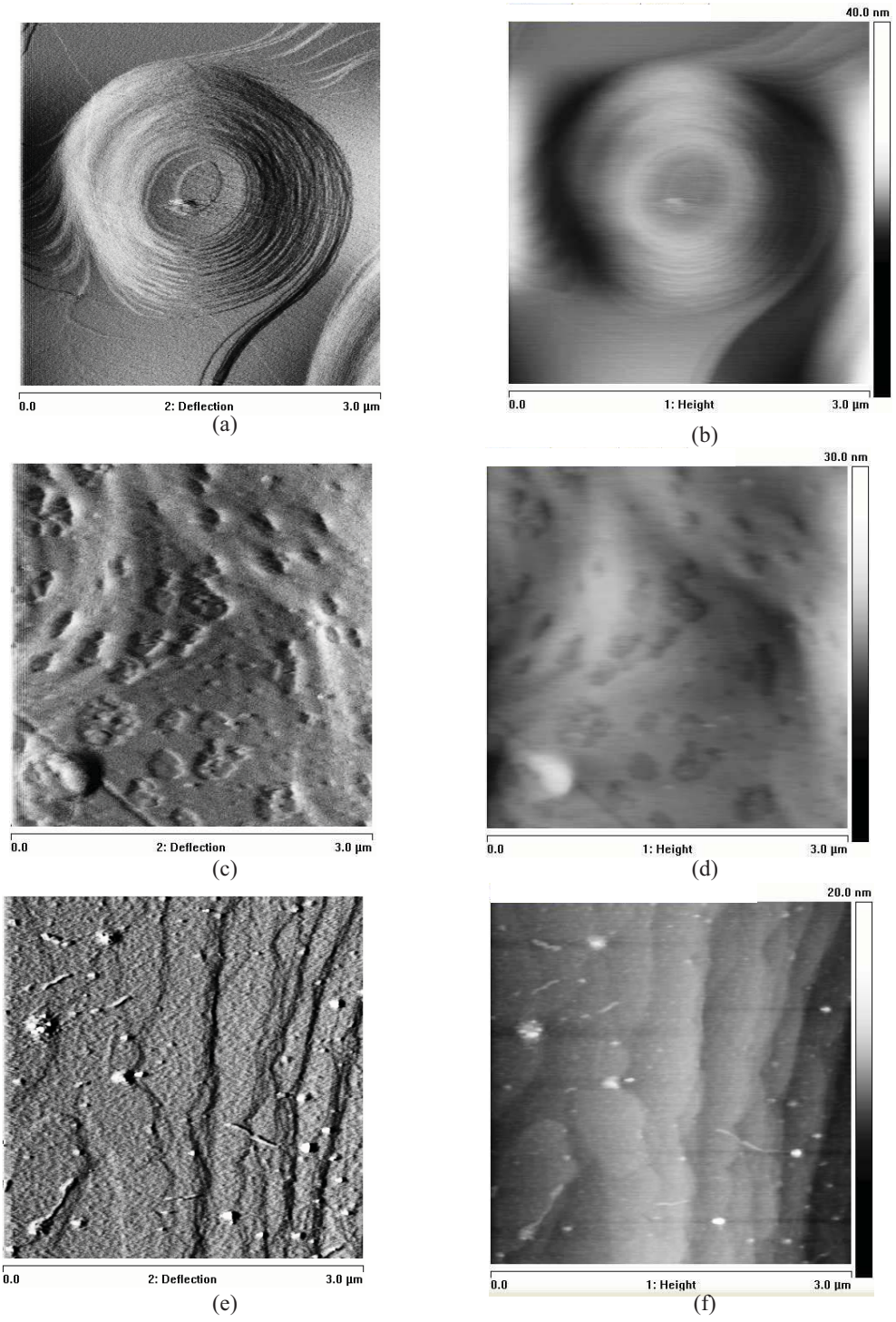

Figure 4-20 AFM deflection (a, c and e) and height (b, d and f) images of a sodium nitrate crystal (20.0°C σ = 0.04) grown by slow evaporation at room temperature for several days.

When the crystal was grown at 30.0°C, steps were also observed as shown in Figure 4-21 (a) and (b), which are not as thick in comparison to the steps observed at 20.0°C (Figure 4-20 (e)), and when the crystal was grown at 40.0°C the growth hillock features were mainly observed to occur at step edges and they were also not random (Figure 4-21 (c) and (d)). This observation is consistent with literature where an increase in supersaturation and a decrease in growth temperature results in a larger number of thick steps appearing on the crystal surface (Sangwal & Rodriguez-Clemente 1991).

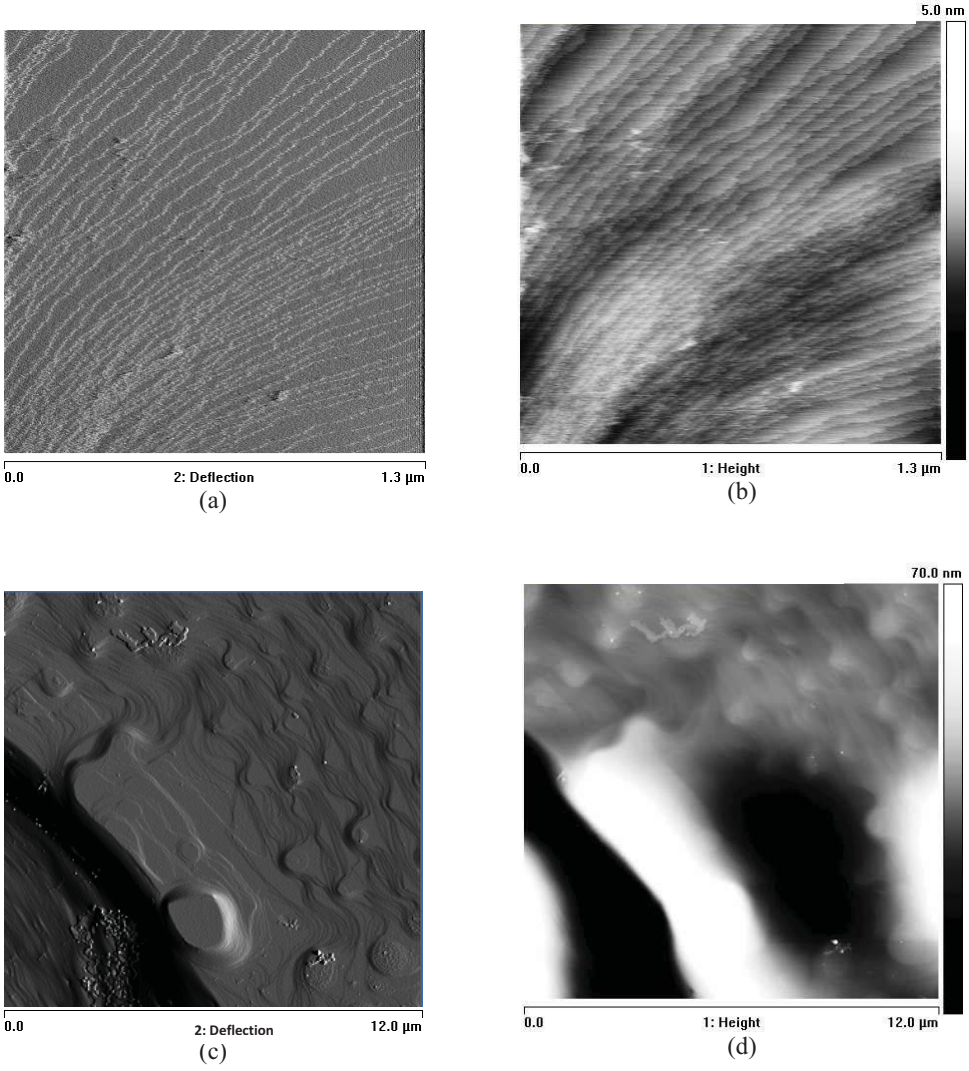

Figure 4-21 AFM deflection (a and c) and height (b and d) images of sodium nitrate crystals grown at (a, b) 30.0°C σ = 0.04, and (c, d) 40.0°C σ = 0.04 for several days.

AFM images of sodium nitrate crystals grown in the batch cell at 20.0°C σ = 0.02 and 0.1, and 40.0°C σ = 0.1 are shown in Figure 4-22 (a) to (e), respectively. No clear difference in surface topography other than crystal surface roughness was observed between the crystals. Etch pits were also observed (not shown) due to the high solubility of sodium nitrate. Growth hillocks were also observed, however in Figure 4-22 (a) it was not clear whether the growth hillocks were due to spiral or two-dimensional nucleation, as no centre was clear for the hillock.

The growth hillock is also different to that observed in Figure 4-20 (a), probably because the crystal in Figure 4-20 was grown by slow evaporation at room temperature where the temperature conditions were not controlled and the supersaturation would have increased with time as the solution evaporated. The crystal would have also grown at a much slower rate and a much larger crystal was grown. On crystals grown at 20.0°C σ = 0.1 (Figure 4-22 (c)), steps were also observed, and at 40.0°C σ = 0.1 (Figure 4-22 (e)) the growth hillock features were mainly observed to occur at step edges and they were also not random, which was also observed in Figure 4-21 (c).

These preliminary AFM results suggest that sodium nitrate crystal growth is surface integration controlled due to the presence of the growth hillocks on the crystal surface. However, it is also possible that the crystals were not dried properly after being taken out of the in situ growth cell and solution adhering to the crystal surface may have caused the formation of some nuclei and surface artefacts. Also, due to its high solubility it is very difficult to image sodium nitrate crystals in air without drying effects or with a completely clean surface.

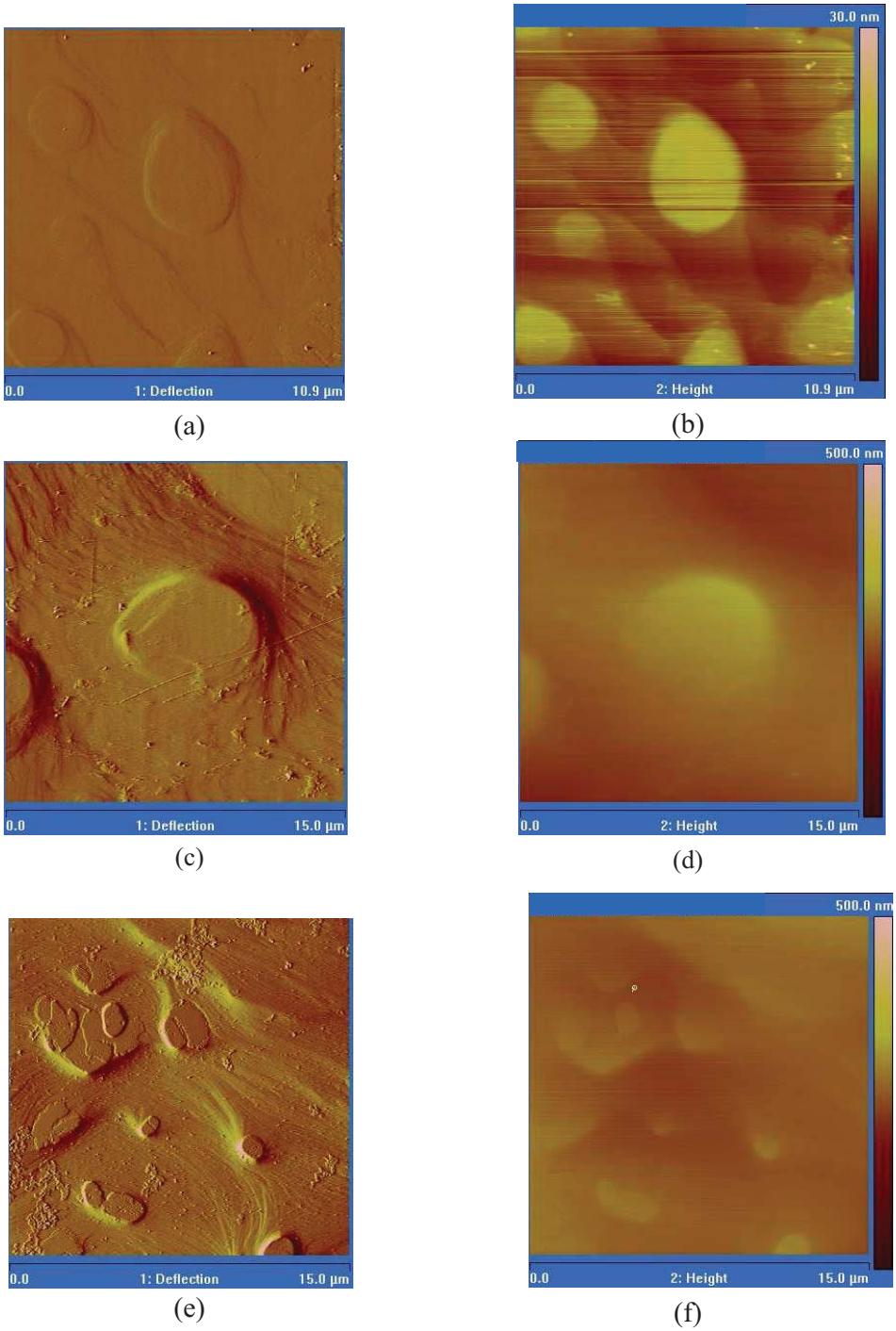

Figure 4-22 AFM deflection (a, c and e) and height (b, d and f) images of a sodium nitrate crystal grown at (a, b) 20.0°C σ = 0.02 and taken out of the batch cell after 250 minutes of growth (c, d) 20.0°C σ = 0.1 and taken out of the batch cell after 80 minutes of growth, and (e, f) 40.0°C σ = 0.1 and taken out of the batch cell after 10 minutes of growth.

4.3.5 Effect of solvent composition

Absolute ethanol solutions were prepared at different weight percents (20, 50 and 90) and relative supersaturations (0.02, 0.04 and 0.08) at 30.0°C using the solubility data from Taylor (Taylor 1897). Due to the volatility of the alcohol solutions, the solutions were prepared by refluxing in a round bottom flask with a condenser to minimise evaporation of the solvent. Solutions were filtered by vacuum through a Millipore 47mm sterifil aseptic system using a 0.2μm Supor membrane filter prior to being placed in the growth cell as shown in Figure 4-1.

4.3.5.1 *Crystal growth rates*

Crystal growth rates were determined as described in Section 4.3.1. Growth rate measurements were made on one to six crystals in each growth cell experiment, with the typical growth rate profile similar to the pure sodium nitrate system (Figure 4-5). The early stages of crystal growth was analysed when the supersaturation was assumed to be constant. Table 4-6 summarises the crystal growth rates obtained at 30.0°C for different weight percents of ethanol (20, 50 and 90) at σ = 0.02, 0.04 and 0.08, and the number of crystals that were analysed in the growth cell during an experiment or when replicate experiments were carried out (see Appendix C2).

Table 4-6 Average growth rates of sodium nitrate in aqueous ethanol grown in the batch cell at 30.0°C σ = 0.02, 0.04 and 0.08

Weight percent of ethanol	σ	Growth rate (μm/min)	Number of crystals analysed
20	0.02	2.27 ± 0.66	14
	0.04	6.01 ± 0.70	10
50	0.02	2.23 ± 0.69	11
	0.04	3.33 ± 0.36	18
	0.08	4.93 ± 0.93	29
90	0.02	0.80 ± 0.11	16
	0.04	0.82 ± 0.09	13
	0.08	1.14 ± 0.16	9

From Table 4-6 it can be observed that the growth rates decrease with increasing amounts of ethanol, which is consistent with the results obtained from Table 4-2 for

the pure aqueous system (0 weight percent ethanol), which has a much higher growth rate. As expected the growth rates also increase with increasing supersaturation at different weight percents of ethanol. Oosterhof *et al* (Oosterhof et al. 1999) also observed this trend of decreasing growth rates with increasing amounts of solvent for sodium nitrate grown in mixtures of IPE and water. Lopes and Farelo (Lopes & Farelo 2006) also observed that growth rates of potassium chloride were significantly reduced by the presence of ethanol and concluded that this was because the ethanol hinders the integration of the solute in the crystalline lattice thus retarding the solute deposition.

4.3.5.2 *Growth rate dispersion*

In order to determine the effect of crystal size on the growth rate, initial crystal size (characteristic dimension) of when the crystals were first observed in the growth cell was plotted against growth rate of the crystal. Figure 4-23 to Figure 4-25 shows the growth rates of crystals at different relative supersaturations (0.02, 0.04 and 0.08) at different weight percents of ethanol. The dotted line represents the average crystal growth rates obtained from Table 4-6. It can be clearly seen that there is no increase in growth rate with increasing crystal size, thus the crystals exhibit size independent growth. This observation is consistent with Oosterhof *et al* (Oosterhof et al. 1999) results in IPE with their results showing no evidence for size-dependent growth. From these figures it can also be observed that the initial crystal sizes are much smaller in comparison to the pure aqueous system when no ethanol was present (Figure 4-14) and with increasing weight percent of ethanol the initial crystal size decreases. This is probably due to the lower solubility of sodium nitrate in ethanol in comparison to the pure aqueous system, so there is not as much solute available in the ethanol system for the crystals to form and grow to a larger size which also accounts for the lower growth rates observed for the ethanol system.

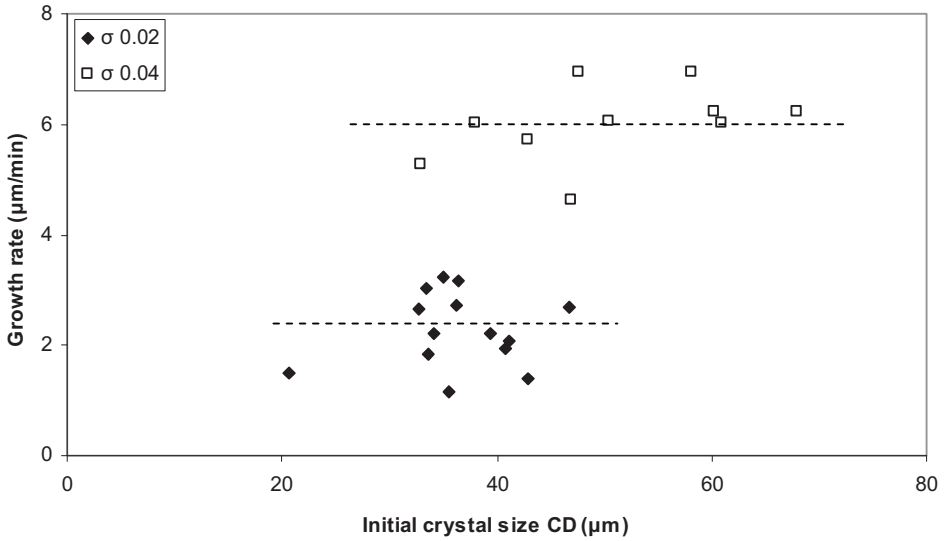

Figure 4-23 Growth rates of sodium nitrate grown at 20 weight percent ethanol, at different supersaturations ($\sigma = 0.02, 0.04$) at 30.0°C

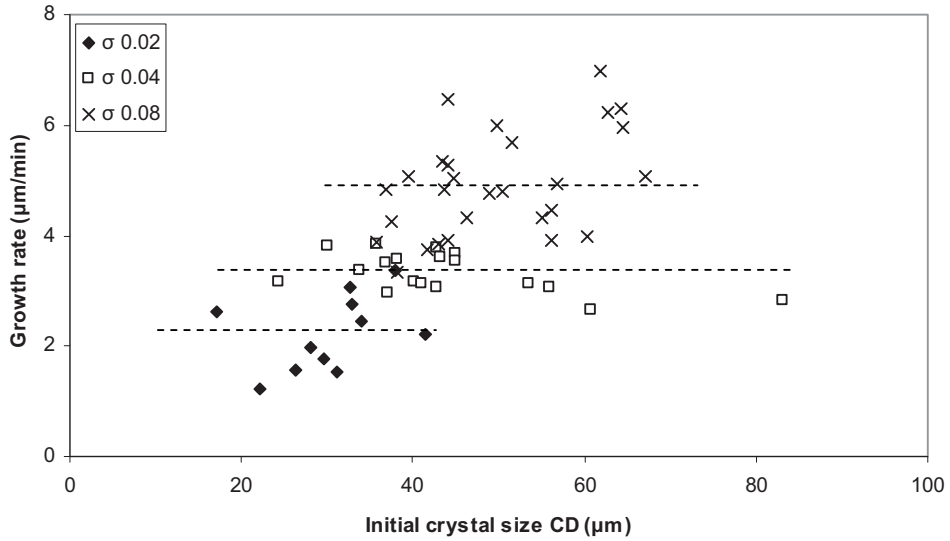

Figure 4-24 Growth rates of sodium nitrate grown at 50 weight percent ethanol, at different supersaturations ($\sigma = 0.02, 0.04, 0.08$) at 30.0°C

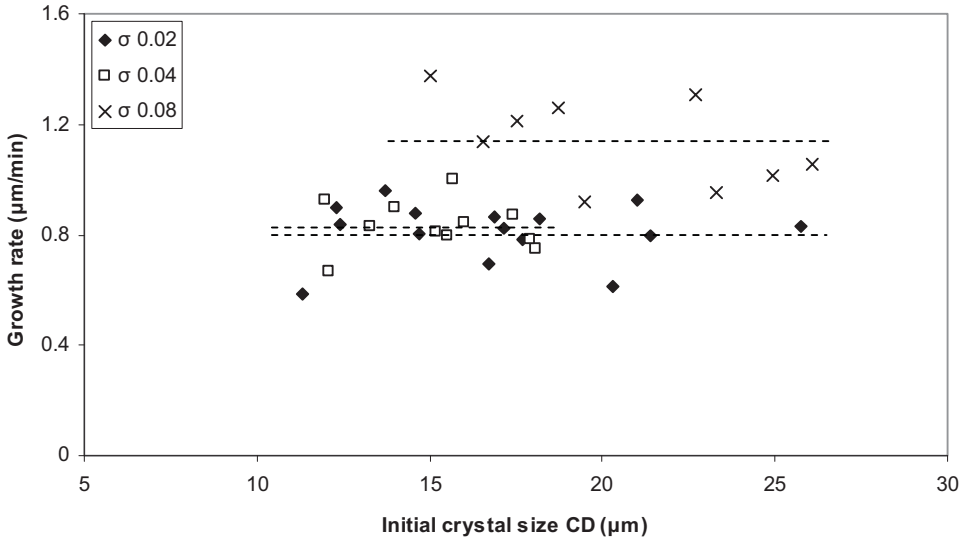

Figure 4-25 Growth rates of sodium nitrate grown at 90 weight percent ethanol, at different supersaturations (σ = 0.02, 0.04, 0.08) at 30.0°C

4.3.5.3 *Surface morphology and habit modification*

Figure 4-26 shows a growth sequence of a typical sodium nitrate crystal (30.0°C σ = 0.02, 50 weight percent ethanol) taken with the optical microscope and grown in the growth cell at different time intervals. From these images it can be observed that the crystals grow in a layer type fashion, with solute first depositing on the top left hand corner, then to the bottom left hand corner (Figure 4-26 (c)) and then back again to the bottom left hand corner (Figure 4-26 (e)). It can also be observed that the crystal surface is free from inclusions, even after 170 minutes of growth at 30.0°C. In general inclusions were not observed on crystal surfaces that were grown at low supersaturation. However, as the supersaturation increased, the weight percent of ethanol decreased, and the crystal size increased, the number of inclusions observed on the crystal surfaces increased. This is observed in Figure 4-27 where inclusions are observed at 20 weight percent ethanol at σ = 0.04, at high supersaturation (σ = 0.08) for 50 weight percent ethanol, and at 90 weight percent ethanol where only a tiny inclusion was observed in the middle of the crystal. As previously mentioned in Section 4.3.4.1, fast growth rates are often linked to inclusion formation, which is consistent with these observations since 90 weight percent ethanol has the lowest

growth rate and hardly any inclusions were observed. Also, another contributing factor could be due to the crystal size, since crystals grow regularly when they are quite small, but when a critical size is reached (65μm for crystals of hexamethylene tetramine (HMT)), cavities begin to form at the centres of the faces and these subsequently seal off forming a pattern of inclusions (Denbigh & White 1966). For 90 weight percent of ethanol the initial crystal sizes were all below 30μm (see Figure 4-25). These observations are consistent with Denbigh and White (Denbigh & White 1966) who observed that HMT crystals readily form inclusions from aqueous solutions under most conditions, but rarely when crystallised from methanol or ethanol.

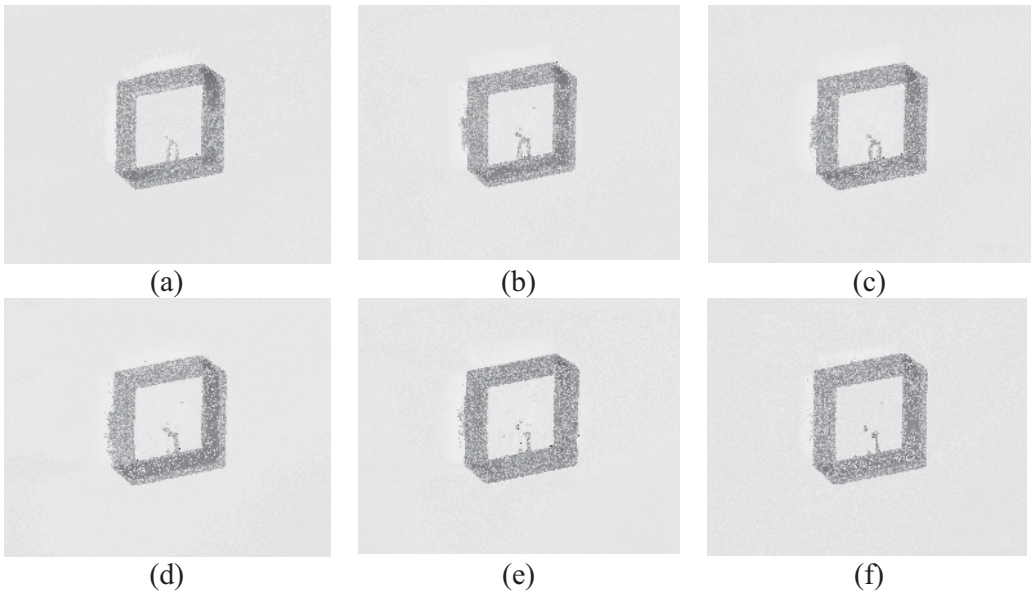

Figure 4-26 Optical images of a growth sequence of a sodium nitrate crystal grown in situ in the batch cell, grown at 30.0^{o}C σ = 0.02, 50 weight percent ethanol (a) after 158 minutes of growth (b) after 160 minutes of growth (c) after 162 minutes of growth, (d) after 166 minutes of growth (e) after 168 minutes of growth, and (f) after 170 minutes of growth

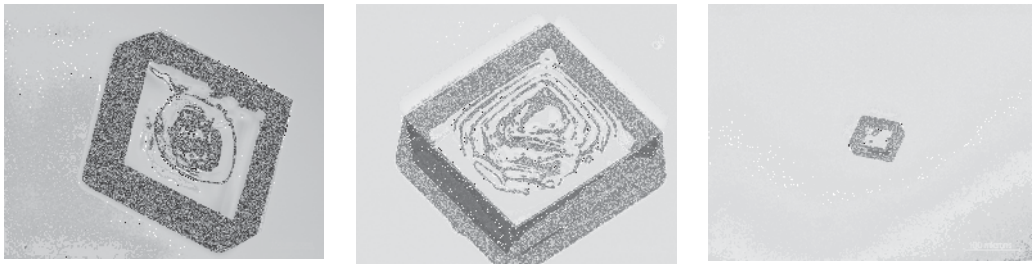

(a) (b) (c)

Figure 4-27 Optical images of sodium nitrate crystals grown in situ in the batch cell, grown at 30.0°C (a) 20 weight percent ethanol, σ = 0.04 after 95 minutes of growth (b) 50 weight percent ethanol, σ = 0.08 after 93 minutes of growth, and (c) 90 weight percent ethanol, σ = 0.04 after 120 minutes of growth

It can also be observed that the habit of the crystal remains unchanged, with this observation consistent with Oosterhof *et al* (Oosterhof et al. 1999) results in IPE who observed that the solvent composition does not effect the crystal morphology. This observation is also consistent with literature which mentions that large solvent effects are expected in crystalline systems that have faces of significant different polarity, such as succinic and adipic acid (Myerson 1993).

4.4 SEEDED CRYSTAL GROWTH EXPERIMENTS IN THE MODIFIED FLOW THROUGH CELL

Seed crystals were prepared by dissolving 85g of sodium nitrate in 100g of deionised water. A range of supersaturation levels were tested and this concentration was found to obtain the optimum sized crystals for viewing under the microscope. The solution was filtered by vacuum through a Millipore 47mm sterifil aseptic system using a 0.45μm Supor membrane filter. The solution was left in a refrigerator at approximately 4°C for four hours and the crystals formed were then filtered by vacuum and washed using a 90% ethanol solution. Seed crystals for growth rate experiments were individually selected under microscopic examination to ensure crystals were free of macroscopic defects and were of suitable size. Typical crystal seeds used in the growth cell experiments are shown in Figure 4-28.

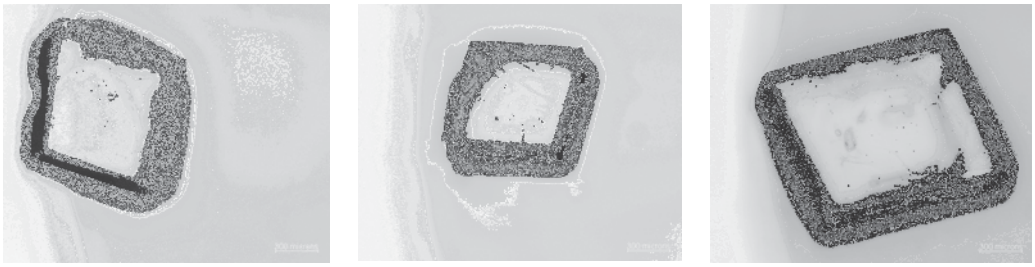

(a) (b) (c)

Figure 4-28 Typical crystal seeds used in the growth cell experiments

Sodium nitrate solutions (approximately 60g) were prepared at relative supersaturations (σ) of 0.02 and 0.04 at 20.0°C following the same procedure as for homogeneous nucleation experiments described in Section 4.3. The solutions were filtered by vacuum through a Millipore 47mm sterifil aseptic system using a 0.2μm Supor membrane filter prior to being placed in the solution reservoir as shown in Figure 4-3. The solution reservoir was covered with parafilm to minimise evaporation and contamination of the solution. Between four to six crystals were added to the upper compartment of the growth cell and the solution was circulated by a peristaltic pump at a flow rate of 4mL/min. This flow rate was chosen since higher flow rates resulted in washing away the crystals from the cell and caused nucleation in the cell. The in-situ cell was sealed after all air bubbles were removed from the system.

4.4.1 Crystal growth rates

Crystal growth rates were determined as described in Section 4.3.1. Growth rate measurements were made on two to six crystals in each growth cell experiment. Figure 4-29 shows the typical growth rate profile, the CD plotted against time. From Figure 4-29 it can be observed that the growth rate increases slightly over time in comparison to Figure 4-5 when the solution in the growth cell was stagnant. Even though the solution in the growth cell was constantly circulating it was assumed that the supersaturation only remains constant in the early stages of crystal growth, so data in this region was only analysed. This is because during growth there was some nucleation observed in the tubing connecting the solution reservoir to the peristaltic

pump and also in the growth cell and solution reservoir. This effect was minimised by insulating the tubing lines.

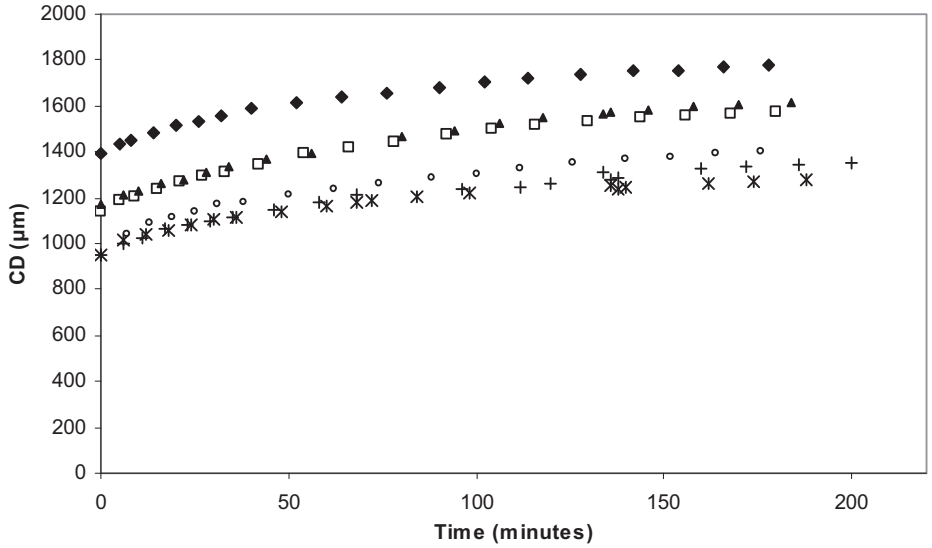

Figure 4-29 Typical plot of the growth rate profile, CD versus time for 20.0°C, σ = 0.04

Table 4-7 summarises the crystal growth rates obtained at 20.0°C at a relative supersaturation of 0.02 and 0.04 and the number of crystals that were analysed in the growth cell during an experiment or when replicate experiments were carried out (see Appendix C3). Different supersaturation levels were also trialled out at 0.01 and 0.06. However, at a supersaturation level of 0.01 the crystal seeds were observed to dissolve due to the solution being close to saturation and at 0.06 the supersaturation level was found to be too high as lots of nucleation in the growth cell was observed. Also, at higher temperatures there was a lot of nucleation observed in the tubing and growth cell so only growth at 20.0°C was investigated.

Table 4-7 Average growth rates of sodium nitrate grown in the modified growth cell at 20.0°C

σ	Growth rate (µm/min)	Number of crystals analysed
0.02	3.09 ± 0.59	13
0.04	5.48 ± 0.96	9

From Table 4-7 it can be observed that the growth rates obtained are lower than the growth rates obtained in the unseeded homogeneous nucleation experiments (Table 4-1). The growth rate at σ = 0.02 is not much different in comparison to the unseeded experiments (5.31μm/min), differing by a factor of about 2. This is reasonable since from Table 4-4 when the effect of flow rate on crystal growth rates at 20.0°C σ = 0.04 was investigated, the growth rates at different flow rates ranged from 7.37 to 10.64μm/min, differing by a factor of 2 from the mean growth rate (9.74μm/min). However, the growth rate at σ = 0.04 differs by a factor of about 4. However, it could also be attributed to the fact that homogeneous nucleation is spontaneous and not predictable, which is also why a wider dispersion in growth rates (standard deviation) was observed in comparison to the seeded experiments.

4.4.2 Fluid dynamics

The solution flowing over the crystal surface in the growth cell was checked for its dynamic condition to determine if laminar or turbulent flow was present. If turbulent flow is present this will add onto the mass transfer and it will also act in a very complex manner on the formation of liquid incorporation (Garside et al. 2002). The Reynolds number (Equation 4-3) was used to calculate the type of flow present in this "porous medium", which is defined as a collection of particles (in this case crystal seeds) with sufficient open space in or around them to enable a fluid to pass through or around them (Darby 2001). If the Reynolds number is less than 10 the flow is defined as laminar (*Australian Gas Association code AG 703* 1974).

$$N_{\mathrm{Re}} = \frac{\rho_{solution} v L}{\mu_{solution}} \tag{4-3}$$

where ρ is the density of the solution, v is the velocity of the fluid passing over the crystal surface, L is the diameter of the growth cell and μ is the viscosity of the solution.

The density and the viscosity values of the sodium nitrate solution can be described by the following equations from Graber *et al* (Graber et al. 1999).

Density of the $NaNO_3$ solution (kg/m^3):

$$\rho = 765.7535C_2 - 0.52705T + 1006 \quad (4\text{-}4)$$

where C_2 is the concentration of the solution in mass fraction and T the temperature in ^oC

Viscosity of the $NaNO_3$ solution (mPaS):

$$\mu = 0.00188508Exp\left(\frac{1833.45022}{T}\right)Exp\left(0.0837004C_1 + 0.00237765C_1^{\,2}\right) \quad (4\text{-}5)$$

where C_1 is the concentration (mol/kg H_2O) and T the temperature in K

The Reynolds number for sodium nitrate crystals grown in the modified growth cell at 20.0^{o}C and a relative supersaturation of 0.02 and 0.04 was calculated (see Appendix D for details) and the results are tabulated in Table 4-8. From the table it can be seen that the Reynolds number is less than 10 thus the flow of the solution in the growth cell over the crystal surface is laminar.

Table 4-8 Reynolds number for the sodium nitrate system grown in the modified growth cell at 20.0^{o}C σ = 0.02 and 0.04

σ	ρ solution (kg/m^3)	v (m/s)	D (m)	μ solution (PaS)	N_{re}
0.02	1683.1	$7.07x10^{-5}$	0.03	$3.10x10^{-3}$	1.15
0.04	1696.3	$7.07x10^{-5}$	0.03	$3.19x10^{-3}$	1.13

4.4.3 Growth rate dispersion

In order to determine the effect of crystal size on the growth rate, initial crystal size (characteristic dimension) was plotted against growth rate of the crystal. Crystal seeds varying in different sizes were selected so the effect of growth rate dispersion could be measured. Figure 4-30 shows the growth rates of crystals at different relative supersaturations of 0.02 and 0.04. The dotted line represents the average crystal growth rates obtained from Table 4-7. It can be clearly seen that there is no increase in growth rate with increasing crystal size, thus the crystals exhibit size independent growth.

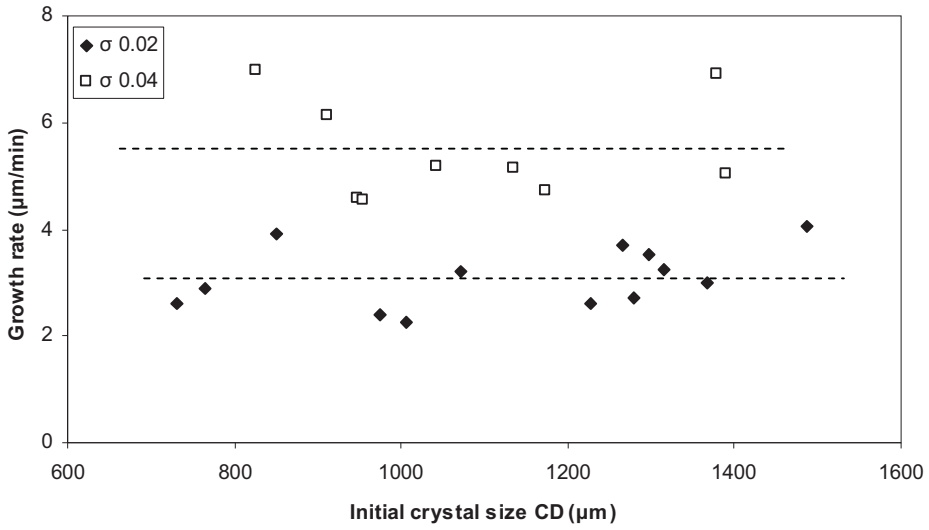

Figure 4-30 Growth rates of sodium nitrate grown at 20.0°C σ = 0.02 and 0.04

4.4.4 Surface morphology

Figure 4-31 shows a growth sequence of a typical sodium nitrate crystal (20.0°C σ = 0.02) taken with the optical microscope and grown in the growth cell at different time intervals, with Figure 4-28 (a) showing the crystal seed before it was placed in the growth cell. From Figure 4-31 it can be observed that in comparison to the homogeneous nucleation experiments (Figure 4-17) liquid inclusions at the centre of the crystal face were not observed. It can also be observed that on the top left hand corner and bottom right hand corner of the crystal that the solute deposits on the crystal surface, probably due to the crystal growth mechanism. This effect is more pronounced when the crystals were grown in the presence of alcohol (Figure 4-35). This is due to the reason as explained in Section 4.3.4.1 that there is a supersaturation difference on the surface of the crystal such that the supersaturation is the highest at the edges and corners of the face, and is the lowest at the centre of the face, thus causing more solute to be delivered to the centre of the crystal.

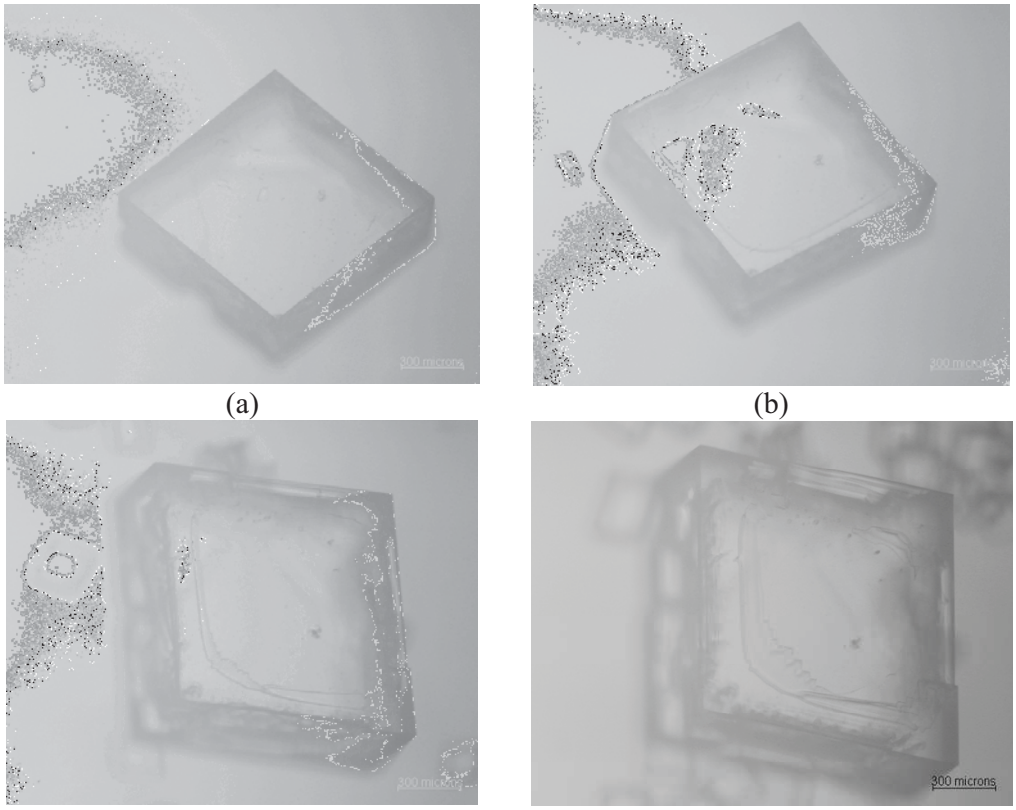

(a) (b)

(c) (d)

Figure 4-31 Optical images of a growth sequence of a sodium nitrate crystal grown in situ in the growth cell, grown at 20.0°C σ = 0.02 (a) after 1 minute of growth (b) after 16 minutes of growth (c) after 76 minutes of growth, and (d) after 148 minutes of growth

4.4.5 Effect of solvent composition

Absolute ethanol solutions were prepared at different weight percents (30, 50 and 90) and relative supersaturations (0.02 and 0.04) at 20.4°C using the experimental solubility data obtained from Chapter 3. Only selected methanol solutions at different weight percents (30, 50 and 90) and relative supersaturations (0.02) were prepared at 20.0°C. Due to the volatility of the alcohol solutions, the solutions were prepared by refluxing in a round bottom flask with a condenser to minimise evaporation of the solvent. Solutions were filtered by vacuum through a Millipore 47mm sterifil aseptic system using a 0.2μm Supor membrane filter prior to being placed in the growth cell as shown in Figure 4-3.

4.4.5.1 *Crystal growth rates*

Crystal growth rates were determined as described in Section 4.3.1. Growth rate measurements were made on three to six crystals in each growth cell experiment, with the typical growth rate profile similar to the pure sodium nitrate system (Figure 4-29). The early stages of crystal growth was analysed when the supersaturation was assumed to be constant, except for 90 weight percent in which the full duration of the experiment was analysed due to the relative low growth rates obtained. Table 4-9 and Table 4-10 summarises the crystal growth rates obtained at 20.4°C for different weight percents of ethanol (30, 50 and 90) at σ = 0.02 and 0.04 and the crystal growth rates obtained at 20.0°C for 50 weight percent methanol at σ = 0.02 respectively, and the number of crystals that were analysed in the growth cell during an experiment or when replicate experiments were carried out (see Appendix C4).

Table 4-9 Average growth rates of sodium nitrate in aqueous ethanol grown in the growth cell at 20.4°C σ = 0.02 and 0.04

Weight percent of ethanol	σ	Growth rate (μm/min)	Number of crystals analysed
30	0.02	2.34 ± 0.62	10
	0.04	4.40 ± 0.73	5
50	0.02	2.19 ± 0.44	9
	0.04	2.64 ± 0.32	6
90	0.02	0.16 ± 0.02	4
	0.04	0.14 ± 0.03	3

Table 4-10 Average growth rates of sodium nitrate in aqueous methanol grown in the growth cell at 20.0°C σ = 0.02

Weight percent of methanol	σ	Growth rate (μm/min)	Number of crystals analysed
50	0.02	1.12 ± 0.12	6

From Table 4-9 it can be observed that the growth rates decrease with increasing amounts of ethanol, which is consistent with the results obtained from Table 4-7 for the pure aqueous system (0 weight percent ethanol), which has a much higher growth rate, and was also observed in Section 4.3.5.1 for the homogeneous nucleation ethanol experiments. Oosterhof *et al* (Oosterhof et al. 1999) also observed this trend

of decreasing growth rates with increasing amounts of solvent for sodium nitrate grown in mixtures of IPE and water. As expected the growth rate also increases with increasing supersaturation at different weight percents of ethanol. However, at 90 weight percent the growth rate of the crystals are low and the values are quite similar. In comparison to the methanol system at 50 weight percent σ = 0.02 (Table 4-10) it can be observed that the growth rate is much lower than the ethanol system.

4.4.5.2 *Growth rate dispersion*

In order to determine the effect of crystal size on the growth rate, initial crystal size (characteristic dimension) was plotted against growth rate of the crystal. Figure 4-32 to Figure 4-34 show the growth rates of crystals at different relative supersaturations (0.02 and 0.04) at each different weight percent of ethanol. The dotted line represents the average crystal growth rates obtained from Table 4-9. It can be clearly seen that there is no increase in growth rate with increasing crystal size, thus the crystals exhibit size independent growth which was also observed in Section 4.3.5.2 for the homogeneous nucleation ethanol experiments. This observation is also consistent with Oosterhof *et al* (Oosterhof et al. 1999) results in IPE with their results showing no evidence for size-dependent growth.

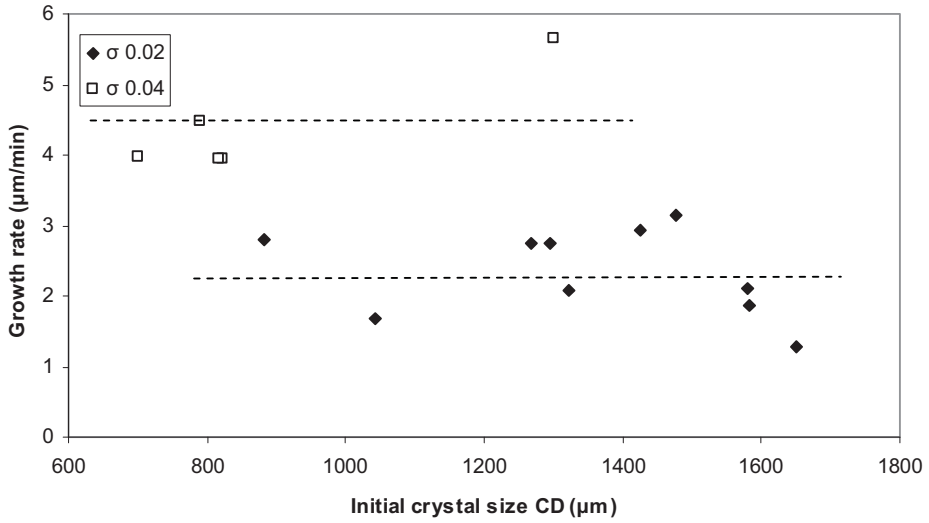

Figure 4-32 Growth rates of sodium nitrate at 20.4°C, 30 weight percent ethanol σ = 0.02 and 0.04

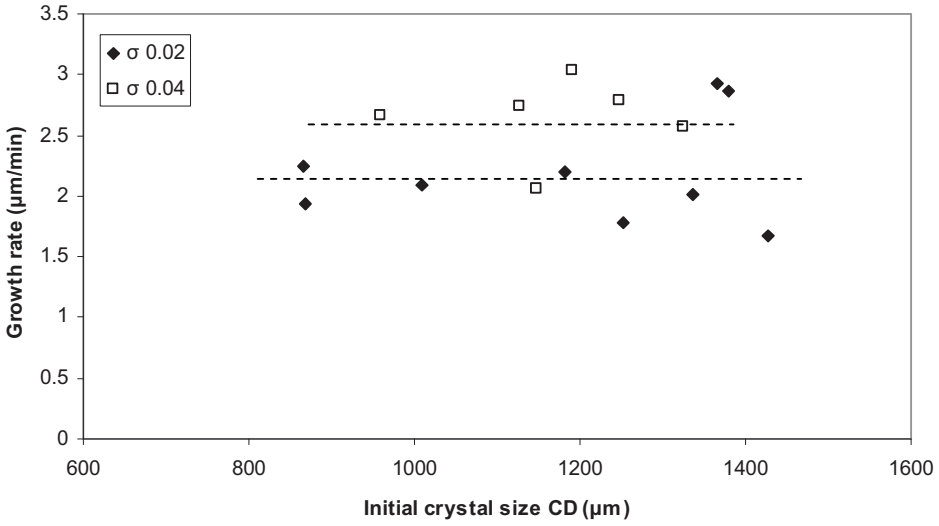

Figure 4-33 Growth rates of sodium nitrate at 20.4°C, 50 weight percent ethanol σ = 0.02 and 0.04

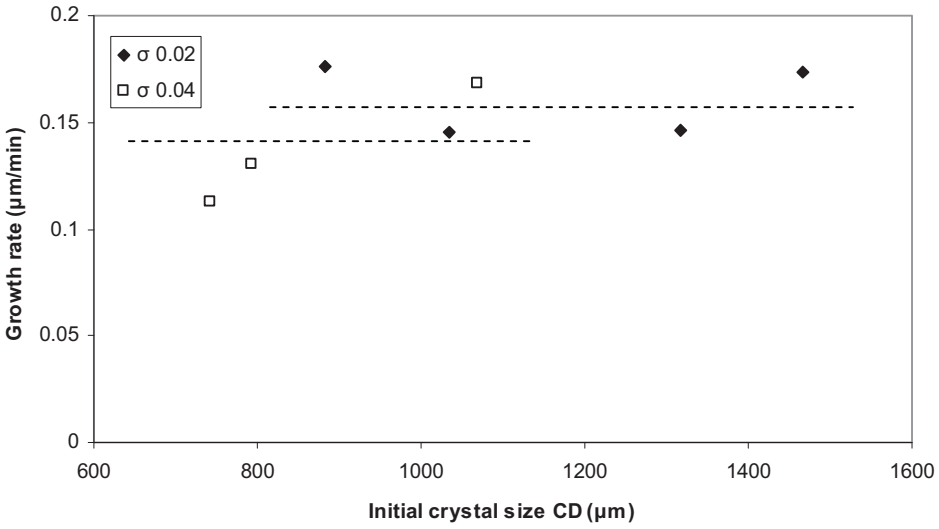

Figure 4-34 Growth rates of sodium nitrate at 20.4°C, 90 weight percent ethanol σ = 0.02 and 0.04

4.4.5.3 *Surface morphology and habit modification*

Figure 4-35 shows a growth sequence of a typical sodium nitrate crystal (20.4°C σ = 0.02, 50 weight percent ethanol) taken with the optical microscope and grown in the

growth cell at different time intervals. It can be observed that on the surface of the crystal there are some liquid inclusions which are different to what was observed in the homogeneous nucleation experiments for ethanol (Figure 4-27), and the solute also deposits on the crystal surface.

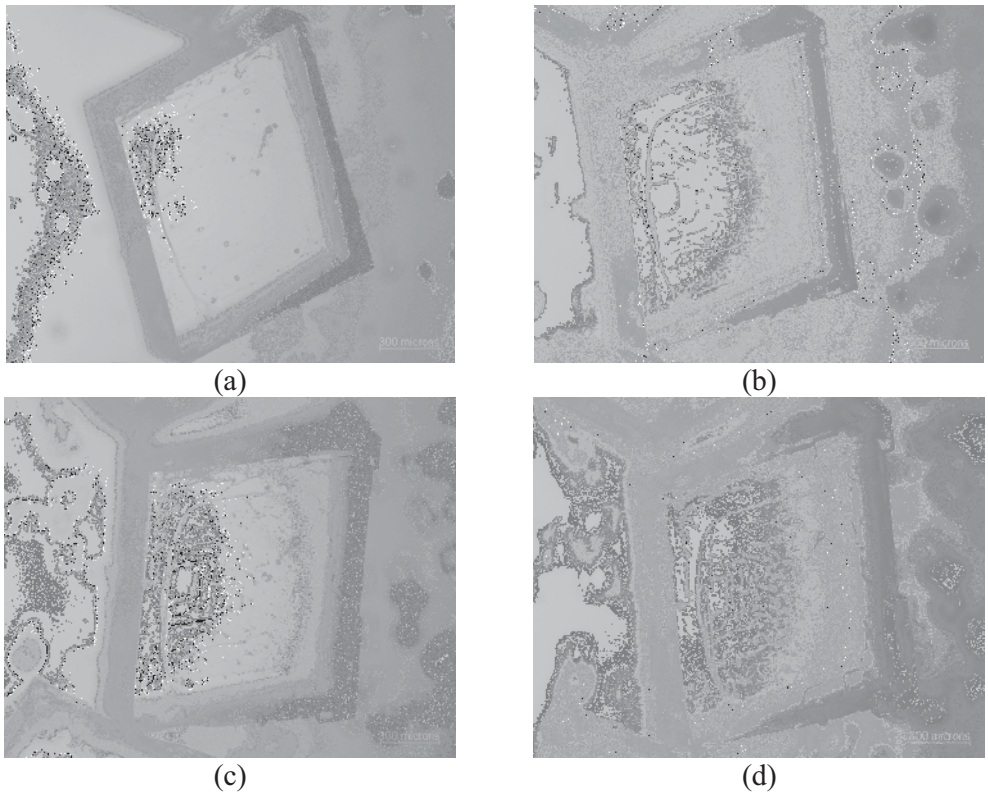

Figure 4-35 Optical images of a growth sequence of a sodium nitrate crystal grown in situ in the growth cell, grown at 20.4^{o}C σ = 0.02, 50 weight percent ethanol (a) after 8 minutes of growth (b) after 38 minutes of growth (c) after 86 minutes of growth, and (d) after 176 minutes of growth

The same surface morphology was also observed at different supersaturations and at 30 and 50 weight percent of ethanol as shown in Figure 4-36. However, at 90 weight percent of ethanol no liquid inclusions can be observed on the crystal surface and also the solute does not deposit on the crystal surface even after 226 minutes of growth (Figure 4-36 (c)). This observation is consistent with the low crystal growth rates obtained at this weight percent. The habit of the crystal also remains unchanged, as was also observed in Section 4.3.5.3 for the homogeneous nucleation

ethanol experiments. This observation is consistent with Oosterhof *et al* (Oosterhof et al. 1999) results in IPE who observed that the solvent composition does not effect the crystal morphology.

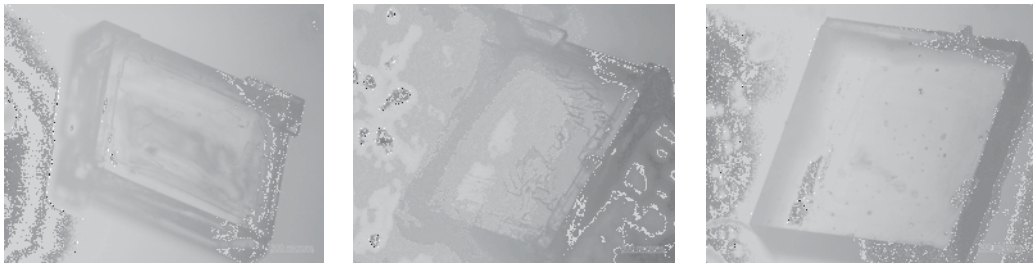

(a) (b) (c)

Figure 4-36 Optical images of sodium nitrate crystals grown in situ in the growth cell, grown at 20.4°C (a) 30 weight percent ethanol, σ = 0.02 after 90 minutes of growth (b) 50 weight percent ethanol, σ = 0.04 after 90 minutes of growth, and (c) 90 weight percent ethanol, σ = 0.02 after 226 minutes of growth

The effect of changing the solvent system to methanol was also studied as shown in Figure 4-37 below, where it can be observed that there is no change in the crystal habit with different weight percents of methanol (30, 50 and 90) at 20.0°C. In comparison to the ethanol system for the same weight percent of alcohol (30 and 50) and time of growth (~90 minutes), it can be observed that the solute only deposits a small amount on the crystals grown in methanol.

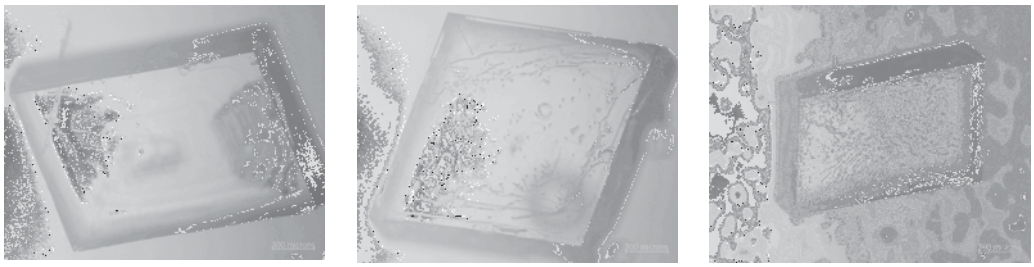

(a) (b) (c)

Figure 4-37 Optical images of sodium nitrate crystals grown in situ in the growth cell, grown at 20.0°C (a) 30 weight percent methanol, σ = 0.02 after 90 minutes of growth (b) 50 weight percent methanol, σ = 0.02 after 90 minutes of growth, and (c) 90 weight percent methanol, σ = 0.02 after 88 minutes of growth

This observation is consistent with the lower growth rates obtained in methanol than in ethanol. It can also be observed that liquid inclusions are observed on the surface of the crystals, which are affected at much higher weight percents of alcohol, the opposite trend to what was observed for the ethanol system.

Summary

- In the batch cell crystal growth rates were obtained for homongeneous nucleation experiments at different temperatures (20.0^{o}C, 30.0^{o}C and 40.0^{o}C) and relative supersaturations, σ (0.02, 0.04, 0.06, 0.08 and 0.1) to determine the kinetics of growth. A combined growth order, g of 1 and activation energy of 23,580 J/mol was obtained which suggests that crystal growth might be controlled by diffusion which is consistent with the results obtained from literature.

- To confirm that growth in the batch cell was diffusion controlled the effect of different flow rates on the crystal growth rates were tested in a modified growth cell, and higher flow rates did not increase the crystal growth rates, suggesting that growth was surface integration controlled. However, the flow rates tested were in the laminar region due to their low Reynolds number so from these results it could not be concluded that growth was surface integration controlled.

- The effect of initial crystal size on the growth rate was investigated for growth rate dispersion in the homogenous nucleation experiments, seeded crystal growth experiments and when the solvent composition was changed. For all cases size independent growth was observed.

- Sodium nitrate crystals grown by homogeneous nucleation in the batch cell contain liquid inclusions when grown at high temperatures and for a long duration. SEM images revealed the presence of pitting on the crystal surface due to the high solubility of sodium nitrate, while AFM images showed the presence of growth hillocks which suggests that crystal growth is surface integration controlled. However, the presence of the growth hillocks could

have been caused by the formation of some nuclei and surface artefacts when the crystal was taken out from solution.

- In seeded crystal growth experiments for the pure aqueous system and in aqueous ethanol and methanol, the solute deposits on the crystal surface. This was observed mainly to occur in the ethanol system at low alcohol weight percents.

- Sodium nitrate crystals grown in aqueous ethanol by homogeneous nucleation in the batch cell have a lower number of inclusions on the crystal surface in comparison to the pure aqueous system. In general, as the supersaturation increased, the weight percent of ethanol decreased, and the crystal size increased, the number of inclusions observed on the crystal surfaces increased.

- Crystal growth rates obtained in the modified growth cell using seeds were lower in comparison to crystal growth rates obtained in the homogeneous nucleation experiments. This could have been attributed to the fact that homogeneous nucleation is spontaneous and not predictable, which is also why a wider dispersion in growth rates was observed in comparison to the seeded experiments.

- The Reynolds number for the modified growth cell at a flow rate of 4mL/min was calculated and flow in the growth cell was confirmed to be laminar.

- The composition of the solvent system is found to have a significant influence on the crystal growth rates of sodium nitrate. The addition of aqueous ethanol and methanol to the sodium nitrate system results in a decrease in the crystal growth rates compared to the pure aqueous system and the habit of the crystal remains unchanged.

Chapter 5
EFFECT OF ADDITIVES ON THE HABIT MODIFICATION OF SODIUM NITRATE

5.1 INTRODUCTION

The literature review performed in Chapter 2 showed that the crystal habit of sodium nitrate crystals were modified by various researchers (Butchart & Whetstone 1949; Perelman & Strakhova 1938; Weinland & France 1932; Whetstone 1955ab), mainly with the use of dyes. The habit of sodium nitrate was changed by the appearance of triangular truncations or octahedral facets replacing one or more corners of the crystal (Weinland & France 1932). A review of the literature indicates that no recent work has been performed on using dyes or additives to change the crystal habit of sodium nitrate. Also, the sodium nitrate crystal is already isometric, a form preferred over plate or needle like habits, which is perhaps another reason why limited work has been carried out on changing its habit. Therefore in the present study, the effect of additives on the crystal habit modification of sodium nitrate will be studied by using the growth cell and the optical microscope to observe the change in crystal habit.

5.2 METHODOLOGY

5.2.1 Materials

Saturated sodium nitrate solutions were prepared from analytical reagent grade sodium nitrate (BDH AR, ≥99.5%) and deionised water (purified by a Millipore Elix 10). The additives amaranth (dye content ~90%), evans blue (dye content ~85%) and

Bismark Brown R were obtained from Sigma-Aldrich, and the surfactant DOWFAX 3B2 (45% solution) was obtained from the DOW Chemical Company.

5.2.2 Preparation of additive solutions

Stock solutions of the additives ranging in different concentrations were prepared with 60μL of each stock solution added to a supersaturated solution of sodium nitrate (σ = 0.04 20.0°C) so that ppm values (mg/L) of 3.8, 22.5, 90, 225 and 450 resulted for DOWFAX 3B2 and ppm values (mg/L) of 50, 100 and 225 resulted for amaranth. Since such low volumes of additives were used it was assumed that the effect of the additive on the solubility of the sodium nitrate solutions were negligible. The sodium nitrate solutions with 60μL of the stock solution were then dissolved by heat using a hot plate and magnetic stirrer to a temperature slightly higher than the experimental temperature, filtered with 0.2μm acrodisc syringe filters and placed in the batch growth cell (described in Section 4.2.2) set at 20.0°C. In each experiment 3 to 5 crystals were monitored for crystal habit modification.

5.3 REVIEW ON ADDITIVES USED

5.3.1 DOWFAX 3B2

DOWFAX 3B2 is an alkylated diphenyloxide disulfonate with its basic molecular structure shown in Figure 5-1 (Farn 2006). Its composition is decyl(sulfophenoxy) benzene sulfonic acid, disodium salt (C_{10}) and it has a molecular weight of 542 (Evanko et al. 1996). It contains two negatively charged sulfonate groups (head groups) per tail group, which provides increased electrostatic repulsion and potentially greater hard water resistance for the same molar concentration of anionic surfactant (Zimmerman et al. 2004). It is also an anionic surfactant that is supplied as a 45% active solution, with the inactive components water and small amounts of sodium chloride (~0.75%) and sodium sulphate (1.5% max) (Dow) and it finds many applications in textiles, cleaning, pulp and paper, oil field chemicals (Dow), hard water applications since the surfactant is not affected by mono- or divalent ions

(Dow 2002), and crystal habit modification (Arlow 2003; Dow 2002). It also has excellent solubility and stability in acidic and alkaline solutions due to its disulfonated structure (Dow 2002), bleach and other oxidising systems (Dow). In crystallisation studies DOWFAX 3B2 has been used to suppress the growth rate of potassium nitrate (Kipp & Lacmann 1996), its influence on the growth behaviour and habit of potassium nitrate has been studied by Kipp *et al* (Kipp, Lacmann & Rolfs 1997) and it acts as a growth inhibitor for gypsum in phosphoric acid (Arlow 2003).

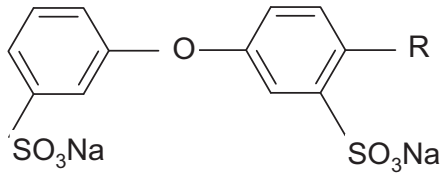

Figure 5-1 Molecular structure of DOWFAX 3B2

5.3.2 Organic dyes

Amaranth, also known as acid red 27, FD & C Red dye No. 2 and azorubin S is a mono-azo-organic dye with its molecular structure shown in Figure 5-2. It has been used in crystallisation studies to make coloured potassium dihydrogen phosphate (KDP) crystals and its influence on supersaturation and dye concentration in the solution on the colour and crystal habit modification of KDP has been studied (Hirota et al. 2002; Kumaresan et al. 2008a; Kumaresan, Babu & Anbarasan 2008b). Kipp *et al* (Kipp, Lacmann & Rolfs 1997) has also used amaranth to determine the face specific growth rates of potassium nitrate in aqueous solution and its effect on crystal habit and surface topographies. Butchart and Whetstone (Butchart & Whetstone 1949) also used amaranth to determine the effect of crystal habit modification on ammonium nitrate IV, ammonium sulphate, potassium nitrate and sodium nitrate. In all cases amaranth was effective in producing habit modification, however for sodium nitrate it was noted that in the change from the orthorhombic to trigonal system, the effectiveness of amaranth in modifying the habit is apparently lost, and dyes such as induline, gallophenine, and acid green GG extra were found effective in bringing about habit modification.

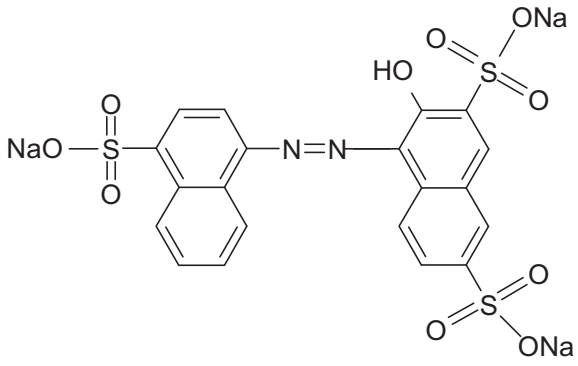

Figure 5-2 Molecular structure of amaranth

5.4 RESULTS AND DISCUSSION

5.4.1 Effect of DOWFAX 3B2 on morphology of sodium nitrate crystals

Figure 5-3 shows the growth sequence of a typical sodium nitrate crystal that was grown with 3.8ppm DOWFAX 3B2, where it can be observed that even after 462 minutes of growth in the batch cell that the crystal habit was not modified. This is probably due to the low concentration of additive added and also due to the growth cell design since the solution is stagnant so a constant liquor composition cannot be maintained for a long duration. This type of behaviour has also been observed for the potassium dihydrogen phosphate (KDP) system using the organic dyes amaranth and sky blue. When low concentrations of amaranth are present in the solution the crystal is not modified, whereas higher concentrations of amaranth produce hourglass crystals (Hirota et al. 2002). In a continuous mixed suspension mixed product remover (MSMPR) crystalliser, crystals in solutions with low dye-concentrations (sky blue) generate regular-shaped KDP crystals, whereas crystals from solution with high dye-concentration form special shaped KDP crystals (Miki et al. 2005).

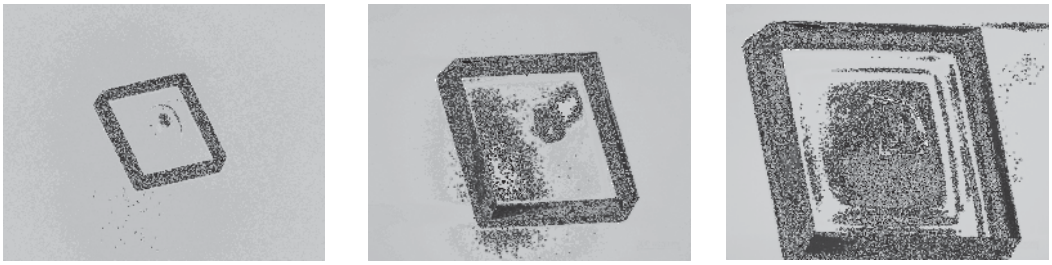

(a) (b) (c)

Figure 5-3 Growth sequence of a sodium nitrate crystal (20.0°C σ =0.04) grown with 3.8ppm DOWFAX 3B2 (a) after 82 minutes from first observation (b) after 174 minutes from first observation, and (c) after 462 minutes from first observation

When 22.5ppm DOWFAX 3B2 was used as shown in Figure 5-4, triangular truncations or octahedral faces at the corners of the sodium nitrate crystal was observed which Weinland and France (Weinland & France 1932) also observed when studying the influence of various dyes on the crystal habit of sodium nitrate which are induced artificially through the process of adsorption of these faces. They also concluded that since adsorption slows up the rate of displacement of these faces and since the rate of perpendicular displacement of the regular faces is not interfered with, by the adsorption of the additive, the octahedral faces at the corners of the rhombohedron must of necessity develop, as shown by (a) and (b) in Figure 5-5. This figure which is drawn from x-ray data, shows that the octahedral faces are populated by ions of like charge whereas the normally occurring cube faces are made up of mixtures of positive and negative ions. The adsorptive effects are greater at the octahedral faces due to the partial polarisation of the residual valencies on the cube faces (Weinland & France 1932).

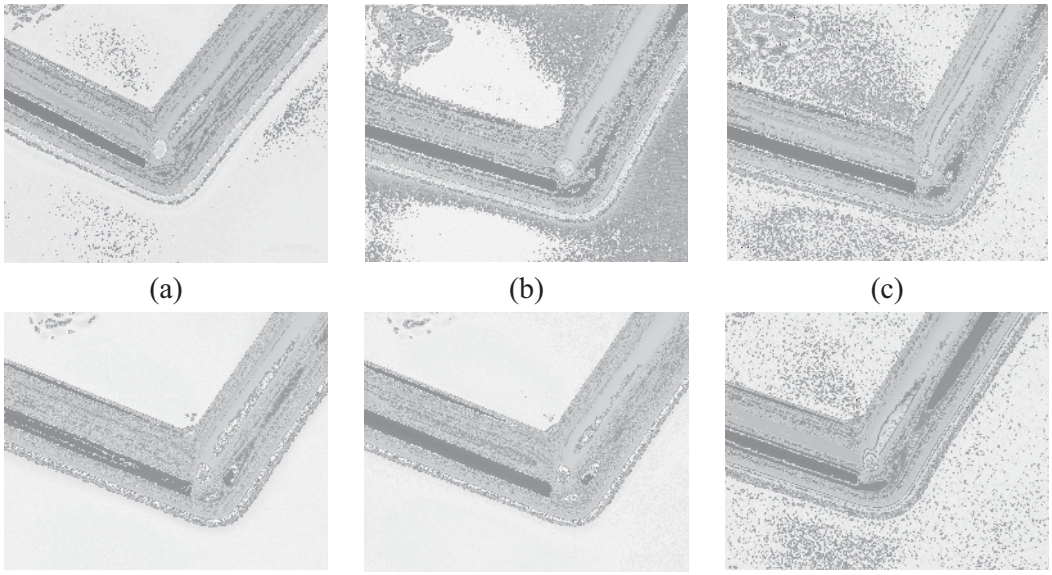

Figure 5-4 Growth sequence of a sodium nitrate crystal (20.0°C σ =0.04) grown with 22.5ppm DOWFAX 3B2 (a) after 244 minutes from first observation (b) after 262 minutes from first observation (c) after 264 minutes from first observation (d) after 308 minutes from first observation (e) after 310 minutes from first observation, and (f) after 346 minutes from first observation

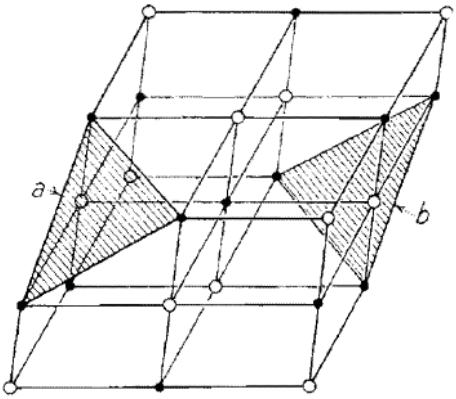

Figure 5-5 Arrangement of Na^+, (°) and NO_3^-, (•) ions in sodium nitrate rhombohedron (Weinland & France 1932)

From Figure 5-4 it can also be observed that once the crystal is modified, after about 20 minutes of growth the corner of the crystals then starts to recover and return to its original form (Figure 5-4 (c)). This process is again repeated as shown in Figure 5-4 (d) and (e), but the corner of the crystal recovers back to its original form much quicker in about 2 minutes. This is also observed when a concentration of 90ppm is used as shown in Figure 5-6. This is probably due to the adsorption process of the additive onto the growing crystal surface, most probably at kink sites, since the additive is present a low concentration and also because such sites offer the highest binding energy. The additive blocks the surface of the crystal and prevents access of the growth molecules and diffuses "two-dimensionally" on the surface as it is swept away in the advancement of steps, therefore decreasing the velocity of growth layers and hence the crystal growth rate. However, since the additive is present at low concentrations not all sites on the crystal surface are blocked and the crystal can proceed to grow as normal at a higher growth rate thus causing the crystal habit to return back to its original form. This is only speculation since this type of behaviour was not observed at high additive concentrations and needs to be confirmed.

(a) (b) (c)

Figure 5-6 Growth sequence of a sodium nitrate crystal (20.0°C σ =0.04) grown with 90ppm DOWFAX 3B2 (a) after 204 minutes from first observation (b) after 226 minutes from first observation, and (c) after 236 minutes from first observation

When higher concentrations of 225 and 450ppm of DOWFAX 3B2 was used the crystal habit was modified in a similar fashion to when lower concentrations of DOWFAX 3B2 was added, except once the crystal was modified it did not return to its original habit. Adding concentrations of 225 and 450ppm of DOWFAX 3B2 also resulted in all of the corners of the crystal being affected by the additive with the

corners of the crystal displaced at a much faster rate, as shown in Figure 5-7 and Figure 5-8 respectively. In general at higher concentration of additives the corners of the crystals are modified much earlier in comparison to lower additive concentrations and more inclusions are observed on the crystal surfaces. For instance when 22.5, 90, 225 and 450ppm of the additive was added respectively, the habit of the crystal was observed to be modified after 256, 204, 88 and 46 minutes, respectively The habit of the crystal was also observed to be affected at much higher concentrations of additive in comparison to lower concentrations as illustrated in Figure 5-9. Crystal habit modification at high additive concentration (above 2000ppm) have also been observed for the KDP system when the dye sun-set yellow FCF was used (Hirota et al. 2002).

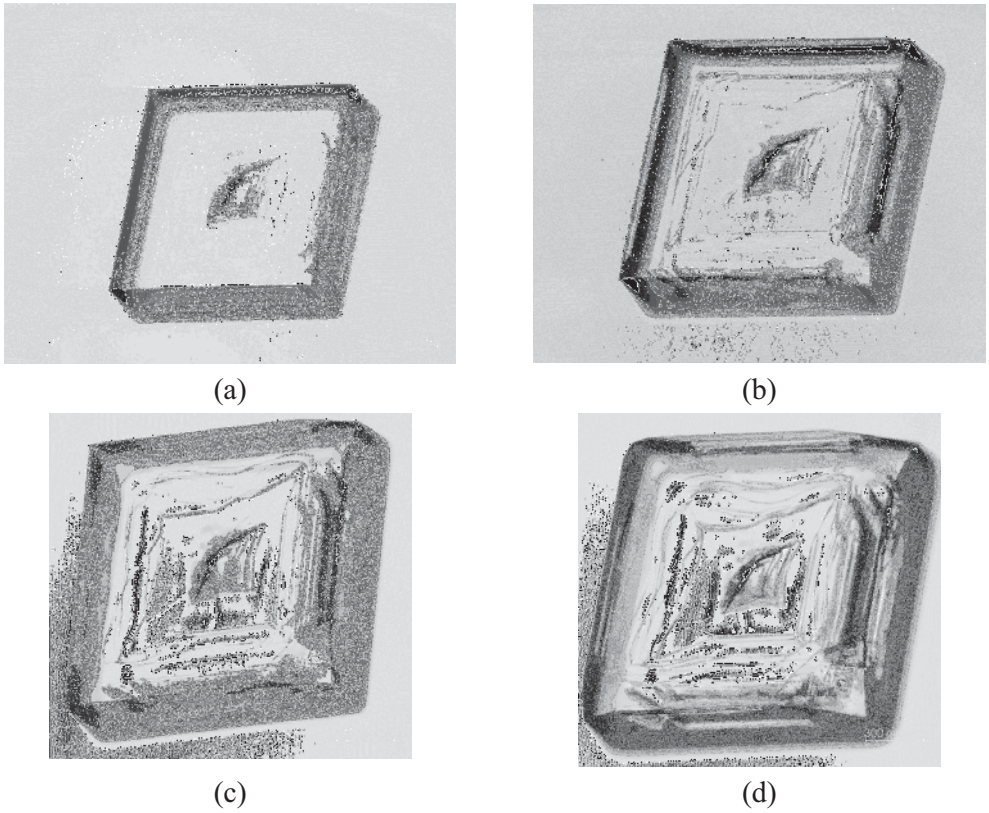

(a) (b)

(c) (d)

Figure 5-7 Growth sequence of a sodium nitrate crystal (20.0°C σ =0.04) grown with 225ppm DOWFAX 3B2 (a) after 88 minutes from first observation (b) after 108 minutes from first observation (c) after 124 minutes from first observation, and (d) after 140 minutes from first observation

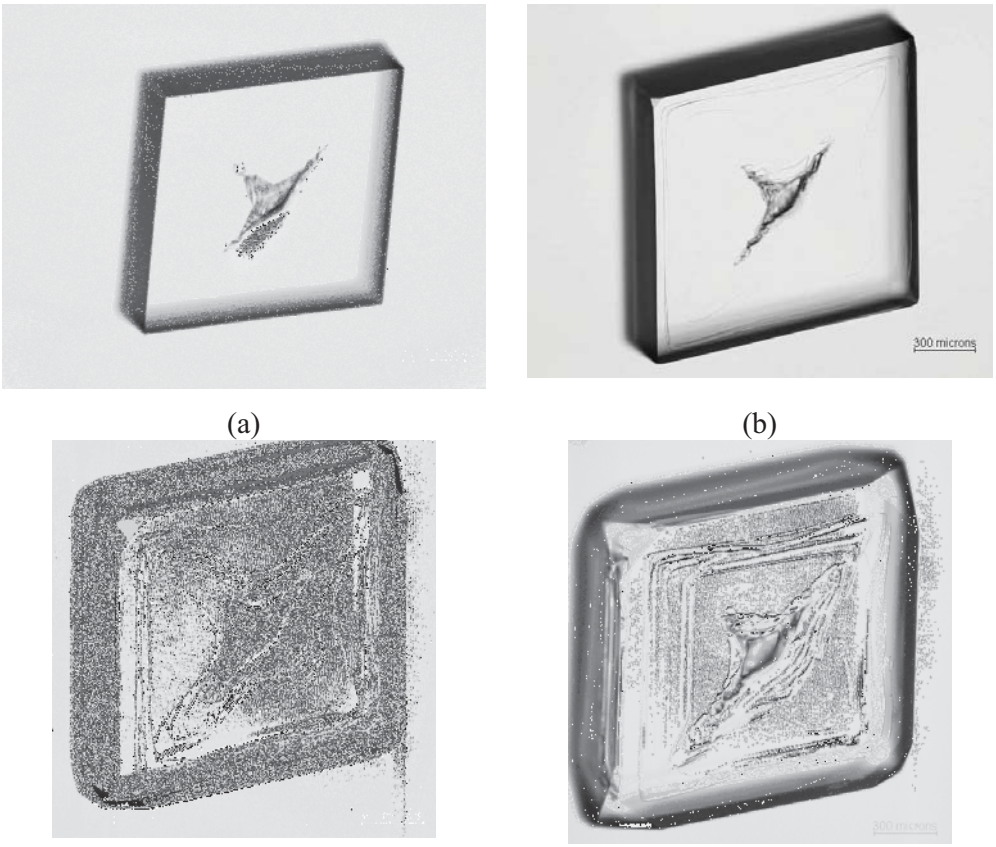

Figure 5-8 Growth sequence of a sodium nitrate crystal (20.0°C σ =0.04) grown with 450ppm DOWFAX 3B2 (a) after 28 minutes from first observation (no crystal habit modification observed) (b) after 46 minutes from first observation (c) after 60 minutes from first observation, and (d) after 98 minutes from first observation

The influence of DOWFAX 3B2 on the crystal habit modification of sodium nitrate can be explained due to the presence of its anionic polar group, the sulphonate group, since surfactants and organic dyestuffs are attracted to the crystal surface through their polar or hydrocarbon portion (J Nyvlt & Ulrich 1995), which has also been shown to play an important part in the adsorption process for dyes (Weinland & France 1932; Whetstone 1955ab). Weinland and France (Weinland & France 1932) concluded that strong polar groups play an important part in the adsorption process, since these groups were present in all cases in their experiments where adsorption had occurred. Whetstone (Whetstone 1955a) also determined that the type of interaction between a dye in solution and a growing crystal was due to the adsorption

of the dye molecules on the habit modified plane, due to interactions of the surface ions for the polar groups of the dye molecules. The effect of many polar group orientations in increasing aggregation tendencies of dye molecules is also an important consideration in determining whether or not a dye shall be a habit modifier (Whetstone 1955b).

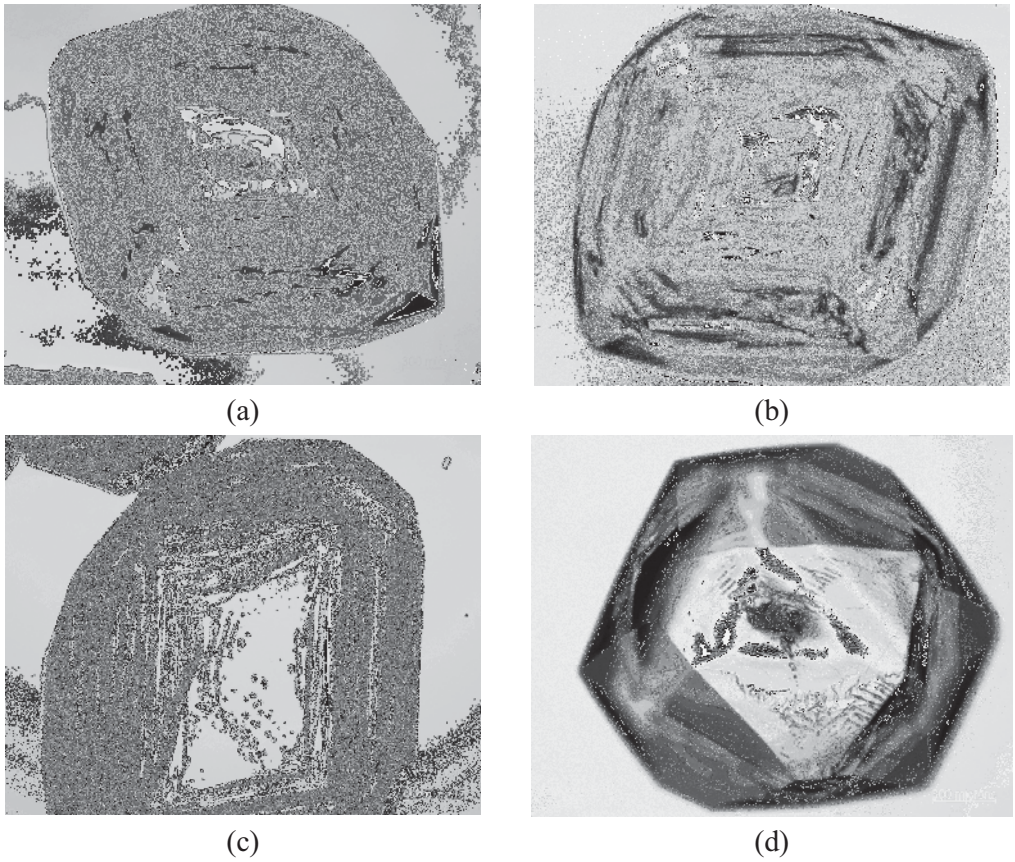

Figure 5-9 Optical images of sodium nitrate crystals grown in situ in the batch cell, grown with 450ppm DOWFAX 3B2 at 20.0°C σ =0.04 (a) after 135 minutes from first observation (b) after 137 minutes from first observation (c) after 138 minutes from first observation, and (d) after 138 minutes from first observation

5.4.1.1 *Effect of DOWFAX 3B2 on crystal growth rate measurements*

The crystal growth rates of the sodium nitrate crystals that were grown at 225 (Figure 5-7) and 450ppm DOWFAX 3B2 (Figure 5-8) were measured by using the growth ratio, which is the displacement of the artificially developed faces relative to that of the regular face of the sodium nitrate crystal as shown in Figure 5-10. The growth ratio measurement for different crystals grown at 225 and 450ppm DOWFAX 3B2 that were monitored in the same experiment is shown in Figure 5-11. For a concentration of 225ppm DOWFAX 3B2, crystal 1 is the growth ratio measurement of the bottom right hand corner of the crystal shown in Figure 5-7, and for 450ppm DOWFAX 3B2 crystal 1 is the growth ratio measurement of the top left hand corner of the crystal shown in Figure 5-8. From Figure 5-7 it can be observed that after 88 minutes of growth, triangular truncation on the corner of the crystals are observed as indicated by the increase in growth ratio in Figure 5-11, and growth is rapid until about 120 minutes and then starts to plateau to a constant growth ratio. A similar trend is also observed for the crystals grown at 450ppm DOWFAX 3B2 except the increase in growth ratio is observed to occur much earlier at 46 minutes and growth is rapid until about 100 minutes and then starts to plateau to a constant growth ratio, which could be due to the sodium nitrate solution in the batch cell almost becoming saturated due to the growth cell design in which the solution is stagnant. The growth ratio at 450ppm DOWFAX 3B2 was also observed to be lower in comparison to 225ppm DOWFAX 3B2. This observation is consistent with Weinland and France (Weinland & France 1932) observation that with increasing concentration of the dye the adsorption becomes greater and the growth ratio values becomes progressively smaller, until a limiting concentration is reached at which the growth ratio values becomes zero and growth stops. This is also consistent with observations in other systems that have used organic dyes (Girolami & Rousseau 1985; Kipp, Lacmann & Rolfs 1997; Rousseau, Tai & McCabe 1976) and DOWFAX 3B2 (Kipp, Lacmann & Rolfs 1997) where the crystal growth rate can be reduced to zero using a sufficient concentration of the additive.

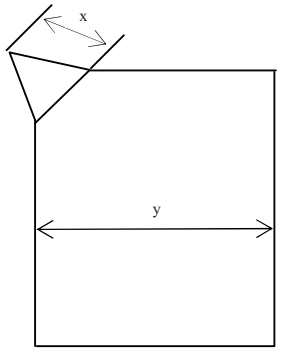

Growth ratio = x/y

Figure 5-10 Definition of growth ratio

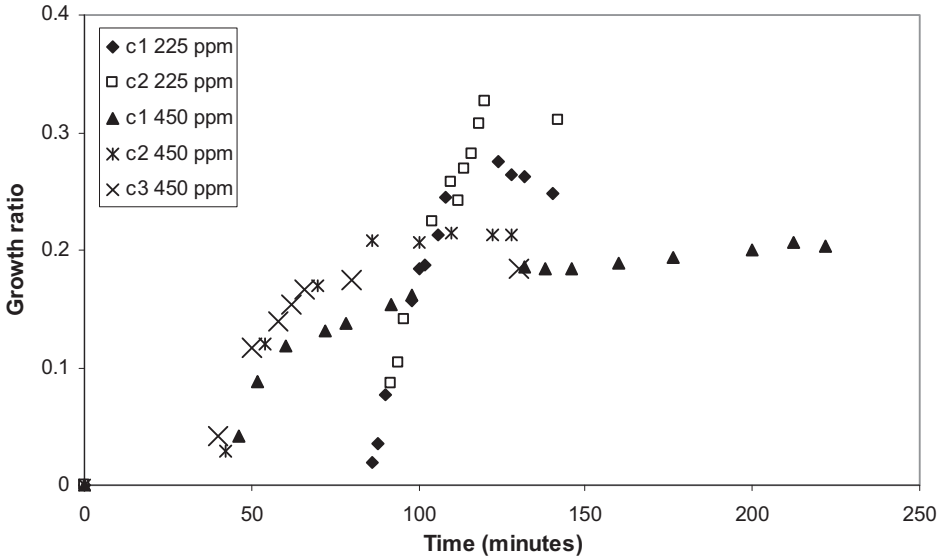

Figure 5-11 Growth ratio of the displacement of the artificially developed faces relative to that of the regular face of the sodium nitrate crystal, for two different crystals at 225ppm DOWFAX 3B2 and for three different crystals at 450ppm DOWFAX 3B2, that were monitored in the same experiment

5.4.2 Effect of organic dyes on morphology of sodium nitrate crystals

Figure 5-12 shows the growth sequence of the same crystal of sodium nitrate that was grown with 50ppm amaranth. From Figure 5-12 (b) it can be observed that at the top left hand corner and at the bottom left and bottom right hand corner of the crystal

there are triangular truncations or octahedral facets (as indicated by the circles) as observed for DOWFAX 3B2. In Figure 5-12 (c) the top left hand corner of the crystal starts to recover and in Figure 5-12 (d) the corner is back to its original form. This phenomena was also observed when sodium nitrate crystals were grown in the presence of DOWFAX 3B2 at low concentration (see section 5.4.1). It can also be observed that the surface of the crystal is not affected by the additive and only liquid inclusions are observed to be present.

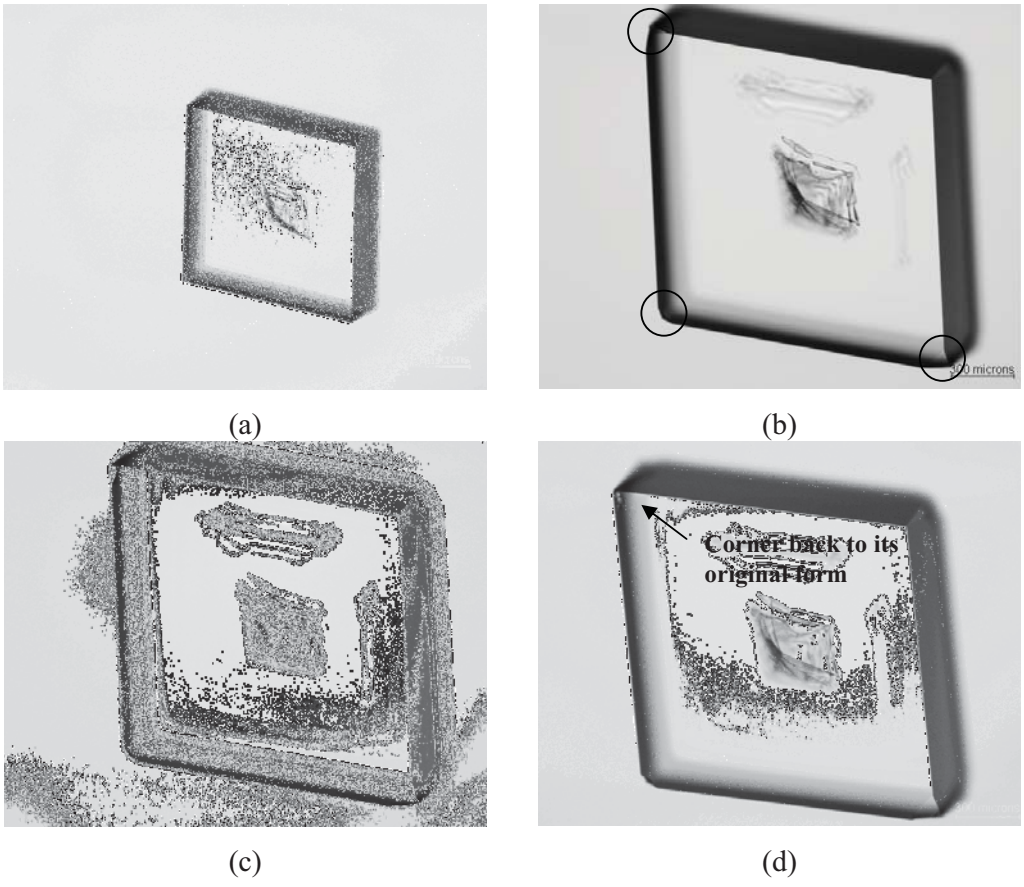

Figure 5-12 Growth sequence of a sodium nitrate crystal (20.0°C σ =0.04) grown with 50ppm amaranth (a) after 60 minutes from first observation (no crystal habit modification observed) (b) after 190 minutes from first observation (c) after 198 minutes from first observation, and (d) after 204 minutes from first observation.

When the concentration of amaranth was increased to 100ppm the crystal habit was modified in a similar fashion to 50ppm, where triangular truncations or octahedral facets were observed as shown in Figure 5-13 (d) on the bottom right hand corner of the crystal. Also, the edges of the crystal faces were affected. It can be observed that crystal A in Figure 5-13 (a) whose edges are affected becomes smooth again as shown in Figure 5-13 (b), (d) and (f). However, the edge of crystal B in Figure 5-13 (a), (b), (c) and (e) still remains affected during growth.

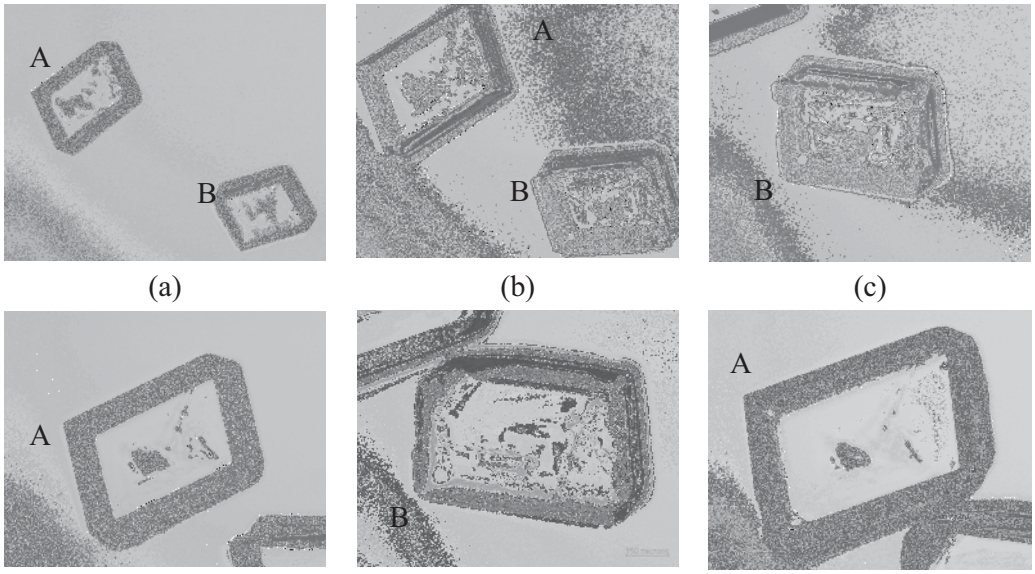

Figure 5-13 Growth sequence of sodium nitrate crystals (20.0°C σ =0.04) grown with 100ppm amaranth (a) after 20 minutes from first observation (b) after 48 minutes from first observation (c) after 72 minutes from first observation (d) after 80 minutes from first observation (e) after 148 minutes from first observation, and (f) after 150 minutes from first observation.

Figure 5-14 shows the growth sequence of the same crystal of sodium nitrate that was grown with 225ppm amaranth. From Figure 5-14 (a) a pyramid shaped growth hillock can be observed which Kipp *et al* (Kipp, Lacmann & Rolfs 1997) also observed on the {110} face of potassium nitrate when the crystal was grown in a solution containing 500ppm amaranth. After 15 minutes of growth it was observed that the crystal surface became rough and the edges of the crystal were also affected

by the additive, as was observed for 100ppm amaranth. Therefore with increasing amaranth concentration the crystal was affected much quicker by the additive since for 50ppm it took 190 minutes before any change to the crystal habit was observed, in comparison to 20 minutes for 100ppm and 8 minutes for 225ppm, and the surface and the edges of the crystal are also affected at higher concentrations.

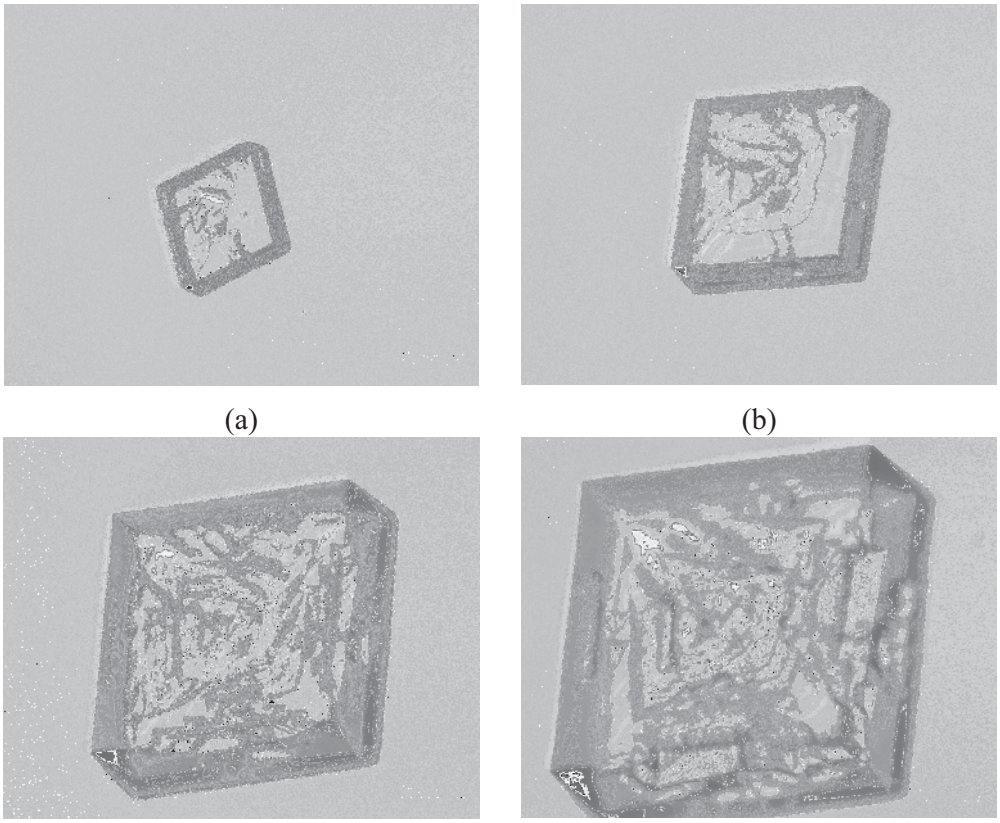

(a) (b)

(c) (d)

Figure 5-14 Growth sequence of a sodium nitrate crystal (20.0°C σ =0.04) grown with 225ppm amaranth (a) after 2 minutes from first observation (b) after 8 minutes from first observation (c) after 15 minutes from first observation, and (d) after 21 minutes from first observation.

The effect of amaranth on the crystal habit modification of sodium nitrate can also be explained due to the presence of its polar groups which has been shown to play an important part in the adsorption process for dyes (Weinland & France 1932; Whetstone 1955ab) as discussed in Section 5.4.1. In comparison to DOWFAX 3B2,

although amaranth affected the corners of the sodium nitrate crystal at low concentrations, it had a greater effect in modifying the crystal surface and edges. It is likely that this is the case since the amaranth molecule is larger than the DOWFAX 3B2 molecule since normally the habit modifying powers of a large dye molecule is greater than that of a small one owing to the greater ease of overgrowth (Whetstone 1955a). However, since the DOWFAX 3B2 is a surfactant it is also likely that a different mechanism was involved. It is extremely unlikely that amaranth would have been incorporated into the crystal lattice, which is normally the case for strongly adsorbing impurities that have certain structural and chemical characteristics of the "host" (crystalline) phase. Also, x-ray spectrographs of the adsorption of quinoline yellow on sodium nitrate indicates that the adsorption occurs interstitially rather than as individual planes or by the replacement of ions in the unit cell (Weinland & France 1932).

The effect of other organic dyes such as Evans blue and Bismark brown on the crystal habit of sodium nitrate was also trialled. However, the additive's solubility was found to be poor since when 60µL of the additive was added to the sodium nitrate solution (equivalent to 50ppm of the additive), the additive did not properly dissolve. Therefore no further experiments were carried out on these additives.

Summary

- The surfactant DOWFAX 3B2 was found to be effective in changing the crystal habit of sodium nitrate. Triangular truncations or octahedral facets at the corners of the sodium nitrate crystal were observed which Weinland and France (Weinland & France 1932) also observed when studying the influence of various dyes on the crystal habit of sodium nitrate, due to the additive being adsorbed onto the crystal surface. In general at higher concentration of additives the corners of the crystals are modified much earlier in comparison to lower additive concentrations and more inclusions are observed on the crystal surfaces. The habit of the crystal was also observed to be affected at much higher concentrations of additive in comparison to lower concentrations.

- The growth ratio of the sodium nitrate crystals grown with 225 and 450ppm DOWFAX 3B2 was measured and it was observed as expected that the growth ratio of the displacement of these artificially developed faces relative to that of the regular face of the sodium nitrate crystal, rapidly increases and then starts to plateau to a constant growth ratio when no crystal growth is observed. This observation could be due to the sodium nitrate solution in the batch cell almost becoming saturated since the solution is stagnant so constant liquor composition cannot be maintained for a long duration. The growth ratio value was also found to decrease with increasing additive concentration.

- The organic dye amaranth was found to be effective in changing the crystal habit as observed for DOWFAX 3B2 due to the adsorption process, and the surface of the sodium nitrate crystal depending on the concentration used. 50ppm amaranth resulted in triangular truncations or octahedral facets at the corners of the sodium nitrate crystal whereas at much higher concentration of amaranth (100 and 225ppm) the surface and edges of the crystal became rougher and the edges of the crystal were affected.

Chapter 6
CONCLUSIONS AND RECOMMENDATIONS

6.1 CONCLUSIONS

The conclusions obtained from each of the chapters are presented below, divided into their chapter headings.

6.1.1 Solubility

- Due to sodium nitrate's high solubility in water, data on its solubility in aqueous alcohol is essential for salting out crystallisation studies. A survey of the literature indicated that solubility data for sodium nitrate in the presence of ethanol is quite outdated, while solubility data with either methanol or isopropanol does not exist at the temperature range of interest.

- The effect of the addition of methanol, ethanol and isopropanol (the latter only at 20.0°C) on the solubility of sodium nitrate in water was experimentally investigated in the different temperature ranges and various weight percents of alcohol. In all cases the solubility of sodium nitrate in water was significantly reduced by the presence of methanol and ethanol.

- Splitting into two liquid phases was observed when using isopropanol. However, this phase separation did not occur at low mass fractions (0.0549) and high mass fractions (0.90) of alcohol, as at lower concentrations of one solvent the two solvents are miscible.

- The order of decreasing solubility of sodium nitrate and water is of methanol<ethanol<isopropanol (only for low or high mass fractions). In other words, the solubility of sodium nitrate and water decreases with increasing molecular weight of the alcohol.

- The experimental data was used for the determination of the ion-specific NRTL parameters by correlating with the modified extended NRTL model. It was observed for both methanol and ethanol that the model was found to satisfactorily correlate the data at low to moderate concentrations of alcohol. However, as the concentration of alcohol rises the model prediction is less satisfactory, probably due to the interaction parameters of NRTL between alcohol and the ions not being able to represent the low solubility of electrolytes.

6.1.2 Crystal growth and surface morphology

- In the batch cell crystal growth rates were obtained for homongeneous nucleation experiments at different temperatures (20.0^{o}C, 30.0^{o}C and 40.0^{o}C) and relative supersaturations, σ (0.02, 0.04, 0.06, 0.08 and 0.1) to determine the kinetics of growth. A combined growth order, g of 1 and activation energy of 23,580 J/mol was obtained which suggests that crystal growth might be controlled by diffusion which is consistent with the results obtained from literature.

- To confirm that growth in the batch cell was diffusion controlled the effect of different flow rates on the crystal growth rates were tested in a modified growth cell, and higher flow rates did not increase the crystal growth rates, suggesting that growth was surface integration controlled. However, the flow rates tested were in the laminar region due to their low Reynolds number so from these results it could not be concluded that growth was surface integration controlled.

- The effect of initial crystal size on the growth rate was investigated for growth rate dispersion in the homogenous nucleation experiments, seeded crystal growth experiments and when the solvent composition was changed. For all cases size independent growth was observed.

- Sodium nitrate crystals grown by homogeneous nucleation in the batch cell contain liquid inclusions when grown at high temperatures and for a long

duration. SEM images revealed the presence of pitting on the crystal surface due to the high solubility of sodium nitrate, while AFM images showed the presence of growth hillocks which suggests that crystal growth is surface integration controlled. However, the presence of the growth hillocks could have been caused by the formation of some nuclei and surface artefacts when the crystal was taken out from solution.

- In seeded crystal growth experiments for the pure aqueous system and in aqueous ethanol and methanol, the solute deposits on the crystal surface. This was observed mainly to occur in the ethanol system at low alcohol weight percents.

- Sodium nitrate crystals grown in aqueous ethanol by homogeneous nucleation in the batch cell have a lower number of inclusions on the crystal surface in comparison to the pure aqueous system. In general, as the supersaturation increased, the weight percent of ethanol decreased, and the crystal size increased, the number of inclusions observed on the crystal surfaces increased.

- Crystal growth rates obtained in the modified growth cell using seeds were lower in comparison to crystal growth rates obtained in the homogeneous nucleation experiments. This could have been attributed to the fact that homogeneous nucleation is spontaneous and not predictable, which is also why a wider dispersion in growth rates was observed in comparison to the seeded experiments.

- The Reynolds number for the modified growth cell at a flow rate of 4mL/min was calculated and flow in the growth cell was confirmed to be laminar.

- The composition of the solvent system is found to have a significant influence on the crystal growth rates of sodium nitrate. The addition of aqueous ethanol and methanol to the sodium nitrate system results in a decrease in the crystal growth rates compared to the pure aqueous system and the habit of the crystal remains unchanged.

6.1.3 Effect of additives on crystal habit

- The surfactant DOWFAX 3B2 was found to be effective in changing the crystal habit of sodium nitrate. Triangular truncations or octahedral faces at the corners of the sodium nitrate crystal was observed which Weinland and France (Weinland & France 1932) also observed when studying the influence of various dyes on the crystal habit of sodium nitrate, due to the additive being adsorbed onto the crystal surface. In general at higher concentration of additives the corners of the crystals are modified much earlier in comparison to lower additive concentrations and more inclusions are observed on the crystal surfaces. The habit of the crystal was also observed to be affected at much higher concentrations of additive in comparison to lower concentrations.

- The growth ratio of the sodium nitrate crystals grown with 225 and 450ppm DOWFAX 3B2 was measured and it was observed as expected that the growth ratio of the displacement of these artificially developed faces relative to that of the regular face of the sodium nitrate crystal, rapidly increases and then starts to plateau to a constant growth ratio when no crystal growth is observed. This observation could be due to the sodium nitrate solution in the batch cell almost becoming saturated since the solution is stagnant so constant liquor composition cannot be maintained for a long duration. The growth ratio value was also found to decrease with increasing additive concentration.

- The organic dye amaranth was found to be effective in changing the crystal habit as observed for DOWFAX 3B2 due to the adsorption process, and the surface of the sodium nitrate crystal depending on the concentration used. 50ppm amaranth resulted in triangular truncations or octahedral faces at the corners of the sodium nitrate crystal whereas at much higher concentration of amaranth (100 and 225ppm) the surface and edges of the crystal became rougher and the edges of the crystal were affected.

6.2 RECOMMENDATIONS FOR FUTURE WORK

6.2.1 Solubility

- Further work is required on the solubility of sodium nitrate in isopropanol which was observed to split into two liquid phases. This phase separation does not occur at low and high mass fractions of alcohol, as at lower concentrations of one solvent the two solvents are miscible.

- The model prediction for the determination of the ion-specific NRTL parameters for the methanol and ethanol system was found not to be satisfactory at high concentrations of alcohol, due to the interaction parameters of NRTL between alcohol and the ions not being able to represent the low solubility of electrolytes. Thus further work is required on the model to see if a better correlation can be obtained.

6.2.2 Crystal growth and surface morphology

- It is recommended that in situ AFM studies be carried out on the sodium nitrate crystals grown from pure aqueous solution and aqueous ethanol to study more quantitative properties which can represent the actual growth processes more closely and determine the mechanism of growth.

- Further work is required to obtain the kinetics of growth of sodium nitrate in the pure aqueous system for seeded crystal growth experiments and for the aqueous ethanol and methanol solutions in both the homogeneous and seeded crystal growth experiments.

6.2.3 Effect of additives on crystal habit

- Further work is required in measuring the growth ratios of the sodium nitrate crystal in amaranth and DOWFAX 3B2.

- It is recommended that in situ AFM studies be carried out to establish the mechanism of DOWFAX 3B2 and amaranth on the crystal habit modification and growth of sodium nitrate.

- It is recommended that more additives be trialled out to see if they have an effect on changing the crystal habit of sodium nitrate.

REFERENCES

Algra, RE, Graswinckel, WS, Van Enckevort, WJP & Vlieg, E 2005, 'Alizarin crystals: An extreme case of solvent induced morphology change', *Journal of Crystal Growth,* vol. 285, pp. 168-77.

Anuradha, P, Murthy, MR & Raju, IVKB 1982, 'Study of growth and gross defects of NaNO3 single crystals', *Physica Status Solid A: Applied Research* vol. 74, no. 2, pp. 93-6.

Archer, DG 2000, 'Thermodynamic properties of the NaNO3 + H2O System', *Journal of Physical and Chemical Reference data,* vol. 29, pp. 1141-56.

Arlow, A 2003, *Crystallisation aspects of the wet-process phosphoric acid industry*, Masters Thesis, University of Pretoria, Pretoria.

Asakuma, Y, Ukita, E, Maeda, K, Fukui, K, Iimura, K, Suzuki, M & Hirota, M 2007, 'Surface Topography of Dyed Potassium Dihydrogen Phosphate (KDP) Crystals ', *Crystal Growth & Design,* vol. 7, no. 2, pp. 420-4.

Australian Gas Association code AG 703 1974.

Bathrick, HA 1896, 'Precipitation of salts', *Journal of Physical Chemistry,* vol. 1, no. 3, pp. 157-69.

Berglund, KA, Kaufman, EL & Larson, MA 1983, 'Growth of contact nuclei of potassium nitrate', *AIChE Journal,* vol. 29, no. 5, pp. 867-9.

Berglund, KA & Larson, MA 1982, 'Growth of contact nuclei of citric acid monohydrate', *AIChE Symposium Series,* vol. 78, no. 215, p. 9.

Berthoud, A 1912, 'Theorie de la formation des faces d'un crystal', *Journal de Chimique Physique* vol. 10, pp. 624-35.

Bhat, HL, Sherwood, JN & Shripathi, T 1987, 'The influence of stress, strain and fracture of crystals on the crystal growth process', *Chemical Engineering Science,* vol. 42, no. 4, pp. 609-18.

Bourne, JR & Davey, RJ 1976, 'The growth of hexamethylene tetramine crystals from ethanolic solutions', *Journal of Crystal Growth,* vol. 34, pp. 230-8.

Brecevic, L & Kralj, D 2000, 'Kinetics and mechanisms of crystal growth in aqueous systems', in N Kallay (ed.), *Interfacial Dynamics*, Marcel Dekker, New York.

Buckley, HE 1951, *Crystal Growth*, John Wiley & Sons, New York.

Burton, WK, Cabrera, N & Frank, FC 1951, *The Philosophical Transactions of the Royal Society A,* vol. 243, p. 299.

Butchart, A & Whetstone, J 1949, 'The effect of dyes on the crystal habits of some oxy-salts', *Transactions of the Faraday Society,* vol. 5, pp. 254-61.

Cang, HX, Huang, WD & Zhou, YH 1998, 'Effects of organic solvents on the morphology of the meta-nitroaniline crystal', *Journal of Crystal Growth,* vol. 192, pp. 236-42.

Cano, H, Gabas, N & Canselier, JP 2001, 'Experimental study on the ibuprofen crystal growth morphology in solution', *Journal of Crystal Growth,* vol. 224, pp. 335-41.

Carter, DJ 2004, *Mechanism of dye incorporation into potassium sulfate*, Curtin University of Technology.

Chen, C, Britt, HI, Boston, JF & Evans, LB 1982, 'Local composition model for excess Gibbs energy of electrolyte systems', *AIChE Journal,* vol. 28, no. 4, pp. 588-96.

Chen, C & Evans, LB 1986, 'A local composition model for the excess Gibbs energy of aqueous electrolyte systems', *AIChE Journal,* vol. 32, no. 3, pp. 444-54.

Chen, C & Song, Y 2004, 'Solubility modeling with a nonrandom two-liquid segment activity coefficient model', *Industrial & Engineering Chemistry Research,* vol. 43, pp. 8354-62.

Chirico, RD, Frenkel, M, Diky, VV, Marsh, KN & Wilhoit, RC 2003, 'ThermoML - An XML based approach for storage and exchange of experimental and critically evaluated thermophysical and thermochemical property data. 2. Uncertainties', *Journal of Chemical and Engineering Data,* vol. 48, pp. 1344-59.

Cho, J, Cho, JK, Lee, J, Lee, D, Park, C & Kim, S 2009, 'Optimization of salting-out crystallization for an efficient in situ separation of synthetic anthraquinone- and azo-type reactive dyes', *Separation and Purification Technology,* vol. In press doi:10.1016/j.seppur.2009.04.015.

Colfen, H & Qi, L 2001, 'A systematic examination of the morphogenesis of calcium carbonate in the presence of a double-hydrophilic block copolymer', *Chemistry - A European Journal,* vol. 7, no. 1, pp. 106-16.

Cruz, J & Renon, H 1978, 'A new thermodynamic representation of binary electrolyte solutions nonideality in the whole range of concentrations', *AIChE Journal,* vol. 24, no. 5, pp. 817-30.

Czech Patent 1964.

Darby, R 2001, *Chemical Engineering Fluid Mechanics, 2nd edition*, Marcel Dekker, Inc, New York, USA.

Davey, RJ, Milisavljevic, B & Bourne, JR 1988, 'Solvent interactions at crystal services: the kinetic story of alpha-resorcinol', *The Journal of Physical Chemistry,* vol. 92, no. 7, pp. 2032-6.

Davey, RJ & Mullin, JW 1974, 'Growth of the {100} faces of ammonium dihydrogen phosphate crystals in the presence of ionic species', *Journal of Crystal Growth,* vol. 26, no. 1, pp. 45-51.

Davey, RJ, Mullin, JW & Whiting, MJL 1982, 'Habit modification of succinic acid crystals grown from different solvents', *Journal of Crystal Growth,* vol. 58, pp. 304-12.

Denbigh, KG & White, ET 1966, 'Studies on liquid inclusions in crystals', *Chemical Engineering Science,* vol. 21, pp. 739-54.

Dincer, TD 2000, *Mechanisms of lactose crystallisation*, Curtin university of Technology.

Dow, *Technical Data Sheet DOWFAX 3B2 surfactant*. Retrieved 2007, from http://www.dow.com/PublishedLiterature/dh_00af/0901b803800af1b6.pdf?filepath=surfactants/pdfs/noreg/119-01968.pdf&fromPage=GetDoc

Dow 2002, *Alkyl diphenyl oxide sulfonates (ADPODS) HPV Challenge Program - Category, test plan and robust summaries of data for HPV/SIDS endpoints*. Retrieved 2008, from http://www.epa.gov/hpv/pubs/summaries/adpods/c14165tp.pdf

Eckstein, J, Perinova, M, Rubinova, E & Urusovskaja, AA 1967, 'Influence of growth conditions and thermal history on the constitution of NaNO3 single crystals', *Kristall und Technik,* vol. 2, no. 3, pp. 359-70.

Evanko, CR, Dzombak, DA & Novak, JW 1996, 'Influence of surfactant addition on the stability of concentrated alumina dispersions in water', *Colloids and Surfaces A: Physicochemical and Engineering Aspects* vol. 110, pp. 219-33.

Farn, RJ 2006, *Chemistry and Technology of Surfactants*, Blackwell Publishing.

Franke, VD, Treivus, EB, Filippov, VK & Antonova, VA 1981, 'Crystallisation of nitrates in the presence of HNO3 and its relation to physical and chemical properties of the systems', *Journal of Crystal Growth,* vol. 52, pp. 795-800.

Freij, AJ 2007, *Crystallization of Lactose from Whey and Permeate*, Curtin University of Technology.

Freij, SJ & Parkinson, G 2005, 'Surface morphology and crystal growth mechanism of gibbsite in industrial Bayer liquors', *Hydrometallurgy,* vol. 78, pp. 246-55.

Freij, SJ, Parkinson, G & Reyhani, M 2004, 'Direct observation of the growth of gibbsite crystals by atomic force microscopy', *Journal of Crystal Growth,* vol. 260, pp. 232-42.

Furves, WT & Larson, MA 1980, *Institution of Chemical Engineering Symposium. Ser. 58, Sol. Separ Proceedings. 7/5/1-7/5/18*.

Garside, J & Larson, MA 1978, 'Direct observation of secondary nuclei production', *Journal of Crystal Growth,* vol. 43, no. 6, pp. 694-704.

Garside, J, Mersmann, A & Nyvlt, J 2002, *Measurement of crystal growth and nucleation rates*, Insitute of Chemical Engineers, U.K.

Garti, N, Leci, CL & Sarig, S 1981, 'The effect of solvents on crystal habit of 1,4-di-tert-butylbenzene (DTBB)', *Journal of Crystal Growth,* vol. 54, pp. 227-31.

Girolami, MW & Rousseau, RW 1985, 'Effects of bismark brown R on the growth rates of large and small potassium alum crystals', *Journal of Crystal Growth,* vol. 71, pp. 220-4.

Gonzalez, X & Rasmuson, AC 1997, 'Drowning-out crystallization of benzoic acid from water-ethanol mixtures', in *Fourth International Workshop on Crystal Growth of Organic Materials*, University of Bremen, Sept 17-19.

Gopalakrishnan, R, Arivuoli, D & Ramasamy, P 1991, 'Growth and characterisation of NaNO3 single crystals', *Crystal Research and Technology,* vol. 26, no. 6, pp. 141-6.

Graber, TA, Taboada, ME, Alvarez, MN & Schmidt, EH 1999, 'Determination of Mass Transfer Coefficients for Crystal Growth of Nitrate Salts', *Crystal Research and Technology,* vol. 34, no. 10, pp. 1269-77.

Granberg, RA & Bloch, DGR, A.C 1999, 'Crystallisation of paracetamol in acetone-water mixtures', *Journal of Crystal Growth,* vol. 198/199, pp. 1287-93.

Granberg, RA & Rasmuson, AC 2005, 'Crystal growth rates of paracetamol in mixtures of water + acetone + toluene', *AIChE Journal,* vol. 51, no. 9, pp. 2441-56.

Guzman, LA, Maeda, K, Hirota, S, Yokota, M & Kubota, N 1997, 'Unsteady-state impurity effect of chromium (III) on the growth rate of potassium sulfate crystal in aqueous solution', *Journal of Crystal Growth,* vol. 181, no. 3, pp. 272-80.

Hartel, RW 2001, 'Crystal Growth', in *Crystallization in Foods*, Aspen Publishers, Gaithersburg.

Hash, J & Okorafor, OC 2008, 'Crystal size distrubtion (CSD) of batch salting-out crystallisation process for sodium sulfate', *Chemical Engineering and Processing,* vol. 47, pp. 622-32.

Herricks, T, Chen, J & Xia, Y 2004, 'Polyol synthesis of platinum nanoparticles: Control of morphology with sodium nitrate', *Nano Letters,* vol. 4, no. 12, pp. 2367-71.

Hirota, S, Miki, H, Fukui, K & Maeda, K 2002, 'Coloring and habit modification of dyed KDP crystals as functions of supersaturation and dye concentration', *Journal of Crystal Growth,* vol. 235, pp. 541-6.

Human, HJ, van der Eerden, JP, Jetten, LAMJ & Odekerken, JGM 1981, 'On the roughening transition of biphenyl: transition of faceted to non-faceted growth of biphenyl for growth from different organic solvents and the melt', *Journal of Crystal Growth,* vol. 51, no. 3, pp. 589-600.

Hurley, LA, Jones, AG & Drummond, JN 1997, 'Growth and dissolution kinetics of cyanazine crystals in aqueous ethanol solutions', *Journal of Crystal Growth,* vol. 172, pp. 499-507.

Iskhakova, LD, Korotkevich, IB, Sorokina, RI, Bolotina, II & Bomshtein, VE 1979, *Issled. v Obl. Khimii i Tekhnol. Osobo Chist. Veshch. M,* vol. 38.

Jaretun, A & Aly, G 1999, 'New local composition model for electrolyte solutions: single solvent, single electrolyte systems', *Fluid Phase Equilibria,* vol. 163, no. 2, pp. 175-93.

Jaretun, A & Aly, G 2000, 'New local composition model for electrolyte solutions: multicomponent systems', *Fluid Phase Equilibria,* vol. 175, no. 1/2, pp. 213-28.

Jones, CM & Larson, MA 1999, 'Characterizing growth-rate dispersion of NaNO3 secondary nuclei', *AIChE Journal,* vol. 45, no. 10, pp. 2128-35.

Jones, CM & Larson, MA 2000, 'Using dislocations and integral strain to model the growth rates of secondary nuclei', *Chemical Engineering Science,* vol. 55, no. 14, pp. 2563-70.

Jones, CM, Larson, MA, Ristic, RI & Sherwood, JN 2000, 'The role of dislocations, integral strain, and supersaturation on the growth rates of sodium nitrate', *Journal of Crystal Growth,* vol. 208, no. 1-4, pp. 520-4.

Kahr, B, Chow, JK & Peterson, ML 1994, 'Organic hourglass inclusions: A review of past and recent work and a student experiment', *Journal of Chemical Education,* vol. 71, no. 7, pp. 584-6.

Kahr, B & Gurney, RW 2001, 'Dyeing Crystals', *Chemical Reviews,* vol. 101, pp. 893-951.

Karunanithi, AT, Acquah, C, Achenie, LEK, Sithambaram, S & Suib, SL 2009, 'Solvent design for crystallisation of carboxylic acids', *Computers and Chemical Engineering,* vol. 33, pp. 1014-21.

Keum, D, Naka, K & Chujo, Y 2003, 'Unique crystal morphology of hydrophobic CaCO3 composite by sodium trisilanolate in a mixture of a water-miscible organic solvent and water', *Journal of Crystal Growth,* vol. 259, pp. 411-8.

Kim, YK, Williard, JW & Frazier, AW 1988, 'Solubility relationship in the system NaNO3-NH4NO3-Urea-H2O at 0oC', *Journal of Chemical and Engineering Data,* vol. 33, no. 3, pp. 306-9.

Kipp, S & Lacmann, R 1996, 'Cooling Crystallization experiments observed by in situ scanning force microscopy', *Journal of Crystal Growth,* vol. 160, no. 3-4, pp. 320-9.

Kipp, S, Lacmann, R & Rolfs, J 1997, 'Crystallization of potassium nitrate (KNO3) in aqueous solution Part II. Kinetical studies under the influence of additives', *Journal of Crystal Growth,* vol. 171, pp. 183-9.

Kiryanova, EV 2003, 'New effects of crystal-solution phase equilibria in a model system NaNO3-H2O', *Journal of Crystal Growth,* vol. 253, pp. 452-9.

Komnik, SN & Startsev, VI 1969, 'On the growth of large and perfect crystals of sodium nitrate', *Journal of Crystal Growth,* vol. 5, pp. 207-9.

Kracek, FC 1931, 'Gradual transition in sodium nitrate. I. Physico-chemical criteria of the transition', *Journal of the American Chemical Society,* vol. 53, no. 7, pp. 2609-24.

Kracek, FC, Posnjak, E & Hendricks, SB 1931, 'Gradual transition in sodium nitrate II. The structure at various temperatures and its bearing on molecular rotation', *Journal of the American Chemical Society,* vol. 53, no. 9, pp. 3339-48.

Kubota, N, Uchiyama, I, Nakai, K, Shimizu, K & Mullin, JW 1988, 'Change of solubility of potassium sulfate in water caused by traces of chromium(III)', *Industrial & Engineering Chemistry Research,* vol. 27, no. 6, pp. 930-4.

Kumaresan, P, Babu, SM & Anbarasan, PM 2008a, 'Effect of irradiation of swift heavy ions on dyes-doped KDP crystals for laser applications', *Journal of Crystal Growth,* vol. 310, pp. 1999-2004.

Kumaresan, P, Babu, SM & Anbarasan, PM 2008b, 'Growth and characterization of metal ions and dyes doped KDP single crystals for laser applications', *Materials Research Bulletin,* vol. 43, no. 7, pp. 1716-23.

Kuramochi, H, Osako, M, Kida, A, Nishimura, K, Kawamoto, K, Asakuma, Y, Fukui, K & Maeda, K 2005, 'Determination of Ion-specific NRTL parameters for predicting phase equilibria in aqueous multielectrolyte solutions', *Industrial & Engineering Chemistry Research,* vol. 44, pp. 3289-97.

Kuznetsov, VA, Okhrimenko, TM & Rak, M 1998, 'Growth promoting effect of organic impurities on growth kinetics of KAP and KDP crystals', *Journal of Crystal Growth,* vol. 193, pp. 164-73.

Lacmann, R, Herden, A & Mayer, C 1999, 'Review - Kinetics of Nucleation and crystal growth', *Chemical Engineering & Technology,* vol. 22, no. 4, pp. 279-89.

Linke, WF 1965, *Solubilities: inorganic and metal-organic compounds: a compilation of solubility data from the periodical literature,* 4th edn, American Chemical Society Washington, D.C.

Loehe, J & Donohue, M 1997, 'Recent advances in modeling thermodynamic properties of aqueous strong electrolyte systems', *AIChE Journal,* vol. 43, no. 1, pp. 180-95.

Lopes, A & Farelo, F 2006, 'Growth kinetics of potassium chloride II - Water ethanol systems', *Journal of Crystal Growth,* vol. 290, pp. 220-4.

Lowe, J, Ogden, M, McKinnon, A & Parkinson, G 2002, 'Crystal growth of sodium oxalate from aqueous solution', *Journal of Crystal Growth,* vol. 237-239, pp. 408-13.

Lu, X & Maurer, G 1993, 'Model for describing activity coefficients in mixed electrolyte aqueous solutions', *AIChE Journal,* vol. 39, no. 9, pp. 1527-38.

Maeda, K, Kuramochi, H, Shinkawa, T & Fukui, K 2002, 'Solubility of two salts containing sulfate and chloride ions in water for ternary systems at 313K', *Journal of Chemical and Engineering Data,* vol. 47, pp. 1472-5.

Maeda, K, Sonoda, A, Miki, H, Asakuma, Y & Fukui, K 2004, 'Synergy of organic dyes for KDP crystal growth', *Crystal Research and Technology,* vol. 39, no. 11, pp. 1006-13.

Mahmoud, MHH, Rashad, MM, Ibrahim, IA & Abdel-Aal, EA 2004, 'Crystal modification of calcium sulfate dihydrate in the presence of some surface-active agents', *Journal of Colloid and Interface Science,* vol. 270, pp. 99-105.

Martino, P, Censi, R, Malaj, L, Capsoni, D, Massarotti, V & Martelli, S 2007, 'Influence of solvent and crystallisation method on the crystal habit of metronidazole', *Crystal Research and Technology,* vol. 42, no. 8, pp. 800-6.

Mathis-Lilley, JJ & Berglund, KA 1985, 'Contact nucleation from aqueous potash alum solutions', *AIChE Journal,* vol. 31, no. 5, pp. 865-7.

Mauri, A & Moret, M 2000, 'Growth of potassium sulfate crystals in the presence of organic dyes: in situ characterization by atomic force microscopy', *Journal of Crystal Growth,* vol. 208, pp. 599-614.

McCabe, WL 1929, 'Crystal Growth in Aqueous Solutions I - Theory', *Industrial and Engineering Chemistry* vol. 21, no. 1, pp. 30-3.

Michaels, AS & Tausch Jr, FW 1961, 'Modification of growth rate and habit of adipic acid crystals with surfactants', *The Journal of Physical Chemistry,* vol. 65, no. 10, pp. 1730-7.

Miki, H, Fukunaga, R, Asakuma, Y, Maeda, K & Fukui, K 2005, 'Distribution of dye into KDP crystals in a continuous MSMPR crystallizer', *Separation and Purification Technology,* vol. 43, pp. 77-83.

Mock, B, Evans, LB & Chen, C 1986, 'Thermodynamic representation of phases equilibria of mixed-solvent electrolyte systems', *AIChE Journal,* vol. 32, no. 10, pp. 1655-64.

Moret, M 2000, 'Influence of organic dyes on potassium sulfate crystal growth: a joint morphological and atomic force microscopy analysis', *Materials Chemistry and Physics,* vol. 66, pp. 177-88.

Mullin, JW 1993, *Crystallization,* Third edn, Butterworth Heinemann.

Mullin, JW & Davey, RJ 1974, 'Growth of the {101} faces of ammonium dihydrogen phosphate crystals in the presence of ionic species', *Journal of Crystal Growth,* vol. 23, no. 2, pp. 89-94.

Myers, JA 1899, 'A review of the present knowledge of sodium nitrate, together with the origin, production, and destruction of nitrates in the soil', *Journal of the American Chemical Society,* vol. 21, no. 5, pp. 455-68.

Myerson, AS (ed.) 1993, *Handbook of Industrial Crystallisation* Butterworth-Heinemann.

NationMaster, *Sodium nitrate*. Retrieved 21/01/2009, from http://www.nationmaster.com/encyclopedia/Sodium-nitrate

Nernst, W 1904, 'Theorie de Reaktionsgeschwindigkeit in heterogenen systemen', *Zeitschrift fur Physikalische Chemie,* vol. 47, pp. 52-5.

Nie, Q, Wang, J, Wang, Y & Bao, Y 2007, 'Effects of solvent and impurity on crystal habit modification of 11alpha-hydroxy-16alpha,17alpha-epoxyprogesterone', *Chinese Journal of Chemical Engineering,* vol. 15, no. 5, pp. 648-53.

Nielsen, AE 1964, *Kinetics of Precipitation*, Pergamon Press, New York.

Nokhodchi, A, Bolourtchian, N & Dinarvand, R 2005, 'Dissolution and mechanical behaviours of recrystallised carbamazepine from alcohol solution in the presence of additives', *Journal of Crystal Growth,* vol. 274, pp. 573-84.

Nowee, SM, Abbas, A & Romagnoli, JA 2008, 'Antisolvent crystallization: Model identification, experimental validation and dynamic simulation', *Chemical Engineering Science,* vol. 63, pp. 5457-67.

Noyes, AA & Whitney, WP 1897, 'Rate of solution of solid substances in their own solution ', *Journal of the American Chemical Society,* vol. 19, pp. 930-4.

Nyvlt, J 1960, 'Conference on Industrial Crystallization', Usti n.L.

Nyvlt, J 1992, 'Batch salting-out crystallisation', *Chemical Engineering and Processing,* vol. 31, no. 1, pp. 39-42.

Nyvlt, J, Sohnel, O, Matuchova, M & Broul, M 1985, *The Kinetics of Industrial Crystallization*, Elsevier, Amsterdam.

Nyvlt, J & Ulrich, J 1995, *Admixtures in Crystallization*, VCH, Weinheim.

Ohara, M & Reid, RC 1973, *Modelling Crystal Growth Rates from Solution*, Prentice-Hall, Englewood Cliffs, NJ.

Olech, AZ & Hodorowicz, SA 1990, 'The growth kinetics of urea monocrystals from 1-propanol-aqueous solutions', *Journal of Crystal Growth,* vol. 102, pp. 562-8.

Omar, W 2006, 'Effect of solvent composition on crystallization process of ascorbic acid', *Chemical Engineering & Technology,* vol. 29, no. 1, pp. 119-23.

Oosterhof, H, Geertman, RM, Witkamp, GJ & van Rosmalen, GM 1999, 'The growth of sodium nitrate from mixtures of water and isopropoxyethanol', *Journal of Crystal Growth,* vol. 198-199, pp. 754-9.

Pamplin, B 1980, *Crystal Growth*, Pergamon Press, Great Britian, UK.

Perelman, S & Strakhova, J 1938, *Zhur. Khim. Prom.,* vol. 26.

Phor, JS, Chaudhary, SK & Maken, S 1990, 'Purification, growth and ESR studies of sodium nitrate', *Crystal Research and Technology,* vol. 25, no. 8, pp. 881-4.

Pitzer, KS 1973, 'Thermodynamics of electrolytes I. Theoretical basis and general equations', *The Journal of Physical Chemistry,* vol. 77, no. 2, pp. 268-77.

Pitzer, KS 1980, 'Electrolytes. From dilute solutions to fused salts', *Journal of the American Chemical Society,* vol. 102, no. 9, pp. 2902 - 6.

Pitzer, KS & Kim, JJ 1974, 'Thermodynamics of electrolytes IV. Activity and osmotic coefficients for mixed electrolytes', *Journal of the American Chemical Society,* vol. 96, pp. 5701-7.

Pitzer, KS & Mayorga, G 1973, 'Thermodynamics of electroytes II. Activity and osmotic coefficients for strong electrolytes with one or both ions univalent', *The Journal of Physical Chemistry,* vol. 77, no. 19, pp. 2300-8.

Pol. Patent. 1966*,* 50 990.

Prymak, O, Sokolova, V, Peitsch, T & Epple, M 2006, 'The crystallization of fluoroapatite dumbbells from supersaturated aqueous solution', *Crystal Growth & Design,* vol. 6, no. 2, pp. 498-506.

Punin, YO & Franke, VD 2004, 'Curved-Face growth of NaNO3 crystals', *Crystallography Reports,* vol. 49, no. 2, pp. 256-60.

Randolph, AD & Larson, MA 1988, *Theory of Particulate Processes - Analysis and techniques of continuous crystallisation,* second edn, Academic Press, Inc, San Diego, California.

Rauls, M, Bartosch, K, Kind, M, Kuch, S, Lacmann, R & Mersmann, A 2000, 'The influence of impurities on crystallisation kinetics - a case study on ammonium sulfate', *Journal of Crystal Growth,* vol. 213, pp. 116-28.

Rifani, M, Yin, Y & Elliott, DS 1995, 'Solid State Dye Lasers from Stereospecific Host-Guest Interactions', *Journal of the American Chemical Society,* vol. 117, pp. 7572-3.

Ristic, RI, Shekunov, BY & Sherwood, JN 1997, 'The influence of synchrotron radiation-induced strain on the growth and dissolution of brittle and ductile materials', *Journal of Crystal Growth,* vol. 179, no. 1-2, pp. 205-12.

Robinson, RA & Stokes, RH 1965, *Electrolyte Solutions, revised ed*, Butterworth London.

Rolfs, J, Lacmann, R & Kipp, S 1997, 'Crystallization of potassium nitrate (KNO3) in aqueous solution I. Growth Kinetics of the pure system', *Journal of Crystal Growth,* vol. 171, pp. 174-82.

Rousseau, RW, Tai, CY & McCabe, WL 1976, 'The influence of quinoline yellow on potassium alum growth rates', *Journal of Crystal Growth,* vol. 32, pp. 73-6.

Ruiz-Agudo, E, Putnis, CV & Rodriguez-Navarro, C 2008, 'Interaction between Epsomite Crystals and Organic Additives', *Crystal Growth & Design,* vol. 8, no. 8, pp. 2665-73.

Safaeefar, P 2007, *Crystallisation of manganese sulphate from mix solvents*, Curtin University of Technology.

Sangwal, K & Rodriguez-Clemente, R 1991, *Surface morphology of crystalline materials*, Trans Tech publications, Zurich, Switzerland.

Sarig, S 1994, 'Fundamentals of aqueous solution growth', in DTJ Hurle (ed.), *Handbook of Crystal Growth 2 - Bulk Crystal Growth Part B: Growth mechanisms and dynamics*, Elsevier Science B.V, North-Holland.

Sawada, T & Shichiri, T 1984, 'Morphology and kinetics in ionic crystals growing from their melts', *Journal of Crystal Growth,* vol. 67, pp. 233-40.

Selvaraj, D, Toghiani, RK & Linder, JS 2008, 'Solubility in the Na + F + NO3 and Na + PO4 + NO3 systems in water and in sodium hydroxide solutions', *Journal of Chemical and Engineering Data,* vol. 53, no. 6, pp. 1250-5.

Shangfeng, Y, Genbo, S, Jing, T, Bingwei, M, Jianmin, W & Zhengdong, L 1999, 'Surface topography of rapidly grown KH2PO4 crystals with additives: ex situ investigation by atomic force microscopy', *Journal of Crystal Growth,* vol. 203, pp. 425-33.

Shanks, BH & Berglund, KA 1985, 'Contact nucleation from aqueous sucrose solutions', *AIChE Journal,* vol. 31, no. 1, pp. 152-4.

Shiau, LD & Berglund, KA 1987, 'Growth Kinetics of Fructose Crystals formed by contact nucleation', *AIChE Journal,* vol. 33, no. 6, pp. 1028-33.

Skoda, W & van den Tempel, M 1967, 'Growth kinetics of triglyceride crystals', *Journal of Crystal Growth,* vol. 1, no. 4, pp. 207-17.

Sohnel, O & Garside, J 1992, *Precipitation: Basic principles and industrial applications*, Butterworth Heinemann, Great Britain.

Sorensen, JM & Arlt, W 1980, *Vapour-Liquid Equilibrium Data Collection, Binary Systems, Chemistry Data Series, volume 1, Part 1*, DECHEMA, Frankfurt/Main.

Stephen, H & Stephen, T 1964, *Solubilities of inorganic and organic compounds*, Pergamon Press Ltd, Great Britain.

Subra-Paternault, P, Roy, C, Vrel, D, Vega-Gonzalez, A & Domingo, C 2007, 'Solvent effect on tolbutamide crystallisation induced by compressed CO2 as antisolvent', *Journal of Crystal Growth,* vol. 309, pp. 76-85.

Taylor, AE 1897, 'Precipitation of salts', *Journal of Physical Chemistry,* vol. 1, no. 2, pp. 718-33.

The Columbia Encyclopedia, SE 2008, *Sodium nitrate*. Retrieved 21/01/2009, from http://www.encyclopedia.com/doc/1E1-sodiumni.html

Thomsen, K, Rasmussen, P & Gani, R 1996, 'Correlation and prediction of thermal properties and phase behaviour for a class of aqueous electrolyte systems', *Chemical Engineering Science,* vol. 51, no. 14, pp. 3675-83.

Toghiani, RK, Phillips, VA, Smith, LT & Linder, JS 2008, 'Solubility in the Na + SO4 + NO3 and Na + SO4 + NO2 systems in water and in sodium hydroxide solutions', *Journal of Chemical and Engineering Data,* vol. 53, no. 3, pp. 798-804.

Toth, J, Kardos-Fodor, A & Halasz-Peterfi, S 2005, 'The formation of fine particles by salting-out precipitation', *Chemical Engineering and Processing,* vol. 44, no. 2, pp. 193-200.

Trypuc, M & Druzynski, S 2007, 'Investigation of the solubility in the NaVO3-NaNO3-H2O system', *Industrial & Engineering Chemistry Research,* vol. 46, no. 9, pp. 2688-92.

Trypuc, M & Druzynski, S 2008, 'Solubility in the NH4NO3 + NaNO3 + H2O system', *Industrial & Engineering Chemistry Research,* vol. 47, no. 10, pp. 3767-70.

Usui, H 2009, 'The effect of surfactants on the morphology and optical properties of precipitated wurtzite ZnO', *Materials Letters,* vol. 63, pp. 1489-92.

Valeton, JJP 1924, 'Wachstum and Auflosungder Kristalle', *Zeitschrift fur Physikalische Kristallographie,* vol. 59, p. 483.

Vargas, P, Salavera, D, Galleguillos, HR & Coronas, A 2008, 'Solubility of aqueous mixtures of alkaline nitrates and nitrites determined by differential scanning calorimetry', *Journal of Chemical and Engineering Data,* vol. 53, no. 2, pp. 403-6.

Villamagna, F & Whitehead, MA 1995, 'Determination of the ionic strength and degree of crystallisation in nitrate salt based emulsions using 14N NMR', *Journal of Molecular Structure,* vol. 356, no. 2, pp. 149-58.

Vitali, G & Berchiesi, G 1989, 'Solubility data of some sodium salts in 2-hydroxyacetamide', *Thermochimica Acta,* vol. 142, pp. 13-8.

Volmer, M 1939, *Kinetic der Phasenbildung*, Steinkoff, Dresden, Germany.

Wakihara, T, Sugiyama, A & Okubo, T 2004, 'Crystal growth of faujasite observed by atomic force microscopy', *Microporous and Mesoporous Materials* vol. 70, pp. 7-13.

Weinland, LA & France, WG 1932, 'Adsorption at crystal solution interfaces VI. Macroscopic sodium nitrate crystals grown in the presence of dyes and other foreign materials', *The Journal of Physical Chemistry,* vol. 36, no. 2, pp. 2832-9.

West, CD 1945, 'A method of growing oriented sections of certain optical crystals', *Journal of the Optical Society of America,* vol. 35, no. 1, pp. 26-31.

Whetstone, J 1955a, 'The crystal habit modification of inorganic salts with dyes: Part 1 - General considerations', *Transactions of the Faraday Society,* vol. 51, pp. 973-80.

Whetstone, J 1955b, 'The crystal habit modification of inorganic salts with dyes: Part 2 - the relationship between the structure of crystals and habit modifying dyes', *Transactions of the Faraday Society,* vol. 51, pp. 1142-53.

White, ET & Wright, AG 1971, 'Magnitude of size dispersion effects in crystallization', *Chemical Engineering Progress Symposium Series,* vol. 110, pp. 67-81.

Wikipedia 2007, *Sodium nitrate*. Retrieved 19/06/2007, from http://en.wikipedia.org/wiki/Sodium_nitrate

Winzer, A 1979, 'Freiberger Forschungsh A', vol. 600, p. 121.

Wolf, F & Holzweissig, J 1968, *Chemical Technology,* vol. 20, p. 477.

Wyckoff, RWG 1964, *Crystal Structures,* second edn, Interscience Publishers.

Xu, D, Xue, D & Ratajczak, H 2005, 'Morphology and structure studies of KDP and ADP crystallites in the water and ethanol solutions', *Journal of Molecular Structure,* vol. 740, pp. 37-45.

Zimmerman, JB, Hayes, KF & Skerlos, SJ 2004, 'Influence of Ion Accumulation on the Emulsion Stability and Performance of Semi-Synthetic Metalworking Fluids', *Environmental Science & Technology,* vol. 38, no. 8, pp. 2482-90.

NOMENCLATURE

General notation

A	single solute ion or molecule which contains n ion or molecules A_n pre-exponential factor surface area of the crystal a temperature dependent constant
A_ϕ	Pitzer-Debye-Huckel parameter
a	activity in units of mole fraction
B	a temperature dependent constant
C	a temperature dependent constant
C_1	concentration of the solution (mol/kg H_2O) empirical parameters obtained from experimental data
C_2	concentration of the solution in mass fraction empirical parameters obtained from experimental data
C_3	empirical parameters obtained from experimental data
C_4	empirical parameters obtained from experimental data
C_5	empirical parameters obtained from experimental data
c	solution concentration
c_i	interfacial concentration (solute concentration in the solution at the crystal-solution interface)
c*	equilibrium saturation at the given temperature
c-c*	'overall' concentration driving force
Δc	concentration driving force
D	coefficient of diffusion of the solute
dm/dt	mass of deposited solute in time t
E	activation energy (J/mol)

g	order of the overall crystal growth process
G	linear growth rate
Δg_{ij}	the difference in the interaction energy between the i-j and j-j combinations
ΔG	Gibbs free energy (overall excess free energy between a small solid particle of solute and the solute in solution)
ΔG_{crit}	Critical Gibbs free energy
ΔG_{het}	Gibbs free energy for heterogeneous nucleation
ΔG_{hom}	Gibbs free energy for homogeneous nucleation
ΔG_s	surface excess free energy
ΔG_v	volume excess free energy
ΔG_v	free energy change of the transformation per unit volume
h	step height
I	two-dimensional nucleation rate ion strength
J	rate of nucleation
k	Boltzmann constant, the gas constant per molecule ($1.3805 \times 10^{-23} JK^{-1}$)
k_0	a constant
k_d	coefficient of mass transfer by diffusion
k_g	a temperature dependent constant
K_g	a temperature dependent constant
K_G	overall crystal growth coefficient
k_m	coefficient of mass transfer
k_r	rate constant for the surface reaction (integration) process
K_s	solubility product of a salt in solution

L	diameter of the growth cell (m)
m	molality solubility (mol/kg solvent)
m_i^{calc}	calculated mole fraction solubility
m^{cor}	correlated solubility data
m^{exp}	experimental solubility data
m_i^{exp}	experimental mole fraction solubility
M_s	molecular weight of the solvent
N	number of experimental data points
N_{Re}	Reynolds number
r	nucleus radius
R	crystal growth rate universal gas constant, 8.314J/Kmol)
r_c	critical nucleus radius radius of a critical cluster
R_G	increase of mass per unit time per unit surface area
S	supersaturation ratio solubility (g /100g solvent)
$_+$ (subscript)	cation
$_-$ (subscript)	anion
T	temperature in K or ° C (as specified)
v	velocity of the fluid (m/s) molecular volume
v_a	stoichiometric coefficient of the anion
v_c	stoichiometric coefficient of the cation
$v_\pm$	stoichiometric number when the salt is perfectly dissociated

W	mass fraction of the alcohol
x	solubility in units of mole fraction
X	mole fraction
z	ion charge

Greek notation

α	non-random factor
δ	length of the diffusion path
ϕ	a factor
γ	interfacial tension
γ^*	unsymmetrical activity coefficient
$(\gamma_{i,NRTL})$	symmetrical NRTL derived activity coefficient
$(\gamma^*_{i,NRTL})$	unsymmetrical NRTL activity coefficient
$(\gamma^\infty_{i,NRTL})$	NRTL derived infinite dilution activity coefficient
$(\gamma^*_{\pm,ac})$	mean ionic activity coefficient of neutral electrolytes a-c
$i(\gamma^*_i)$	activity coefficient of an individual ion
μ	viscosity of the solution
θ	angle of wetting in liquid-solid systems
ρ	density of the solution (kg/m^3)
ρ	closest approach parameter
σ	absolute or relative supersaturation
τ_{ij}	NRTL binary interaction parameter of the i-j combination for any species

Abbreviations

AFM	atomic force microscopy
BCF	Burton-Cabrera-Frank
CCG	constant crystal growth
CD	characteristic dimension
EDS	energy dispersive detector
GRD	growth rate dispersion
MSMPR	mixed suspension mixed product removal
NRTL	non random two liquid
RF	random fluctuation
Rmsd	Root-mean-square-deviation
SEM	scanning electron microscopy
UNIQUAC	Universal Quasichemical

Appendix A Solubility data

Appendix A1 Solubility of sodium nitrate in water from literature

Table A1-1 Solubility of sodium nitrate in water from literature (Mullin 1993)

Temperature (°C)	Solubility ($gNaNO_3$/100g water)
0	73
10	80
20	88
30	96
40	104
60	124
80	148
100	180

Appendix A2 Experimental solubility data of sodium nitrate in water

Table A2-1 Experimental solubility data of sodium nitrate in water at 10.0, 20.0, 30.0 and 40.0 °C

Temperature (^oC)	Solubility ($gNaNO_3$/100g water)							average	stdev
	1	2	3	4	5	6	7		
10.0	82.55	82.01	81.85	81.97				82.10	0.31
20.0	88.43	88.81	88.39	88.19				88.46	0.26
30.0	95.7	96.07	95.06					95.57	0.71
40.0	104.79	104.6	103.47	103.65	103.92	104.55	103.75	104.10	0.53

Appendix A3 Experimental solubility data of sodium nitrate in aqueous methanol, ethanol and isopropanol at different temperatures

Table A3-1 Experimental solubility data of sodium nitrate in aqueous methanol at 20.0°C

Wt % in alcohol	Solubility ($gNaNO_3$/100g solvent mixture[a])					average	stdev
	1	2	3	4	5		
0	88.43	88.81	88.39	88.19		88.46	0.26
5.49	79.03	79.12	79.19	79.53		79.22	0.22
13.59	66.23	66.08	66.05	66.56		66.23	0.23
19.09	57.81	57.82	58.07	58		57.93	0.13
30	42.75	42.83	42.94			42.84	0.10
40	31.62	31.5	31.63			31.58	0.07
50	23.04	22.77	22.9	22.69	23.39	22.96	0.28
60	15.7	15.6	15.82			15.71	0.11
90	4.12	4.03	4.29	4.32		4.19	0.14

a) Solvent refers to the mixed solvent of water and methanol

Table A3-2 Experimental solubility data of sodium nitrate in aqueous methanol at 30.0°C

Wt % in alcohol	Solubility ($gNaNO_3$/100g solvent mixture[a])				average	stdev
	1	2	3	4		
0	95.7	96.07	95.06		95.61	0.51
10	79.78	79.88	79.96		79.87	0.09
20	63.01	63.93	64.1		63.68	0.59
30	49.17	49.38	49.2	48.8	49.14	0.24
40	36.77	36.88	36.53		36.73	0.18
50	26.94	26.55	26.21	26.22	26.48	0.34
60	18.6	18.56	18.62	18.7	18.62	0.06
70	12.46	12.79	12.26		12.50	0.27
90	4.76	4.68	4.71	4.67	4.71	0.04

a) Solvent refers to the mixed solvent of water and methanol

Table A3-3 Experimental solubility data of sodium nitrate in aqueous methanol at 40.0°C

Wt % in alcohol	Solubility ($gNaNO_3$/100g solvent mixture[a])							average	stdev
	1	2	3	4	5	6	7		
0	104.79	104.6	103.47	103.65	103.92	104.55	103.75	104.10	0.53
10	88.81	88.09	88.38	88.63	88.4	88.56	88.28	88.45	0.24
20	70.83	70.48	71.08	70.9				70.82	0.25
30	55.96	55.62	55.8					55.79	0.17
40	42.3	42.21	43.03	43.04	42.94	42.11		42.61	0.44
50	31.35	31.02	30.76	30.72	31.49	31.5		31.14	0.36
60	21.6	21.67	22.04	22.19				21.88	0.29
70	14.09	14.38	14.2	14.4	14.2			14.25	0.13
90	5.64	5.23	5.19	5.58				5.41	0.23

a) Solvent refers to the mixed solvent of water and methanol

Table A3-4 Experimental solubility data of sodium nitrate in aqueous ethanol at 20.4°C

Wt % in alcohol	Solubility ($gNaNO_3$/100g solvent mixture[a])						average	stdev
	1	2	3	4	5	6		
0	89.48	89.82	89.48	89.53	89.59		89.58	0.14
5.49	78.26	78.1	78.74	78.45			78.39	0.28
13.59	63	62.65	63.52	63.14			63.08	0.36
19.09	54.87	54.33	54.46	54.5			54.54	0.23
30	39.6	40.16	39.83	39.47			39.77	0.30
40	28.61	28.53	28.83	28.54			28.63	0.14
50	20.1	20.37	20.4	19.5	19.55	19.92	19.97	0.39
60	12.63	13.27	13.17	13	12.55		12.92	0.32
90	1.11	1.07	1.02	1.05			1.06	0.04

a) Solvent refers to the mixed solvent of water and ethanol

Table A3-5 Experimental solubility data of sodium nitrate in aqueous ethanol at 30.0°C

Wt % in alcohol	Solubility ($gNaNO_3$/100g solvent mixture[a])					average	stdev
	1	2	3	4	5		
0	95.7	96.07	95.06			95.61	0.51
5	85.81	86.3	85.66	85.18	86.15	85.82	0.44
20	59.97	59.53	59.42			59.64	0.29
40	33.38	33.33	33.76			33.49	0.24
60	14.82	14.8				14.81	0.01
70	8.23	8.31				8.27	0.06
90	1.28	1.25	1.2			1.24	0.04

a) Solvent refers to the mixed solvent of water and ethanol

Table A3-6 Experimental solubility data of sodium nitrate in aqueous ethanol at 40.0°C

Wt % in alcohol	Solubility ($gNaNO_3$/100g solvent mixture[a])								average	stdev
	1	2	3	4	5	6	7	8		
0	104.79	103.47	104.6	103.65	103.92	104.55	103.74		104.10	0.53
8.22	87.9	87.89	88.55	88.13	89.15	88.79	88.2	89.26	88.48	0.54
26	57.75	57.47	57.84						57.69	0.19
42.8	35.9	35.43	35.88	35.6	35.55				35.67	0.21
65.1	13.65	13.26	13.34	13.46	13.45				13.43	0.15
87.2	2.33	2.08	2.02	2.5	2.05	2.32	2.15	2.31	2.22	0.17
	2.29	2.2	2.12	2.07						

a) Solvent refers to the mixed solvent of water and ethanol

Table A3-7 Experimental solubility data of sodium nitrate in aqueous isopropanol at 20.0 °C

Wt % in alcohol	Solubility ($gNaNO_3$/100g solvent mixture[a])				average	stdev
	1	2	3	4		
0	88.43	88.81	88.39	88.19	88.46	0.26
*5.49	77.53	77.36	77.13		77.34	0.20
**13.59	67.52	67.13			67.33	0.28
**19.09	61.68	61.69	61.91		61.76	0.13
**30	50.83	51.2	51.44	50.88	51.09	0.29
**40	41.05	40.85	40.98		40.96	0.10
**50	30.84	31.16			31.00	0.23
**60	21.01	21.19			21.10	0.13
*90	0.97	0.69	0.79	0.8	0.81	0.12

a) Solvent refers to the mixed solvent of water and isopropanol
* One miscible phase ** Two phases

Appendix A4 Solubility of sodium nitrate in aqueous ethanol from literature

Table A4-1 Solubility of sodium nitrate in aqueous ethanol at 30 °C from literature (Taylor 1897)

Wt % in alcohol	Solubility ($gNaNO_3$/100g solvent mixture[a])
0	96.46
5	86.6
10	76.99
20	59.89
30	45.58
40	33.58
50	23.36
60	14.9
70	8.47
90	1.22

a) Solvent refers to the mixed solvent of water and ethanol

Table A4-2 Solubility of sodium nitrate in aqueous ethanol at 40 °C from literature (Bathrick 1896)

Wt % in alcohol	Solubility ($gNaNO_3$/100g solvent mixture[a])
0	104.5
8.22	90.8
17.4	73.3
26	61.6
36	48.4
42.8	40.6
55.3	27.1
65.1	18.1
77	9.4
87.2	4.2

a) Solvent refers to the mixed solvent of water and ethanol

Appendix B Specifications of sodium nitrate

Table B Specifications of BDH sodium nitrate

Characteristics	Specifications
Assay (acidimetric)	≥ 99.5 %
Insoluble matter	≤ 0.005 %
pH-value (5%, water, 25°C)	5.5 - 8.0
Chloride (Cl)	≤ 0.0005 %
Iodate	≤ 0.0005 %
Magnesium (Mg)	≤ 0.002 %
Ammonium (NH_4)	≤ 0.002 %
Nitrite (NO_2)	≤ 0.001 %
Phosphate (PO_4)	≤ 0.0005 %
Sulphate (SO_4)	≤ 0.003 %
Heavy metals (as Pb)	≤ 0.0005 %
Calcium (Ca)	≤ 0.002 %
Iron (Fe)	≤ 0.0003 %
Potassium (K)	≤ 0.01 %

Appendix C Crystal growth rates

Appendix C1 Summary of sodium nitrate growth rates from homogeneous nucleation in the batch cell at different temperatures and supersaturations

Table C1-1 Summary of sodium nitrate growth rates from homogeneous nucleation in the batch cell at 20.0°C, σ 0.02

Exp #	Growth rate (µm/min)	R^2 fit
1	6.32	0.995
2	5.28	0.993
3	2.79	0.995
4	2.83	0.993
5	6.49	0.993
6	4.54	0.996
7	4.62	0.995
8	7.52	0.986
9	7.37	0.990

Table C1-2 Summary of sodium nitrate growth rates from homogeneous nucleation in the batch cell at 20.0°C, σ 0.04

Exp #	Growth rate (µm/min)	R^2 fit
1	10.42	0.996
2	10.29	0.992
3	8.63	0.997
4	11.72	0.995
5	9.15	0.995
6	12.13	0.995
7	10.74	0.996
8	8.65	0.992
9	11.62	0.997
10	7.87	0.996
11	12.66	0.993
12	7.31	0.993
12	7.36	0.993
13	9.67	0.996
14	8.91	0.995
15	8.76	0.994

Table C1-3 Summary of sodium nitrate growth rates from homogeneous nucleation in the batch cell at 20.0°C, σ 0.06

Exp #	Growth rate (µm/min)	R^2 fit
1	15.54	0.993
2	17.89	0.995
3	14.53	0.995
4	12.54	0.993
5	8.25	0.994
6	13.72	0.994
7	12.77	0.996
8	12.90	0.986
9	12.79	0.995

Table C1-4 Summary of sodium nitrate growth rates from homogeneous nucleation in the batch cell at 20.0°C, σ 0.08

Exp #	Growth rate (µm/min)	R^2 fit
1	16.74 15.62	0.996 0.997
2	21.24	0.997
3	19.84	0.994
4	12.62	0.998
5	14.57	0.999
6	20.87	0.995
7	23.85	0.996
8	18.92	0.999
9	17.55	0.998
10	17.83	0.994
11	19.08	0.996
12	19.79	0.993

Table C1-5 Summary of sodium nitrate growth rates from homogeneous nucleation in the batch cell at 20.0°C, σ 0.1

Exp #	Growth rate (µm/min)	R^2 fit
1	23.38	0.996
2	24.18	0.996
3	25.04	0.997
4	24.21	0.997
5	16.89	0.989
6	23.54	0.999
7	22.93 23.59	0.998 0.997

Table C1-6 Summary of sodium nitrate growth rates from homogeneous nucleation in the batch cell at 30.0°C, σ 0.02

Exp #	Growth rate (μm/min)	R^2 fit
1	8.78	0.990
2	8.11	0.993
3	8.23	0.988
4	9.72	0.995
5	10.42	0.974
6	10.38	0.992
7	8.10	0.993
8	7.95 7.58 10.41	0.988 0.994 0.995
9	9.07	0.992
10	10.05	0.995
11	5.14	0.997
12	6.03	0.997

Table C1-7 Summary of sodium nitrate growth rates from homogeneous nucleation in the batch cell at 30.0°C, σ 0.04

Exp #	Growth rate (μm/min)	R^2 fit
1	13.82	0.999
2	25.83	0.990
3	14.39	0.997
4	13.93	0.998
5	13.61	0.999
6	17.75 11.08	0.993 0.993
7	11.67	0.993
8	10.00	1.000
9	15.99	0.998
10	12.43	1.000
11	15.96	0.987
12	13.46	0.999
13	11.04	0.994
14	13.90	0.989
15	13.72	0.995
16	13.87	0.995
17	14.03	0.994
18	13.83	0.996
19	11.04	0.996
20	12.87	0.995
21	16.22	0.995
22	15.16	0.995
23	11.95	0.994
24	14.02	0.995
25	13.41	0.993

Table C1-8 Summary of sodium nitrate growth rates from homogeneous nucleation in the batch cell at 30.0°C, σ 0.06

Exp #	Growth rate (μm/min)	R^2 fit
1	22.50	0.997
2	19.47	0.993
3	21.54	0.992
4	19.85	0.996
5	19.70	0.997
6	17.84	0.999
7	18.50	0.996
8	18.81	0.997
9	16.96	0.998
10	19.12	0.997
11	14.63	0.997
12	19.27	0.997
13	13.74	0.999
14	17.45	0.993
15	16.11	0.995
16	20.14	0.997
17	18.68	0.996

Table C1-9 Summary of sodium nitrate growth rates from homogeneous nucleation in the batch cell at 30.0°C, σ 0.08

Exp #	Growth rate (μm/min)	R^2 fit
1	31.05	0.993
2	28.03	0.998
3	28.35	0.998
4	28.69	0.998
5	29.26	0.997
6	27.93	1.000
7	26.07	0.997
8	26.61	0.996
9	29.11	0.996
10	28.82	0.996
11	32.40	0.998
12	29.38	0.998
13	31.94	0.996
14	27.83	0.994

Table C1-10 Summary of sodium nitrate growth rates from homogeneous nucleation in the batch cell at 30.0°C, σ 0.1

Exp #	Growth rate (μm/min)	R^2 fit
1	39.91	0.999
2	41.63	0.991
	22.56	0.998
	25.44	0.998
3	23.89	0.998
	26.62	0.994
4	27.56	0.999
	31.73	0.998
5	26.02	0.997
	35.27	0.999
6	28.13	0.998
	30.81	0.996
7	29.88	0.997
	33.17	0.998
8	30.87	0.997
	32.20	0.995
9	27.12	0.996
	31.24	0.993

Table C1-11 Summary of sodium nitrate growth rates from homogeneous nucleation in the batch cell at 40.0°C, σ 0.02

Exp #	Growth rate (μm/min)	R^2 fit
1	9.82	0.995
2	6.77	0.992
3	11.81	0.991
4	14.76	0.992
5	9.10	0.982
6	13.86	0.976
7	9.38	0.990
	10.23	0.990
	7.86	0.989
8	9.73	0.995
9	6.93	0.999
10	8.38	0.994
11	9.31	0.987
12	14.90	0.991
13	11.52	0.993
14	3.85	0.996
15	10.09	0.993
16	19.71	0.991
17	6.39	0.997
18	9.25	0.992

Table C1-12 Summary of sodium nitrate growth rates from homogeneous nucleation in the batch cell at 40.0°C, σ 0.04

Exp #	Growth rate (µm/min)	R^2 fit
1	14.18	0.992
2	18.23	0.991
3	15.33	0.995
4	18.14	0.993
5	11.30	0.992
6	22.29 22.84	0.990 0.993
7	19.30	0.995
8	16.40	0.996
9	18.19	0.994
10	23.18	0.993
11	22.97	0.991
12	20.93	0.993
13	26.09	0.994
14	30.70	0.995
15	24.30	0.992
16	15.86	0.963
17	23.99	0.988
18	29.89	0.995

Table C1-13 Summary of sodium nitrate growth rates from homogeneous nucleation in the batch cell at 40.0°C, σ 0.06

Exp #	Growth rate (µm/min)	R^2 fit
1	26.94	0.995
2	30.28	0.999
3	22.81	0.994
4	30.42	0.987
5	28.25	0.985
6	30.73	0.993
7	25.66	0.999
8	31.32	0.998
9	27.22	0.994
10	31.62	0.993
11	24.98	0.995

Table C1-14 Summary of sodium nitrate growth rates from homogeneous nucleation in the batch cell at 40.0°C, σ 0.08

Exp #	Growth rate (µm/min)	R^2 fit
1	46.01	1.000
2	40.61	0.996
3	43.02	0.997
4	42.27	0.991
5	42.39	0.993
6	36.51	0.996

Table C1-15 Summary of sodium nitrate growth rates from homogeneous nucleation in the batch cell at 40.0°C, σ 0.1

Exp #	Growth rate (µm/min)	R^2 fit
1	43.78	0.999
	41.43	0.993
2	33.66	0.993
3	38.67	0.996
	34.94	0.997
4	40.58	0.998
	36.03	0.995
	31.07	0.985
5	29.06	0.997
	33.58	0.998
6	41.25	0.998
	41.41	0.999
7	47.90	0.998

Appendix C2 Summary of sodium nitrate growth rates in aqueous ethanol at different weights from homogeneous nucleation in the batch cell at 30.0°C

Table C2-1 Summary of sodium nitrate growth rates from homogeneous nucleation in 20 weight percent ethanol 30.0°C, σ 0.02

Exp #	Growth rate (µm/min)	R^2 fit
1	2.21	0.981
	2.69	0.990
	2.06	0.965
	2.21	0.983
	1.94	0.977
	1.85	0.971
2	3.02	0.982
	2.66	0.980
	2.73	0.982
	3.22	0.993
	3.17	0.968
3	1.40	0.982
	1.50	0.971
	1.17	0.990

Table C2-2 Summary of sodium nitrate growth rates from homogeneous nucleation in 20 weight percent ethanol 30.0°C, σ 0.04

Exp #	Growth rate (µm/min)	R^2 fit
1	5.28	0.980
	6.02	0.970
	5.73	0.990
	6.04	0.988
	4.62	0.997
	6.02	0.993
2	6.96	0.979
	6.94	0.990
	6.23	0.995
	6.23	0.994

Table C2-3 Summary of sodium nitrate growth rates from homogeneous nucleation in 50 weight percent ethanol 30.0°C, σ 0.02

Exp #	Growth rate (µm/min)	R^2 fit
1	3.36	0.989
	3.07	0.979
	2.77	0.976
2	2.21	0.998
	1.96	0.986
	1.77	0.987
3	1.56	0.984
	1.22	0.990
4	2.46	0.990
5	2.63	0.989
6	1.52	0.996

Table C2-4 Summary of sodium nitrate growth rates from homogeneous nucleation in 50 weight percent ethanol 30.0°C, σ 0.04

Exp #	Growth rate (µm/min)	R^2 fit
1	3.50	0.965
	2.96	0.983
	3.84	0.984
	3.77	0.991
	3.16	0.989
2	3.13	0.989
	3.67	0.995
	3.60	0.996
3	2.83	0.996
	3.07	0.996
4	3.81	0.990
	3.59	0.986
	3.14	0.992
5	3.17	0.966
	3.38	0.973
	3.54	0.987
	3.07	0.990
6	2.65	0.995

Table C2-5 Summary of sodium nitrate growth rates from homogeneous nucleation in 50 weight percent ethanol 30.0°C, σ 0.08

Exp #	Growth rate (μm/min)	R^2 fit
1	5.27	0.976
	4.84	0.984
	5.36	0.998
	4.81	0.985
2	5.35	0.951
	5.02	0.973
	5.69	0.988
	4.31	0.990
	5.08	0.989
	3.99	0.978
3	3.33	0.970
	4.33	0.992
	4.27	0.991
	3.91	0.977
	3.92	0.992
4	5.97	0.995
	3.76	0.996
	3.85	0.993
5	6.00	0.977
	6.48	0.992
	6.21	0.989
	6.29	0.995
	6.98	0.993
6	4.47	0.984
	5.07	0.981
	4.76	0.985
	4.84	0.988
	3.89	0.970
	4.94	0.992

Table C2-6 Summary of sodium nitrate growth rates from homogeneous nucleation in 90 weight percent ethanol 30.0°C, σ 0.02

Exp #	Growth rate (µm/min)	R^2 fit
1	0.84	0.980
	0.86	0.983
	0.67	0.991
	0.58	0.993
	0.61	0.988
2	0.86	0.981
	0.88	0.986
	0.96	0.981
	0.70	0.938
	0.83	0.980
	0.93	0.992
3	0.90	0.955
	0.78	0.969
	0.80	0.987
	0.80	0.988
	0.83	0.983

Table C2-7 Summary of sodium nitrate growth rates from homogeneous nucleation in 90 weight percent ethanol 30.0°C, σ 0.04

Exp #	Growth rate (µm/min)	R^2 fit
1	0.83	0.942
	0.90	0.977
	0.87	0.973
	0.75	0.971
	0.83	0.997
2	0.93	0.966
	1.00	0.978
	0.81	0.981
	0.78	0.981
3	0.84	0.981
	0.80	0.987
	0.67	0.942
4	0.67	0.985

Table C2-8 Summary of sodium nitrate growth rates from homogeneous nucleation in 90 weight percent ethanol 30.0°C, σ 0.08

Exp #	Growth rate (μm/min)	R^2 fit
1	1.37	0.984
	1.31	0.991
	1.26	0.984
2	1.14	0.983
	0.92	0.981
	0.95	0.976
3	1.21	0.988
	1.01	0.998
	1.06	0.987

Appendix C3 Summary of sodium nitrate growth rates of crystal seeds grown in the modified growth cell at 20.0°C

Table C3-1 Summary of sodium nitrate growth rates of crystal seeds grown in the modified growth cell at 20.0°C, σ 0.02 and 0.04

σ	Exp #	Growth rate (μm/min)	R^2 fit
0.02	1	3.20	0.993
		3.91	0.923
		2.89	0.973
	2	3.25	0.991
	3	2.71	0.994
		2.60	0.991
		2.27	0.864
		2.63	0.965
		2.40	0.989
	4	3.52	0.993
	5	4.06	0.976
		3.71	0.990
		3.01	0.978
0.04	1	5.04	0.980
		4.71	0.993
		5.15	0.977
		4.60	0.948
		5.19	0.984
		4.56	0.943
	2	6.92	0.963
		6.13	0.977
		6.98	0.984

Appendix C4 Summary of sodium nitrate growth rates of crystal seeds in aqueous ethanol and methanol grown in the modified growth cell at 20.4 and 20.0°C respectively

Table C4-1 Summary of sodium nitrate growth rates of crystal seeds in 30 weight percent ethanol at 20.4°C, σ 0.02 and 0.04

σ	Exp #	Growth rate (μm/min)	R^2 fit
0.02	1	2.76	0.977
		2.95	0.960
		3.14	0.996
		2.75	0.989
		2.81	0.997
	2	1.88	0.943
		1.29	0.976
		2.11	0.965
		1.69	0.964
		2.08	0.970
0.04	1	3.95	0.986
		4.49	0.997
		3.95	0.987
		5.64	0.997
		3.97	0.975

Table C4-2 Summary of sodium nitrate growth rates of crystal seeds in 50 weight percent ethanol at 20.4°C, σ 0.02 and 0.04

σ	Exp #	Growth rate (μm/min)	R^2 fit
0.02	1	2.09	0.989
		2.21	0.994
		2.01	0.976
		1.67	0.965
		1.78	0.990
	2	2.86	0.985
		2.93	0.964
		2.25	0.927
		1.93	0.994
0.04	1	2.79	0.933
		2.74	0.989
		2.07	0.984
		2.57	0.960
		2.66	0.997
		3.03	0.986

Table C4-3 Summary of sodium nitrate growth rates of crystal seeds in 90 weight percent ethanol at 20.4°C, σ 0.02 and 0.04

σ	Exp #	Growth rate (µm/min)	R^2 fit
0.02	1	0.146	0.723
		0.174	0.711
		0.146	0.590
		0.176	0.825
0.04	1	0.168	0.702
		0.130	0.711
		0.113	0.623

Table C4-4 Summary of sodium nitrate growth rates of crystal seeds in 50 weight percent methanol at 20.0°C, σ 0.02

Exp #	Growth rate (µm/min)	R^2 fit
1	1.00	0.960
	0.98	0.962
	1.25	0.979
	1.19	0.961
	1.05	0.956
	1.24	0.951

Appendix D Calculation of Reynolds number

Calculation of Reynolds number for sodium nitrate grown in the modified growth cell at 20.0°C σ 0.02

Calculation of the density:

$$\rho = 765.7535C_2 - 0.52705T + 1006$$

C_2 = 89.76g/ 100 = 0.898
T = 20.0°C

Therefore density = 1683.11kg/m^3

Calculation of the velocity:

$$v = \frac{Q}{A} = \frac{Q}{\pi dh}$$

d (diameter of the growth cell): 0.03m
h (height of the upper section of the growth cell): 0.01m
Q: 4mL/min = 4cm^3/min

Therefore velocity = 0.424 cm/min = 7.0735 x 10^{-5} m/s

Calculation of the viscosity of the solution:

$$\mu = 0.00188508Exp\left(\frac{1833.45022}{T}\right)Exp\left(0.0837004C_1 + 0.00237765C_1{}^2\right)$$

T = 293K
C_1 = [(89.76/2)/ 85] x (1000/50) = 10.56

Therefore viscosity = 3.104mPaS = 3.104x10^{-3}PaS

Calculation of Reynolds number:

$$N_{\mathrm{Re}} = \frac{\rho_{solution} vL}{\mu_{solution}}$$

N_{Re} = (1683.11kg/m^3)(7.0735 x 10^{-5} m/s)(0.03m) / (3.104x10^{-3}PaS)
= 1.15

Calculation of Reynolds number for sodium nitrate grown in the modified growth cell at 20.0°C σ 0.04

Calculation of the density:

$$\rho = 765.7535C_2 - 0.52705T + 1006$$

C_2 = 91.52g/ 100 = 0.915
T = 20.0°C

Therefore density = 1696.28kg/m^3

Calculation of the velocity:

$$v = \frac{Q}{A} = \frac{Q}{\pi dh}$$

d (diameter of the growth cell): 0.03m
h (height of the upper section of the growth cell): 0.01m
Q: 4mL/min = 4cm^3/min

Therefore velocity = 0.424 cm/min = 7.0735 x 10^{-5} m/s

Calculation of the viscosity of the solution:

$$\mu = 0.00188508Exp\left(\frac{1833.45022}{T}\right)Exp\left(0.0837004C_1 + 0.00237765C_1{}^2\right)$$

T = 293K
C_1 = [(91.52/2)/ 85] x (1000/50) = 10.77

Therefore viscosity = 3.192mPaS = 3.192x10^{-3}PaS

Calculation of Reynolds number:

$$N_{\mathrm{Re}} = \frac{\rho_{solution} vL}{\mu_{solution}}$$

N_{Re} = (1696.28kg/m^3)(7.0735 x 10^{-5} m/s)(0.03m) / (3.192x10^{-3}PaS)
= 1.13